Self-healing Poly(methyl methacrylate) Bone Cement Utilizing Embedded Microencapsulated 2-Octyl Cyanoacrylate Tissue Adhesive

by

Alice Bradbury Welsh Brochu

Department of Biomedical Engineering
Duke University

Date:_____

Approved:

_____
William M. Reichert, Supervisor

_____
Stephen Craig

_____
Jan Genzer

_____
Farshid Guilak

_____
Bruce Klitzman

Dissertation submitted in partial fulfillment of
the requirements for the degree of Doctor
of Philosophy in the Department of
Biomedical Engineering in the Graduate School
of Duke University

2013

ABSTRACT

Self-healing Poly(methyl methacrylate) Bone Cement Utilizing Embedded Microencapsulated 2-Octyl Cyanoacrylate Tissue Adhesive

by

Alice Bradbury Welsh Brochu

Department of Biomedical Engineering
Duke University

Date:_____
Approved:

_____
William M. Reichert, Supervisor

_____
Stephen Craig

_____
Jan Genzer

_____
Farshid Guilak

_____
Bruce Klitzman

An abstract of a dissertation submitted in partial fulfillment of the requirements for the degree of Doctor of Philosophy in the Department of Biomedical Engineering in the Graduate School of Duke University

2013

Abstract

Extending the functional lifetime of acrylic poly(methyl methacrylate) (PMMA) bone cement may reduce the number of revision total joint replacement (TJR) surgeries performed each year. We developed a system utilizing an encapsulated water-reactive, FDA-approved tissue adhesive, 2-octyl cyanoacrylate (OCA), as a healing agent to repair microcracks within a bone cement matrix. The proposed research tested the following hypotheses: (1) reactive OCA can be successfully encapsulated and the resulting capsules thoroughly characterized; (2) the static mechanical properties of the PMMA composite can be improved or maintained through inclusion of an optimal wt% of OCA-containing capsules; (3) PMMA containing encapsulated OCA has a prolonged lifetime when compared with a capsule-free PMMA control as measured by the number of cycles to failure; and (4) the addition of capsules to the PMMA does not significantly alter the biocompatibility of the material. Based on the experiments reported herein, the primary conclusions of this dissertation are as follows: (1) functional OCA can be encapsulated within polyurethane spheres and successfully incorporated into PMMA bone cement; (2) lower wt% of capsules maintained the tensile, compressive, fracture toughness, and bending properties of the PMMA; (3) inclusion of 5 wt% of OCA-containing capsules in the matrix increased the number of cycles to failure when compared to unfilled specimens and those filled with OCA-free capsules; and (4) MG63

human osteosarcoma cell proliferation and viability were unchanged following exposure to OCA-containing PMMA when compared with a capsule-free control.

Dedication

I would like to dedicate this dissertation specifically to my husband, Keegan, and to the rest of our extended family. My husband has been wonderful and supportive throughout all my years in graduate school, giving me confidence and being my cheerleader, especially when I wasn't being one for myself. Even from 3000 miles away he has been patient, devoted, and attentive, helping me power through the toughest stages of my research. I am so lucky and thankful to have him, and I can't wait to start our life together in California!

I have a terrific support system in my immediate family, my extended family, and my husband's family. Everyone has been very understanding and accepting of the demands that being a graduate student has put on my free time and even though I wasn't able to spend as much time with my families as I would have liked, I am very fortunate to have stayed near my hometown where I am surrounded by love on all sides. I hope that no matter what distance separates us, we are always able to maintain the close relationships we have now.

Contents

Abstract iv

List of Tables xiii

List of Figures xiv

Acknowledgements xvii

1. Chapter 1: Background, significance, specific aims, and hypotheses 1

1.1 Background and significance 1

1.1.1 Total joint replacements 1

1.1.1.1 Clinical need for and design of total joint replacements 1

1.1.1.2 Sources of failure observed in total joint replacements 4

1.1.1.3 Strategies to improve the functional lifetime of total joint replacements 7

1.1.2 Self-healing materials 9

1.1.2.1 What are self-healing materials? 9

1.1.2.2 Challenges for extension into biomaterials 13

1.1.2.3 Strategies commonly used to assess self-healing materials 15

1.1.3 Characterization of PMMA bone cement 17

1.1.3.1 Determination of various mechanical properties 17

1.1.3.2 *In vitro* assessments of PMMA toxicity 24

1.1.3.3 Failure of PMMA bone cement 26

1.1.3.4 Biomimetic assessments of PMMA bone cement 29

1.2 Specific aims and hypotheses 33

2. Chapter 2: Microencapsulation of 2-octyl cyanoacrylate tissue adhesive for self-healing acrylic bone cement 38

2.1 Chapter synopsis 38

2.2 Introduction 39

2.3 Experimental section 43

2.3.1 Materials 43

2.3.2 Preparation of polyurethane prepolymer 43

2.3.3 Preparation of microcapsules 44

2.3.4 Characterization of microcapsules 45

2.3.4.1 Capsule morphology, size, and shell thickness 45

2.3.4.2. Characterization of capsule content and reactivity 46

2.3.4.3 Compression testing of individual microcapsules 46

2.3.4.4 Adhesion testing of crushed microcapsules 47

2.3.4.5 Incorporation of capsules into a PMMA matrix 47

2.4 Results 48

2.4.1 Reaction conditions 48

2.4.1.1 Organic solvents 48

2.4.1.2 Surfactants 49

2.4.1.3 Temperature 49

2.4.1.4 Controlling OCA reactivity 50

2.4.2 Effect of agitation rate 50

2.4.3 Capsule thermal properties 53

2.4.4 Capsule mechanical properties 59

2.4.5 Incorporation of capsules into the PMMA matrix 65

2.5 Discussion 67

2.6 Conclusions 71

2.7 Chapter acknowledgements 72

3. Chapter 3: Mechanical testing of acrylic bone cement embedded with microencapsulated 2-octyl cyanoacrylate 73

3.1 Chapter synopsis 73

3.2 Introduction 74

3.3. Experimental section 77

3.3.1 Reagents 77

3.3.2 Microcapsule preparation 77

3.3.3 Preparation of capsule-containing bone cement samples 78

3.3.3.1 Tensile testing of capsule-embedded bone cement 79

3.3.3.2 Compression testing of capsule-embedded bone cement 79

3.3.3.3 Fracture toughness testing of capsule-embedded bone cement 80

3.4 Results 82

3.4.1 Capsule morphology 82

3.4.2 Tensile testing of capsule-embedded bone cement 82

3.4.3 Compression testing of capsule-embedded bone cement 84

3.4.4 Fracture toughness testing of capsule-embedded bone cement 86

3.5 Discussion 88

3.6 Conclusions 91

3.7 Chapter acknowledgements 91

4. Chapter 4: Functional lifetime of acrylic bone cement containing microencapsulated 2-octyl cyanoacrylate 93

4.1 Chapter synopsis 93

4.2 Introduction 94

4.3 Experimental section 99

4.3.1 Reagents 99

4.3.2 Microcapsule preparation 99

4.3.3 Preparation of capsule-containing bone cement samples 100

4.3.3.1 Bending testing of capsule-embedded bone cement 101

4.3.3.2 Fatigue testing of capsule-embedded bone cement 102

4.3.4 Capsule susceptibility to moisture intrusion 104

4.3.5 Statistical analyses 105

4.4 Results 105

4.4.1 Capsule morphology 105

4.4.2 Bending testing of capsule-embedded bone cement 106

4.4.3 Fatigue testing of capsule-embedded bone cement 108

4.4.4 Capsule susceptibility to moisture intrusion 116

4.5 Discussion 120

4.6 Conclusions 126

4.7 Chapter acknowledgements 127

5. Chapter 5: Cytotoxicity testing of acrylic bone cement embedded with microencapsulated 2-octyl cyanoacrylate 128

5.1 Chapter synopsis 128

5.2 Introduction 129

5.3 Experimental section 131

5.3.1 Reagents 131

5.3.2 Microcapsule preparation 132

5.3.3 Biocompatibility of capsule-containing bone cement 133

5.3.3.1 Preparation of bone cement and OCA extracts 133

5.3.3.2 Cell viability and proliferation 135

5.3.4 Statistical analyses 137

5.4 Results 138

5.4.1 Capsule morphology 138

5.4.2 Cytotoxicity testing of OCA and capsule-embedded bone cement 138

5.4.2.1 MG63 viability 138

5.4.2.2 MG63 proliferation 144

5.5 Discussion 152

5.6 Conclusions 154

5.7 Chapter acknowledgements 155

6. Chapter 6: Dissertation summary and future work 156

6.1 Dissertation summary 156

6.2 Future work to complete current studies 162

6.3 Implications of this research 163

6.4 Future directions for the self-healing bone cement project 165

Appendix A: Glossary of Terms 175

Appendix B 177

References 191

Biography 210

List of Tables

Table 1.1: Summary of healing agents, catalysts, and matrix materials studied for applications in SHM based on the matrix repolymerization scheme 12

Table 1.2: Concerns associated with SHM and their extension to biomaterials 14

Table 1.3: Properties of PMMA bone cement 23

Table 2.1: Mechanical properties of single capsules (data presented as average ± one standard deviation) 62

Table 2.2: Detachment forces required to separate aluminum plates bonded by various cyanoacrylate (data presented as average ± one standard deviation) 64

Table 4.1: Mechanical properties of capsule-filled and capsule-free bone cements tested in air 113

Table 6.1: Effect of thiol functionalization on contact angle of PUR films 169

List of Figures

Figure 1.1: Self-healing material scheme[47]. Adopted from[65]. 10

Figure 2.1: (A) Increasing agitation rate results in decreasing average capsule diameter and average shell thickness; (B) smooth surface morphology of microcapsules made at 700 rpm is clearly visible under SEM. 52

Figure 2.2: TGA results provide thermal degradation behaviors of capsules made under various conditions. The weight loss curves of capsules as well as pure samples of MIBK, OCA, and PUR shell material are shown in (A). Derivatives of the TGA data for capsules, MIBK, OCA, and PUR shell material are presented in (B). All experiments were conducted at a heating rate of 10 ºC/min under N_2..... 54

Figure 2.3: TGA data analysis was used to determine the various weight fractions of components of the microcapsules..... 56

Figure 2.4: TGA weight loss curves of microcapsules made at 700 rpm following 56 days of storage. 58

Figure 2.5: Stress-strain curves of microcapsules fabricated at various agitation rates. All compressions performed at a rate of 5 μm/s. Following capsule shell failure, the capsule was removed from the lower DMA compression plate, transferred to carbon tape on an SEM stage, gold-coated, and then imaged. (Inset) An SEM image of a capsules post-DMA testing where the failure plane is clearly visible; the original capsule diameter was 180 μm..... 60

Figure 2.6: (A) An SEM image of PMMA bone cement containing intact microcapsules, (B) a PMMA fracture plane in which ruptured capsules are visible, and (C) a magnified image of a fractured microcapsule within the damage plane of the matrix. 66

Figure 3.1: Palacos R PMMA samples for (A) tension, (B) compression, and (C) fracture toughness testing. 81

Figure 3.2: Relationship between capsule content and (A) ultimate tensile strength and (B) Young's modulus (average ± SEM, n=5)..... 83

Figure 3.3: (A) Relationship between capsule content and the ultimate compressive strength of bone cement (average ± SEM, n=3 with 5 replicates per group). Photographs of samples containing (B) 0 wt% and (C) 40 wt% capsules post-compression testing. 85

Figure 3.4: Load with increasing vertical displacement is shown in (A) for samples containing 0 and 3 wt% capsules. The effect of capsule content on fracture toughness is presented in (B) (average ± SEM, n=5). Fracture plane roughness and sub-surface microcracking are observed in SEM images of the side views of TDCB samples containing (C) 0 wt% and (D) 3 wt% capsules. Direction of crack propagation is indicated by arrows. 87

Figure 4.1: Relationship between capsule content and (A) bending strength and (B) bending modulus (average ± SEM, n=5) for specimens embedded with OCA-containing and OCA-free capsules. 107

Figure 4.2: The reference bending strengths for each sample type are depicted in (A) (n=10). The fatigue test results as applied stress versus the number of cycles to failure for samples tested after 1 d storage in air are summarized in (B). 109

Figure 4.3: Number of cycles to failure in samples tested to a maximum load of 40 N (n=10). OCA-containing specimens underwent approximately two times as many cycles prior to failure at this lower load level. 111

Figure 4.4: The reference bending strengths for each sample type are depicted in (A) (n=10). The fatigue test results as applied stress versus the number of cycles to failure for samples tested after 4 weeks storage in Ringer's solution at 37 ºC are summarized in (B). 115

Figure 4.5: Compressive strength of individual capsules over storage time. Capsules were stored in air at RT and Ringer's solution at RT or 37 ºC (average ± SEM, n=3 with 3 replicates per group). Asterisks indicate significance between the RT and Ringer's 37 ºC samples. 117

Figure 4.6: SEM images of capsule morphology with exposure to (A) Ringer's solution at 37 ºC and (B) air at RT for 15 days of storage time. Note the increased shell thickness of the capsule stored in Ringer's solution when compared with the capsule stored in air. 119

Figure 5.1: (A) Rectangular specimens were prepared and (B) extracted into complete culture medium in a 50 mL conical tube. 134

Figure 5.2: Viability of MG63 cells following 72 h exposure to (A) control media, (B) undiluted extract prepared from unfilled and (C) filled bone cements. Green – calcein; blue – Hoechst 33342. 140

Figure 5.3: Viability of MG63 cells following 72 h exposure to (A) control media and media containing OCA extract diluted to (B) 50%, (C) 25%, and (D)10% using fresh medium. Green – calcein; blue – Hoechst 33342..... 141

Figure 5.4: Viability of MG63 human osteosarcoma cells after 72 h exposure to (A) PMMA bone cement and (B) OCA extracts (average ± SEM, n=4). Coverage by live cells in the positive controls, Cu and Loctite®, were significantly different from all treatment groups though significance is not indicated on the figures. 143

Figure 5.5: Proliferation of MG63 cells after 24 h exposure to (A) control media and undiluted extracts prepared from (B) unfilled and (C) filled bone cements. Green – EdU; blue – Hoechst 33342..... 145

Figure 5.6: Proliferation of MG63 cells following 24 h exposure to (A) control media and media containing OCA extract diluted to (B) 50%, (C) 25%, and (D) 10% using fresh medium. Green – EdU; blue – Hoechst 33342..... 147

Figure 5.7: Proliferation of MG63 cells exposed to OCA extract media diluted to 50% for (A) 24 h, (B) 48 h, and (C) 72 h. Note the recovery of proliferation between 48 and 72 h, suggesting the effects of OCA on MG63 cell proliferation may be transient. Green – EdU; blue – Hoechst 33342. 149

Figure 5.8: Proliferation of MG63 human osteosarcoma cells in response to growth in extract from (A,B,C) bone cement and (D,E,F) OCA after (A,D) 24 h, (B,E) 48 h, and (C,F) 72 h (average ± SEM, n=4). Proliferation of cells in the positive controls, Cu and Loctite®, were significantly different from all treatment groups though significance is not indicated on the figures..... 151

Figure 6.1: The structure of the 1,4-BD chain extender currently used in encapsulation procedures is shown in (A) while the structure of a proposed potential chain extender, 2-allyl-1,3-propanediol, is shown in (B)..... 167

Acknowledgements

I would like to thank my dissertation adviser, Dr. William Reichert, and the rest of my committee for the opportunity to work at Duke and for their guidance and encouragement throughout my graduate career. I would also like to acknowledge Ethicon, Inc. for their generous donation of OCA and specifically Errol Purkett for entertaining conversations and equipment training. Conversations with Matthew Novak and Dr. Steve Wallace are also gratefully acknowledged as they clarified the mysteries surrounding statistics. I would also like to thank Dr. David Katz and his lab for allowing me to use their equipment and hood space for capsule fabrication. Additionally, the staff at the Shared Materials Instrumentation Facility was very helpful for equipment training. I would also like to thank Dr. Ashley Black Ramirez, Dr. James Ogle, and Zachary Kean for their patience and allowing me to occupy space in their lab while fabricating polymers and Dr. Julie Albert for assistance with thin film fabrication.

I have had the distinct pleasure of mentoring several undergraduate and Master's students who assisted me with my research, specifically: William Chyan, Gregory Evans, Oriane Matthys, Sonia George, MS, and Vineela Gandham, MS. Lastly, I want to thank my fellow graduate students for their support, friendship, and for being part of some of best memories of my life; I cherish these relationships and am a better person for having met these amazing people.

1. Chapter 1: Background, significance, specific aims, and hypotheses

Some of the text, figures, and modified versions of the tables included in Chapter 1 were previously published in the February 2011 edition of the Journal of Biomedical Materials Research Part A. The full citation for the article is: Brochu, A. B. W., Craig, S. L. and Reichert, W. M. (2011), Self-healing biomaterials. J. Biomed. Mater. Res., 96A: 492–506. doi: 10.1002/jbm.a.32987. John Wiley & Sons Ltd. does not require permission for authors to reuse their own articles, but an optional grant of license can be obtained and is included in Appendix B.

1.1 Background and significance

1.1.1 Total joint replacements

1.1.1.1 Clinical need for and design of total joint replacements

In the United States, more than 16 million individuals are affected by some form of arthritis, the most common types of which are osteoarthritis (OA) and rheumatoid arthritis[1]. OA is a degenerative condition characterized by joint pain and mild inflammation associated with the mechanical failure of articular cartilage[1, 2]. OA is the leading cause of disability and functional limitation in adults[3] and more than 59 million cases are expected by the year 2020[1]. Primary treatments for arthritis are acetaminophen and non-steroidal anti-inflammatory medications such as Tylenol and Advil; physical therapy is also recommended to reduce pain and improve range of

motion in the affected joint(s). Injections of powerful steroids, such as cortisone, directly into the joint space are also used to temporarily reduce pain and inflammation[4]. However, none of these treatment options repair the cartilage damage and merely serve to manage the symptoms.

Total joint replacements (TJRs) have become the gold standard to manage the pain and cartilage loss associated with OA when the pain becomes unmanageable[5, 6]. Numerous joint replacements are clinically-approved, including those for the hip, knee, shoulder, ankle, wrist, elbow, and finger[7]. Replacements generally involve (1) a metallic endoprosthesis inserted into the boney tissue, (2) polymeric ultra-high molecular weight polyethylene (UHMWPE) articulating surfaces, and (3) an acrylic poly(methyl methacrylate) (PMMA) cement to anchor the prosthesis within the native tissue[8].

PMMA bone cement is a space-filling matrix that forms mechanical interlocks between the implant stem and the surrounding boney tissue[9, 10], serving to transfer loads from the prosthesis to the bone[11]. Bone cement consists of two components: (1) a low molecular weight PMMA powder containing a radiopacifier (e.g. barium sulfate) and an initiator (e.g. benzoyl peroxide) and (2) liquid methyl methacrylate (MMA) monomer. Mixing the two components *in situ* initiates an exothermic polymerization to yield a workable dough, which is applied to the implant and cures into a solid mass after the implant is inserted[8, 9].

While not all joint replacements are cemented, data from 2010 reports that 92% of primary total knee and 12% of primary total hip replacements performed in the United States utilized bone cement[12-14]. There are projected to be 332,000 hip, 719,000 knee, 40,000 total shoulder, 30,000 hemishoulder, and 5,000 elbow replacements per year by 2013[12, 15, 16]; nearly all of shoulder, hemishoulder, and elbow TJRs performed to date are cemented[15]. These numbers do not take into account the number of revision procedures performed each year.

By 2030, demand for primary hip replacement procedures is expected to increase by 174% in the United States[17, 18]; demand for primary knee replacement procedures is expected to be much higher, with a projected increase of 673% over the same time period[18]. These increases are primarily driven by the aging of the baby boomer generation and the obesity epidemic in the United States[19]. However, increased life expectancy and need for joint replacements at younger and more active ages will also play a significant role in the demand for these procedures[6, 20, 21]. Additionally, younger patients are considered at elevated risk for revision due to their higher activity levels in comparison with elderly patients. Approximately 18% of total hip arthroplasties and 8% of total knee arthroplasties performed annually in the United States are revision procedures, indicating failure of the primary replacement[22]. Revision procedures are associated with elevated risks of complications including infection, dislocation, venous thromboembolism, and mortality; their complexity is reflected by higher hospital costs,

longer length of hospital stay, and longer operative time when compared with primary procedures[22]. Moreover, the average lifetime of a revised prosthesis is significantly lower than that of a primary implant[23, 24]. Cement usage is more common in revision procedures to further stabilize the TJR in the event of osteolysis, the active resorption of bone matrix by osteoclasts, resulting from the primary replacement. As the prevalence of revisions increases[22], so will the number of cemented procedures.

1.1.1.2 Sources of failure observed in total joint replacements

Bone resorption, bone fracture, cement/bone separation, cement/prosthesis separation, microcrack formation in the cement, and the generation of wear debris from the articulating surfaces, metallic stem, and the bone cement itself serve to accelerate wear that often leads to loosening and subsequent failure of the implant[11, 18, 20, 25-30]. Aseptic loosening of TJRs is a disabling condition that generally affects patients more than 10 years after surgery; this loosening can result from factors such as inadequate initial implant fixation[31, 32], mechanical loss of fixation over time[33, 34], or biological loss of fixation resulting from osteolysis[33, 35-38]. While loosening can be attributed to various mechanisms, all are interconnected and serve to perpetuate the process that ultimately results in TJR failure and necessitates subsequent revision procedures.

Stress shielding results when the loads within a joint are redistributed following a TJR, ultimately decreasing the loads transmitted to the bone[35]. Shielding is due to the

mismatch in stiffness between the implant and the native bone[39]. Mechanical load stimulates new bone formation[39]; bone is resorbed as the physiological loads sustained by the bone decrease and new bone is not deposited, further exacerbating the issue of bone integrity around the implant[40]. While stress shielding contributes to implant loosening, it is rarely the isolated cause of failure but accelerates failure from other means[35]; even if shielding is not the primary cause of loosening, preservation of the native bone is extremely important to prolong the functional lifetime of the TRJ and improve the success of any subsequent revision procedure. Patient physical health also contributes to the functional lifetime of the implant; conditions such as osteoporosis or obesity can further compromise the success of a TJR[40]. As the initial mechanical fixation of the implant depends partially on the local bone mass and degree of osteolysis[35], stress shielding and osteoporosis both influence local bone density and contribute to the stability of implant fixation.

The biologic response to implant debris is complex and results from multiple factors; wear particles can be generated from all materials within the TJR including the bone cement, metallic stem, and polymeric load-bearing surfaces[33, 35, 39]. The core of the biological response that leads to osteolysis is activation of the receptor activator of nuclear factor-κB (RANK)/RANK ligand (RANKL) axis that enhances osteoclast recruitment and activity at the bone/implant interface, promoting osteolysis[36]. Studies with human macrophages have found that direct interactions between wear particles

and cells are sufficient to activate the osteoclastic signaling pathways that precede osteolysis[37]. Because wear particles are often resistant to enzymatic degradation, their continued presence in the joint space further exacerbates the cell response and continuously promotes osteolysis[35, 36, 41]. Macrophages, fibroblasts and osteoblasts release pro-inflammatory cytokines that directly and indirectly stimulate osteoclast development[35, 37]. Additionally, greater concentrations of wear particles have been associated with more aggressive osteolysis and subsequent aseptic loosening[42].

Implant loosening is the primary cause of TRJ failure, but other factors also influence TJR failure. Infections incurred during the surgical procedure occur in 0.3-2% of primary arthroplasties[43-45]; these infections result in complications such as discharging sinuses and scar tissue formation that produce debilitating patient pain[44] in addition to facilitating implant loosening. Chronic infection also triggers the foreign body response that results in encapsulation of the implant. Osteolysis brought on by infection also contributes to TJR failure but bone loss specifically from infection cannot be separated from that resulting from other mechanisms[44]. Several broad-spectrum antibiotics, including gentamicin sulphate, vancomycin chloride, and tobramycin, have been incorporated into bone cement to fight infection[46]; the costs associated with these additions is estimated to be more than $250 million/year in the United States alone[43].

1.1.1.3 Strategies to improve the functional lifetime of total joint replacements

Straightforward attempts to improve implant stability have focused on improving the fixation between the implant and the native boney tissue. The simplest solution is the use of PMMA bone cement to anchor the stem of the implant and transfer loads between it and the native tissue. As bone cement is considerably weaker than bone[11] and comes with its own set of challenges, researchers have proposed composite designs to improve the mechanical properties of the material; dispersed particulates and fibers have been investigated to increase the toughness, impact strength, and wear resistance of the PMMA by absorbing a greater fraction of the load, inhibiting pathways for crack propagation, and resisting void formation. However, in spite of a long history of development in load-bearing applications, very few composite devices have progressed to widespread clinical use[47].

Glass polyalkenoate cements, bioglass, various glass-ceramic compositions, antibiotic-containing cements[46], and calcium phosphate cements[48] have been investigated to minimize failure and promote integration at the bone/PMMA interface. Other techniques to improve TJR materials include modifying the implant stem with coatings of hydroxyapatite[39, 49-51] or silicate glasses[39] to stimulate bone adhesion; such coatings have also been used in combination with rough and/or sintered stem surfaces to facilitate interlocking with the tissue and promote bone ingrowth in the absence of bone cement[35, 40, 50-52].

In addition to improving implant-bone integration, therapeutic interventions have been investigated to target cells that contribute to osteolysis and subsequent aseptic loosening, such as osteoclast precursor cells and non-osteoclast precursor cells that are stimulated by debris to differentiate into osteoclasts. Direct inhibition of osteoclast differentiation has been investigated using molecules that bind to RANKL to inhibit bone loss, resulting in reduced osteolysis[37, 53, 54]. Strategies to locally inhibit cytokine production could also be used to mediate joint inflammation[36]. For example, strategies to reduce tumor necrosis factor (TNF) or block its receptors on osteoclasts have been investigated as treatments to prevent aseptic loosening[37, 55] by inhibiting the potent osteoclastogenic action of TNF-α[56]. Additionally, drugs such as bisphosphonates that are currently used to treat bone diseases such as osteoporosis have also been proposed to inhibit osteoclast function and induce osteoclast apoptosis[37, 57, 58].

Other strategies focus on the improvement of the properties of the implant materials themselves to reduce the generation of wear debris and resulting osteolysis rather than attempting to mediate it after the fact. Ceramics[33, 59] and highly polished metal heads[39] have been introduced in an attempt to minimize the generation of wear debris from UHMWPE surfaces in joint replacements. There is also significant interest in metal-metal and ceramic-ceramic TJRs[33, 39, 59]. To increase the wear resistance of titanium alloys commonly used in TJRs, nitriding processes such as plasma and laser nitriding as well as ion implantation have been used to enhance the tribological

properties of titanium and its alloys[60]. Variations in the alloy compositions have also been investigated to improve wear and corrosion resistance, decrease the modulus to approach that of native bone, and improve biocompatibility[39, 60-62].

1.1.2 Self-healing materials

1.1.2.1 What are self-healing materials?

Self-healing materials (SHM) are a rapidly emerging class of composites with applications primarily designed for use in the civil, mechanical, electrical, and aerospace industries. These materials hold the potential for significantly extending functional lifetimes by preventing and repairing failures caused by accumulated microdamage. To date, the majority of research conducted on self-healing bulk materials has employed composites, adhesives, and cements intended for traditional engineering applications[63-70]. One of the most broadly reported self-healing schemes is that pioneered by White and Sottos et al. in which a polymer matrix is co-embedded with a catalyst and microcapsules containing a reactive healing agent (Figure 1.1). Once encountered by a propagating microcrack, the microcapsule shell ruptures, releasing the healing agent into the crack plane and exposing it to the catalyst embedded in the matrix. *In situ* curing of the healing agent ensues, halting crack propagation[47, 63-65, 71-73].

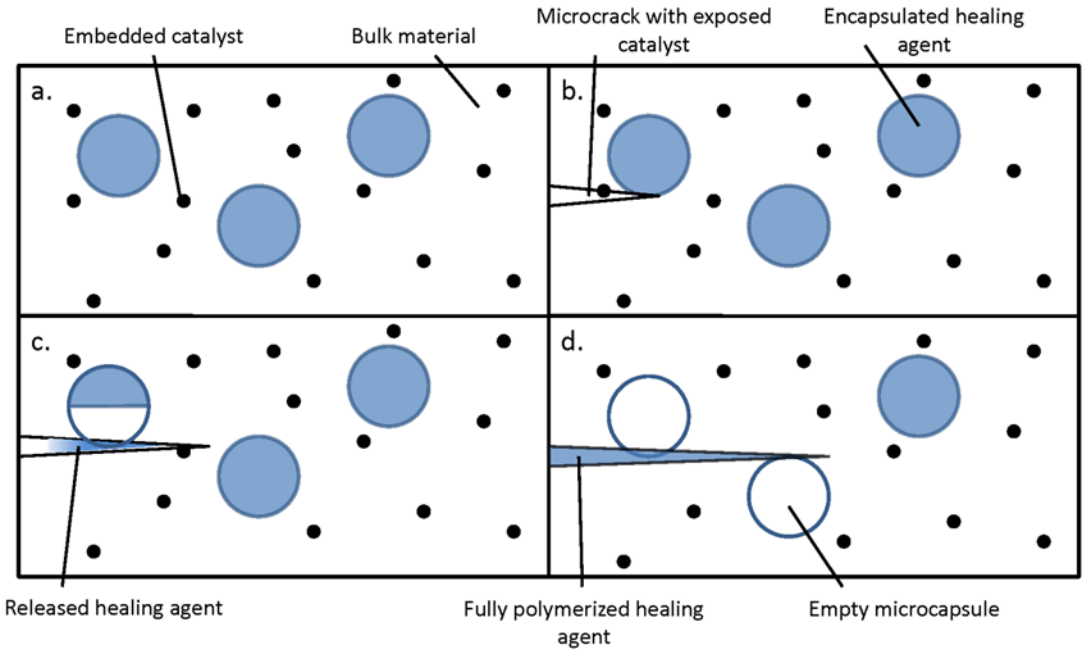

Figure 1.1: Self-healing material scheme[47]. Adopted from[65].

Although this field has been steadily growing over the past 10 years, very little discussion of extension into biomaterials has taken place and none of the existing systems employ materials acceptable for *in vivo* applications. Table 1.1 summarizes some of the many systems proposed for SHM using the matrix repolymerization material design approach[47].

Table 1.1: Summary of healing agents, catalysts, and matrix materials studied for applications in SHM based on the matrix repolymerization scheme

Matrix material	Healing agent	Catalyst	References
Vinyl ester	HOPDMS and PDES (phase separated in matrix)	DBTL in PUR microcapsules	[71, 74]
EPON 828 cured with DETA	DCPD in UF capsules	Grubbs' catalyst in paraffin wax microspheres	[75, 76]
PMMA	DCPD in UF capsules	Grubbs' catalyst	[77]
EPON 828 cured with DETA	EPON 862 or 828 diluted with cholorobenzene, phenylacetate, ethyl phenylacetate in UF capsules	None	[66]
EPON 828 cured with DETA	DCPD in UF capsules	Grubbs' catalyst	[63-65, 78, 79]
YD-115 cured with KH-816	DCPD in UF capsules	Grubbs' catalyst	[78, 79]
YD-115 cured with KH-816	ENB in UF capsules	Grubbs' catalyst	[78, 79]
Silver particle ink lines on a PUR substrate	Silver ink in acrylic capsules	Encapsulated hexyl acetate that, when released, dissolves acrylic capsule to release silver ink	[80]
EPON 828 cured with DETA	EPON 815C in UF capsules	EPIKURE 3274 polyamine	[81]

1.1.2.2 Challenges for extension into biomaterials

Numerous implants fail following the accumulation of damage and are potential candidates for the introduction of self-healing to biomaterials. However, as there are stringent requirements for materials used in clinical applications, any SHM proposed for a biomedical application would need to be assessed from mechanical, biocompatibility, and self-healing perspectives. There are several concerns associated with SHM based on the repolymerization scheme depicted in Figure 1.1; these concerns along with some specific to biomaterials are summarized in Table 1.2[47].

Table 1.2: Concerns associated with SHM and their extension to biomaterials

General Concerns	References
Healing agent/catalyst consumption	[63, 69]
Healing agent stability in microcapsules	[64-66]
Microcapsule shell process survivability	[65, 66]
Effective release of healing agent from capsule	[65, 72]
Capsule/matrix interfacial bonding	[65, 66, 72]
Healing agent viscosity and volatility	[66, 78, 79]
Uneven healing agent/catalyst distribution or ratios within matrix	[64, 69, 75, 82, 83]
Concerns Specific to Biomaterials	
Healing may require times not feasible with cyclically-loaded implants	[64, 71]
Complex and variable loading patterns may limit healing opportunities	[47]
Functional lifetime of encapsulated healing agent	[47]
Toxicity of the healing agent/catalyst system	[47]
Surgeon ease-of-use dictates adoption of material	[47]

Due to its long history of use and significant potential for increased future use, lack of post-polymerization modifications, and need for improvement, the development of a self-healing PMMA bone cement is a very attractive option for the first self-healing biomaterial designed with the aforementioned embedded capsule and catalyst approach[47, 84]. The projections and statistics included in section 1.1.1.1 indicate there are a significant number of potential beneficiaries of any steps taken to improve existing bone cement and extend implant functional lifetime.

1.1.2.3 Strategies commonly used to assess self-healing materials

Tapered and width-tapered double cantilever beam (TDCB and WTDCB, respectively) testing protocols are currently the literature standards used to assess the healing efficiency of existing systems in response to controlled crack propagation. TDCB testing determines mode I fracture toughness (K) and the geometry is designed such that the profile of the taper provides a constant value of K over a desired range of crack lengths[85]. The WTDCB geometry has been used to investigate the healing of delamination and thin film failures and is similarly designed so that the energy release rate remains constant over a desired range of crack lengths[64]. Fracture specimens of each type are tested under displacement control, applying a vertical load to induce crack propagation within a grooved centerline region of the specimen[64, 85].

Typically, the healing efficiency of a SHM is determined by testing the "virgin" specimen until a crack propagates through the center of the material; the separate pieces are reapposed to allow the healing agent to react and bond the surfaces together and the "healed" specimen is then tested again. The most desirable feature of TDCB and WTDCB specimens is that the geometries exhibit a linear relationship between critical load (P_C) and fracture toughness independent of crack length, allowing the healing efficiency (η) to be expressed as show in Equation 1[65, 85]:

$$\eta = \frac{K_{healed}}{K_{virgin}} = \frac{P_{C_{healed}}}{P_{C_{virgin}}} \quad (1)$$

While this equation holds for both geometries, the two methods have several distinctions. For example, each TDCB sample must be molded separately whereas numerous WTDCB samples may be machined from one larger sheet of material. TDCB testing has been used to assess the healing efficiency of numerous systems[65, 74-76]; however, the WTDCB geometry is limited to describe delamination fracture toughness[64] and self-healing for thin adhesive films[86].

Most studies utilizing these geometries to investigate healing efficiency have induced crack propagation through a single, continuously applied load[65, 74-76]. However, given that SHM are designed to prevent accumulated damage, their healing efficiency under cyclic loading has also been investigated[86-89]. Brown et al. reported that when healing agent was released into the crack plane of a cyclically-loaded TDCB specimen it

polymerized to form a polymer wedge, generating a crack tip shielding mechanism[87, 88]. This shielding wedge resulted in temporary crack arrest and extended the fatigue lifetime by 20 times. Hydrodynamic pressure crack-tip shielding due to viscous flow was also found to retard crack growth[87], indicating that the initiation of healing agent polymerization could act to slow crack growth before full polymerization and subsequent polymer wedge formation. The forces required to squeeze a viscous fluid from the crack plane during unloading provided crack-tip shielding.

While TDCB and WTDCB tests currently provide valuable information about the healing efficiency of some systems, these methods introduce very large defects that are not representative of damage likely to be sustained *in vivo*. A more clinically-relevant and informative procedure would involve assessing the healing capabilities of a self-healing bone cement system under *in vivo* conditions to repair microdamage.

1.1.3 Characterization of PMMA bone cement

1.1.3.1 Determination of various mechanical properties

Several protocols for PMMA testing have been developed over its long history of usage in biomaterials. The total loading is a mixture of compressive, bending, tensile, shear, and torsional forces[90] and as such, procedures to determine the mechanical properties involve the application of various static or dynamic stresses.

1.1.3.1.1 Compression testing

A material's ultimate compressive strength (UCS) is the maximum stress it can withstand before failure under compression. ASTM F451 describes compressive testing protocols; it requires the time between the mixing of the cement and the measurement of the compressive strength be no more than 24 ± 2 h, with tests performed at 23 ± 2 ºC and 50 ± 10% relative humidity. Deformation is applied at a cross-head speed of 20-25.4 mm/min. Failure load is determined as the load at the 2.0% offset, upper yield point, or fracture, depending on which occurs first. At least five samples must be tested and the minimum acceptable compressive strength is 70 MPa[91].

1.1.3.1.2 Tensile testing

The ultimate tensile strength (UTS) is the maximum stress a material can withstand before failure under tension. ASTM D638 describes a static, uniaxial tensile test applicable for polymeric materials and requires at least 5 samples be tested at 23 ± 2 ºC on any universal testing machine. Prior to testing, the specimens must be measured within 5 mm of each end of the gage length to confirm cross-sectional area. The specimen is placed between the grips of the testing machine and tightened evenly and firmly to prevent slippage during the test but without crushing the sample[92]. An extension rate of 5 ± 1 mm/min is used to deform the samples. Though there is no minimum acceptable UTS dictated by standards, commercial bone cements have literature-reported values ranging from 25-70 MPa[21, 90, 93].

1.1.3.1.3 Bending testing

Bending is a combination of tensile and compressive loading and is therefore a more realistic test of the bone cement's properties *in vivo*. ISO 5833 describes a four-point bending protocol to determine the bending strength (B) and modulus (E) of materials. The bending modulus is a ratio of stress to strain of the material within the elastic range characterizing the relative stiffness of the material[90]. ISO 5833 requires the time between the mixing of the cement and the measurement of the bending strength and modulus be no more than 24 ± 2 h with tests performed at 23 ± 1 ºC. The inner loading points are separated by 20 mm and the outer loading points separated by 60 mm. A cross-head speed of 5 ± 1 mm/min is applied on the inner loading points and the deflection of the specimen measured as a function of the applied force; the testing is continued through specimen failure. At least five samples must be tested and the minimum acceptable B and E of bone cement are 50 and 1800 MPa, respectively[94].

1.1.3.1.4 Fracture toughness testing

Fracture toughness is a measure of a material's ability to resist unstable crack propagation; crack initiation and propagation rates contribute to this property. Fracture toughness can be determined using a variety of notched specimen types, such as TDCB samples; these samples are tested 24 ± 2 h after fabrication at 23 ± 1 ºC under applied loads at various speeds. The variation of the testing geometries and protocols used results in literature-reported values ranging from 0.88-2.58 MPa $m^{1/2}$ [11, 95-98].

1.1.3.1.5 Fatigue testing

Long-term strength under alternating loads determines the durability of bone cement; therefore, fatigue testing provides information about the reliability of the cement for *in vivo* applications[99, 100]. If applied a sufficient number of times, the stress required to produce fatigue failure is generally much lower than that required to fracture the material under a single application[101]. A variety of procedures can be used to characterize the fatigue behavior of PMMA, including: four-point bending testing following ISO 5833, pure tensile testing following ISO 527, and uniaxial compression-tensile testing following ASTM F2118[90]. In each of these tests, sinusoidal cyclic loading is applied until specimen failure or runout at a predetermined number of cycles. However, due to the simplicity of the four-point bending testing configuration described in ISO 5833 and the complexity of the preparation of samples following ASTM F2118, four-point bending testing is the preferred method of fatigue testing[90, 99, 100]. A protocol and set-up identical to that used for bending testing is followed.

Five specimens must be tested to bending failure to determine the quasi-static strength of the samples and to establish the average strength as a reference value. During fatigue studies, specimens should be submitted to cyclic loading at a physiologically-relevant frequency (i.e. 1-5 Hz[8, 102-105]) that is continued until failure occurs. Various load levels ranging from 35-90% of the reference value are selected as testing conditions and at least five samples are tested at each load level[94, 106]. Under load control, the upper limit of the applied cycling force is kept constant; the standard

does not specify a value for $R = \sigma_{min}/\sigma_{max}$, although values ranging from -1 to 1 have been used previously, depending on the test configuration[100, 105]. Tests should be performed under load control as physiological strain is almost exclusively dictated by force[99, 100]. Displacement-controlled protocols are easier to perform[99, 105], but are less accurate than load-controlled procedures and overestimate material lifetimes, subsequently under-rating the risk of failure[90, 99, 106].

1.1.3.1.6 Other testing procedures

Shear strength plays a role in the debonding sometimes seen at the implant stem-bone cement interface and is assessed following ASTM D732; impact strength is assessed using ISO 179, ISO 180, and DIN 53435. Because PMMA is a viscoelastic material, creep and stress relaxation may contribute to implant loosening[11, 90]; creep measurements are made using ASTM D2990.

1.1.3.1.7 Other considerations

The properties of bone cement vary widely depending on water absorption, preparation variations and subsequent porosity differences (hand versus vacuum mixing), sterilization protocols, composition variations and additives, temperature, strain rate, etc.[11]. For example, hand-mixing results in a more porous matrix, generally decreasing the overall strength[8, 11, 90, 106]. Variability in the preparation and testing protocols complicate cross-comparison of results[105]; however, for the purposes of this research, commercial and self-healing matrices will be manufactured under identical

conditions and therefore similar levels of variability are expected across the experiments.

1.1.3.1.8 Properties of PMMA bone cement

Commercial formulations of PMMA bone cement have widely varying properties based on the aforementioned factors; the ranges of values for several properties are summarized in Table 1.3:

Table 1.3: Properties of PMMA bone cement

Property	Reported value(s)	References
Ultimate tensile strength	25-70 MPa	[11, 21, 90, 93, 107]
Ultimate compression strength	66-103 MPa	[11, 108]
Bending strength	62-77 MPa	[90]
Young's modulus	1.36-3.07 GPa	[11, 107, 109, 110]
Fracture toughness	0.88-2.58 MPa $m^{1/2}$	[11, 95-97, 111]
Density	1.08-1.19 g/cm^3	[11]
Strain to failure	0.0086-0.01	[21]
Poisson's ratio	0.3-0.4	[112]

1.1.3.2 *In vitro* assessments of PMMA toxicity

Due to its extensive usage in biomaterials, PMMA has been thoroughly investigated for adverse biological effects. Primary concerns associated with PMMA-based bone cements include localized cell death due to the exothermic reaction of the MMA and leaching of residual monomer from the matrix[113]. An estimated 3-5% of the MMA remains 15 minutes post-polymerization and is reduced to about 1-2% over time as the residues are eliminated through the bloodstream[114, 115]. *N*,*N*-dimethyl-*p*-toluidine, which is present in small amounts (≤ 2% of the liquid component)[116] and initiates polymerization when it reacts with benzoyl peroxide, is very toxic at low concentrations and is able to inhibit protein synthesis and cause chromosomal mutations[114].

MG63 human osteosarcoma cells have been used in many biocompatibility studies [113, 114, 117-120] because they share numerous features with normal human osteoblasts including secretion of insulin-like growth factor, binding proteins, matrix metalloproteinases, and osteocalcin. Similar to undifferentiated osteoblasts, MG63 cells also synthesize collagen types I and III and have a low basal expression of alkaline phosphatase that is increased in response to 1,25-dihydroxyvitamin D_3[117, 121]. Furthermore, because they are transformed, MG63 cells are readily obtained in large numbers and are unlikely to show growth-related changes in antigen expression with increasing passages[118]. Other cell types, including fibroblast L-929 cells[117] and TE85

human osteosarcoma cells[121, 122], have previously been used to assess bone cement cytotoxicity, but MG63 cells more closely reproduce the qualities of human osteoblasts.

Numerous assays can be used to determine the viability of cells. The 3-(4,5-dimethylthiazolyl-2)-2,5-diphenyltetrazolium bromide[113, 117, 122-126] (MTT) assay, 3-(4,5-dimethylthiazol-2-yl)-5-(3-carboxymethoxyphenyl)-2-(4-sulfophenyl)-2H-tetrazolium (MTS) assay[122], neutral red assay[122], methylene assay[122], and calcein-acetoxymethylester (calcein-AM) studies[127] have all been used to investigate cell viability. These assays work in various ways but cell metabolic activity is generally detected through a response such as a color change or emergence of fluorescence.

Bone proliferation is commonly used as a marker for biocompatibility; techniques such as 5-bromo- 2′-deoxyuridine (BrdU)[124], 5-ethynyl-2′-deoxyuridine (EdU)[128], and propidium iodide (PI) staining[113, 114, 129] have been used to determine if cement leachables interfered with the progression of cells through the cell cycle. BrdU is a halogenated analogue of thymidine and is incorporated into cells that are actively synthesizing DNA during the period of BrdU exposure[114, 124, 130]. A fluorescein isothiocyanate (FITC)-labeled monoclonal antibody against BrdU can be used as a probe for BrdU incorporated into DNA. EdU is a nucleoside analog containing an alkyne that reacts with an azide in a copper-catalyzed reaction to form a covalent bond. These proliferation assays are reported to be more accurate and consistent than BrdU assays, without requiring DNA denaturation or harsh treatments[128]. PI binds by intercalation

to double-stranded DNA and RNA and when used in combination with RNase digestion, it serves as a probe for measuring cellular DNA content[114]; during the G_1 phase of cell proliferation, the DNA in a diploid cell is 2n and, following the successful replication of DNA during the S phase, cells in the G_2 phase are 4n, resulting in double the fluorescence intensity detected by flow cytometry.

1.1.3.3 Failure of PMMA bone cement

Bone cement is a brittle material that is weak in tension and strong in compression. The material has a low fracture energy through which cracks can propagate at stresses below the UTS[93]; however, it is susceptible to crack initiation and subsequent propagation resulting from the cyclic loading it experiences *in vivo*. Crack initiation is generally associated with regions of high stress intensity, such as inclusions, voids, and other microdefects. When the stress concentration at the crack initiation site exceeds the critical load P_c, propagation is initiated. The formation of microcracks causes debonding at the cement/bone and cement/implant interfaces as well as the generation of PMMA wear debris that contributes to chronic inflammation and osteolysis.

During cyclic loading, a material's resistances to crack initiation and propagation are strong determinants of fatigue strength and lifetime. It has been reported that in bone cement, resistance to unstable crack propagation is a more important characteristic

than resistance to crack formation[95] and *in vivo*, crack propagation behavior dominates over crack initiation behavior[30]. Crack growth rates previously observed during fatigue testing of PMMA range from 10^{-2} to 1 μm/cycle[30, 131]. Various groups have found that crack propagation rates are reduced in bone cement containing various fillers including radiopacifiers and carbon fibers[30, 131]. Prior research has demonstrated that propagation is slowed as a crack propagates from a brittle to ductile material[132]. Slower crack growth rates in studies of bone cements containing additives are attributed, at least in part, to the longer crack path required for propagation as well as the number of cycles required to transverse the distance of the additive. An decrease in the rate of crack propagation results increased fatigue life[30].

Intrinsic factors of the bone cement as well as its preparation techniques dictate the fatigue properties of the cured material[105]. Properties such as the composition of the bone cement, type of radiopacifying agent, and polymer molecular weight are intrinsic to the brand of bone cement and contribute to the fatigue properties of the material. Storage temperature, specimen fabrication and curing conditions, and mixing methods are also highly variable and dictate the fatigue properties of the resulting bone cement[105]. Some of these preparation techniques may not be appropriate or feasible for bone cement used clinically; for example, perfectly smooth samples are not representative of the bone cement seen at the bone and implant interfaces *in vivo*.

While microcrack formation contributes to implant loosening, PMMA is a viscoelastic material: creep deformation and stress relaxation may also affect the material and contribute to TJR loosening[11, 90]. Previous studies have found that bone cement subjected to 1% compressive strain showed stress relaxation by 24% within 8 h[11, 133]. Creep deformation of bone cement in response to an applied stress of 10 MPa was also investigated; within the first 24 h, the creep strain varied between 55-70%[133]. Deformation of the cement mantle facilitates debonding at the cement/bone and cement/stem interfaces to contribute to loosening.

In addition to the loosening caused by microcrack formation within the bone cement, the generation of these cracks also releases PMMA wear debris. Wear particles represent loss to the original implant material and their presence is problematic as it facilitates wear particle-induced osteolysis and contributes to third body wear mechanisms within the TRJ[35]. Cement mantle defects have also been shown to act as preferential access pathways for wear debris, enabling the debris to infiltrate the articulating space to further accelerate UHMWPE wear; this debris responsible for the formation of granulomatous tissue that contributes to implant loosening, as discussed previously[134].

1.1.3.4 Biomimetic assessments of PMMA bone cement

1.1.3.4.1 Ex vivo fatigue testing

In addition to PMMA fatigue analyses utilizing simple specimen geometries and loading patterns, a variety of testing set-ups and modified protocols have been proposed to examine the behavior of bone cement in contact with a cyclically-loaded metallic stem[34, 38, 135-140]. These procedures allow for analysis of failure at the cement/stem and cement/bone interfaces, which serve as initiation sites for failure *in vivo*. Reported systems vary drastically, from tensile loading of metal rods in contact with stationary bone cement[38] to complex devices that simulate the damage that occurs during gait and stair climbing[135, 140].

Several investigators have examined simplified systems to mimic the cement interfaces in TRJs by applying a load to a metallic rod encased in bone cement[38, 136, 137]. Raab et al. used a cylindrical shear specimen to investigate fracture formation at or near the cement/metal interface[38]; the metal was inserted into a mass of bone cement that cured around it. The interfaces demonstrated fatigue properties that were far inferior to the fatigue properties of bulk bone cement, particularly following 30-60 d storage in physiological saline at 37 ºC[38].

Other groups employed strategies that are combinations of more complex loading and specimen geometry. For example, Jeffers et al. utilized a simple modified implanted femoral geometry surrounded by bone cement and polyurethane foam to mimic the native bone tissue to investigate creep and cracking of the bone cement[34]; this

model enabled real-time observation of crack formation in the cement mantle. In their system, a load horse applied joint reaction and abductor forces while a sinusoidal compressive force was applied to the head of the horse to mimic gait. The metallic stems were either bonded to the bone cement or fabricated such that the stems were in contact with the bone cement but not bonded with it. Catastrophic cement mantle fracture occurred in all unbonded samples at the distal end of the stem; however, dye penetrant analyses revealed only microcracks with the use of a grit-blasted stem bonded to the bone cement and no catastrophic damage was observed[34].

Race et al. examined crack formation resulting from the cement/stem interface, cement/bone interface, and voids utilizing a custom-built stair climbing fixture in which cadaveric femora implanted with commercial hip stems were tested. The system was designed such that the load and a moment were applied via a cup cemented to the upper part of the fixture to mimic the femoral head and abductor muscle movements *in vivo*[135]. For the first 150,000 cycles, the load varied from 10-80% of the peak load to mimic normal gait and for the next 150,000 cycles, the load varied from 10-100% of the peak load to mimic climbing stairs. This study also recorded stem/cortex micromotion using steel reference spheres monitored by linear variable displacement transducers. They found that significantly more cracks were associated with the cement/bone interface than with the cement/stem interface and voids[135].

Given the number of factors that could be varied in these tests, comparison across such studies is difficult. The loading patterns, specimen geometry, implant surface preparation, conditioning time, mixing time and rate, cement type, testing conditions, pressure used during joining, and testing rates all contribute to the fatigue lifetime of the bulk PMMA and of its interfaces. The general consensus from these *ex vivo* studies is that failure at the cement interfaces dictates the overall success of the implant and that appropriate *ex vivo* testing is crucial to anticipate *in vivo* results.

1.1.3.4.2 In vivo animal models

Several animal studies have examined the *in vivo* responses to bone cement; these include studies investigating tissue response[141], the effects of wear debris on the immune response and subsequent osteolysis[56, 142], and load-bearing properties of new formulations to be used in bone defect repair[143, 144].

Allen et al. examined the tissue response to the *in situ* polymerization of a two-solution bone cement using a non-load bearing sheep model[141]. For their studies, an 11 mm diameter hole was drilled into the trochlear groove of the femur and the bone cement was injected into the void. A steel rod was inserted into the space to simulate the presence of a metallic stem. The tissue response following 12 weeks was assessed by quantifying histomorphometric parameters such as bone volume; the two-solution and commercial bone cements produced similar tissue responses, but this model did not consider the effects of loading on the material and on the body's response.

Other animal studies have investigated the immune response to TJR wear debris; these models attempted to investigate the *in vivo* response to wear debris without a load-bearing implant. Merkel et al. used a transgenic mouse model to examine the effects of TNF-α on osteolysis. Two types of transgenic mice were used: one in which the p55 TNF receptor gene has been deleted and one in which both the p55 and p75 TNF receptor genes had been deleted. PMMA bone cement particles were placed under the external calvarial periosteum in direct contact with the sagittal aspects of both temporal bones for 7 d. Histological sections of the bones from wild type mice revealed the presence of a fibrous membrane with mononuclear cells containing phagocytosed PMMA particles. Additionally, this membrane contained numerous osteoclasts that resorbed the width of the calvarial bone in just 1 week. An inflammatory membrane was not generated in either transgenic mouse model, indicating that targeting TNF and/or its p55 receptor may reduce wear debris-induced osteolysis[56].

A load-bearing rabbit tibia model has been used to investigate repair of segmental bone defects[143, 144]. Okada et al. inserted commercial PMMA and bioactive bone cements into 15 mm defects in rabbit tibia; in this model, the biomaterial was cyclically-loaded throughout the course of the study. Animals were sacrificed 12 and 25 weeks post-implantation and sections of the native tibia removed for tensile testing. The tensile strength of the bone proximal to a defect repaired with a bioactive bone cement was higher than that of bone near a defect repaired with PMMA bone cement. A similar

study was performed by Hautamaki et al. in which a porous fiber-reinforced bone cement was implanted and subsequent bone ingrowth over 8-20 weeks was quantified[144]. These studies utilized load-bearing models, but the *in vivo* forces experienced by rabbits and humans make it difficult to draw comparisons.

While the *in vivo* cytotoxicity of PMMA has been thoroughly documented over its long history of use in cemented TJRs, characterizing the biomaterial response in an animal model is challenging but must be completed before new materials can progress to human testing. In the case of responsive materials (such as SHM), the response *in vivo* could depend on changes in the material following loading and static implantation may not provide the necessary and relevant information. Furthermore, to glean meaningful information from load-bearing orthopedic implant studies, large animals would more closely mimic the forces seen by TJRs in humans and therefore more accurately describe the *in vivo* material response to cyclic loading.

1.2 Specific aims and hypotheses

To assess the practicality of a self-healing PMMA biomaterial concept, we will examine the potential for encapsulating a biocompatible, FDA-approved water-reactive tissue adhesive, 2-octyl cyanoacrylate (OCA), commonly used as a substitute for sutures in surgeries[145]. By selecting a water-reactive monomer, the material design (Figure 1.1) is simplified because a matrix-embedded catalyst is no longer required. Water present

in vivo will polymerize OCA released from ruptured microcapsules. In general, work will focus on successfully encapsulating OCA, characterizing microcapsule properties, investigating the effects of the capsules on the bulk PMMA mechanical properties, assessing the healing efficiency of the incorporated system, and examining the response of cells to the capsule-embedded PMMA formulation. The specific aims and hypotheses of this dissertation are as follows:

Specific Aim 1: Encapsulate 2-octyl cyanoacrylate and thoroughly characterize the physical and mechanical properties of the capsules. Interfacial polymerization of toluene-2,4-diisocyanate (TDI) and 1,4-butanediol (1,4-BD) will be used to encapsulate OCA within polyurethane (PUR) shells. Various properties of the resulting capsules will be investigated, including their morphology, size distribution, shell thickness, thermal degradation behavior, individual compressive strength, contents, and adhesive functionality of the encapsulated agent. Once the capsules have been fully characterized, preliminary PMMA incorporation studies will determine capsule process survivability and their potential to be used in a self-healing bone cement application.

Hypothesis 1: An optimized interfacial polymerization procedure using TDI and 1,4-BD will produce robust PUR capsules containing OCA tissue adhesive retaining its reactivity.

Specific Aim 2: Characterize the static mechanical properties of a microcapsule-embedded PMMA bone cement when compared with an unmodified commercial formulation. Clinically-approved bone cements must undergo extensive testing to characterize their mechanical properties. Although this project aims to develop a self-healing bone cement, any new material proposed must also meet the standards set for commercial formulations. The effects of the inclusion of capsules on the bone cement will be investigated following various ASTM protocols. The capsule content will be incrementally increased so an accurate assessment of matrix strength as a function of capsule content can be determined.

Hypothesis 2: The inclusion of an optimal weight content of capsules will either (1) maintain static mechanical properties within acceptable limits or (2) increase the strengths to values greater than those seen with commercial bone cement formulations, particularly at low capsule wt%.

Specific Aim 3: Assess the bending properties and fatigue lifetime extension of the capsule-containing formulation when compared with the commercial material via load-controlled cyclic testing. To obtain reference values and optimal capsule content for fatigue specimens, the bending strength as a function of capsule content will be measured. The effects of microcapsules on bulk matrix properties only represent one facet of the composite testing - the healing ability of the matrix must also be

characterized. Cyclic loading will be applied to commercial and capsule-embedded specimens using the 4-point bending configuration described in ISO 5833 to determine if fatigue lifetime is increased through the incorporation of encapsulated OCA. The susceptibility of capsules to moisture intrusion will also be analyzed to determine the potential duration of the functional lifetime of the material.

Hypothesis 3: The inclusion of an optimal weight content of capsules will either (1) maintain the bending strength above acceptable limits or (2) increase the strengths to values greater than those seen with commercial bone cement formulations. The number of cycles to failure at load levels that are defined percentages of the reference strength will be increased in specimens containing encapsulated OCA, indicating repair of microcracks in response to cyclic loading.

Specific Aim 4: Perform preliminary evaluations of the *in vitro* cytotoxicity of the self-healing PMMA formulation in comparison with commercial formulations. In this aim, calcein AM and Hoechst 33342 staining will be used to assess viability of MG63 human osteosarcoma cells following exposure to commercial and capsule-embedded cement extracts. Bone proliferation is also a common marker for biocompatibility; therefore, EdU staining will be used to determine if cement leachables interfere with progression through the cell cycle. Response of cells to the healing agent alone (OCA) will also be investigated.

Hypothesis 4: Viability and proliferation of MG63 cells exposed to extracts from the capsule-embedded formulation will not be significantly different from the viability and proliferation of cells exposed to extracts from commercial PMMA bone cement formulations. OCA may affect cell viability and proliferation but only at concentrations much higher than what can be expected from this composite *in vivo*.

2. Chapter 2: Microencapsulation of 2-octyl cyanoacrylate tissue adhesive for self-healing acrylic bone cement

The text and figures included in Chapter 2 were previously published in the October 2012 edition of the Journal of Biomedical Materials Research Part B: Applied Biomaterials. The full citation for the article is: Brochu Alice BW, Chyan WJ, Reichert WM. 2012. Microencapsulation of 2-octylcyanoacrylate tissue adhesive for self-healing acrylic bone cement. J Biomed Mater Res Part B 2012:100B:1764–1772. John Wiley & Sons Ltd. does not require permission for authors to reuse their own articles, but an optional grant of license can be obtained and is included in Appendix B.

2.1 Chapter synopsis

This chapter describes the first phase of developing a self-healing acrylic bone cement: the preparation and characterization of polyurethane microcapsules containing a medical cyanoacrylate tissue adhesive. Capsules were prepared by interfacial polymerization of a toluene-2,4-diisocyanate-based polyurethane prepolymer with 1,4-butanediol to encapsulate 2-octyl cyanoacrylate. Various capsule characteristics, including: resultant morphology, average size and size distribution, shell thickness, content and reactivity of encapsulated agent, and shelf life are investigated and their reliance on solvent type and amount, surfactant type and amount, temperature, pH, agitation rate, reaction time, and mode of addition of the oil phase to the aqueous phase

are presented. Capsules had average diameters ranging from 74 to 222 μm and average shell thicknesses ranging from 1.5 to 6 μm. The capsule content was determined via thermogravimetric analysis and subsequent analysis of the capsules following up to 8 weeks storage revealed minimal loss of core contents. Mechanical testing of OCA-containing capsules showed individual capsules withstood compressive forces up to a few tenths of Newtons, and the contents released from crushed capsules generated tensile adhesive forces of a few Newtons. Capsules were successfully mixed into the poly(methyl methacrylate) bone cement, surviving the mixing process, exposure to methyl methacrylate monomer, and the resulting exothermic matrix curing.

2.2 Introduction

The terms "healing" and "biomaterials" are most commonly linked through the tissue response to the presence of an implant[146]. Ratner has coined the expression "biomaterials that heal" to describe biomaterials that actively promote wound healing as opposed to those aimed at passivity or inertness[147]. While the biology and chemistry of healing have significant impacts on biomaterial performance, biological healing does not address the physical repair of biomaterials that experience mechanical and chemical breakdown as they are subjected to loading and degradation effects *in vivo*. Developing synthetic biomaterials with the intrinsic ability to autonomously repair mechanical and

chemical damage is particularly important for implants that replace tissues also capable of self-repair[148, 149].

Self-healing materials are a rapidly emerging class of composites with applications intended for use in the civil, mechanical, electrical, and aerospace industries. These materials hold the potential for significantly extending material lifetimes by preventing and repairing failures caused by accumulated micro-damage due to microcrack formation. To date, the majority of the research conducted on self-healing bulk materials has employed composites, adhesives, and cements intended for traditional engineering applications[63-70]. The most broadly reported self-healing scheme is that pioneered by White and Sottos et al. in which a polymer matrix is co-embedded with a catalyst and microcapsules containing a reactive healing agent. Once encountered by a propagating microcrack, the capsule shell ruptures, releasing the healing agent into the crack plan and exposing it to the catalyst embedded in the matrix. *In situ* curing of the healing agent ensues, halting crack propagation[47, 63-65, 71-73].

The fixation of total joint replacements with acrylic bone cement is employed in hundreds of thousands of patients each year[18]. Poly(methyl methacrylate) (PMMA) bone cement is a space-filling matrix that forms mechanical interlocks between the stem of the implant and the surrounding boney tissue[9, 10]. Bone cement consists of two components: low molecular weight PMMA powder containing an initiator (e.g. benzoyl peroxide), and liquid methyl methacrylate (MMA) monomer. Mixing the two

components *in situ* forms a slurry that initiates polymerization yielding a workable dough that is applied to the implant and hardens into a solid mass after the implant is inserted into the boney tissue[9]. While broadly successful, cemented implants are subject to failure following prolonged exposure to the harsh environment of the body as well as the cyclic loading patterns seen *in vivo*. Microcrack formation and the generation of wear debris from both the articulating surfaces and the bone cement itself serve to accelerate wear that often leads to subsequent failure of the implant[18, 20, 25-28].

Due to its long history of use, lack of post-polymerization modifications, and need for improvement, the development of a self-healing PMMA bone cement is a very attractive option for the first self-healing biomaterial designed with the aforementioned embedded capsule and catalyst approach. However, none of the existing self-healing systems are suitable for *in vivo* deployment due to reagent toxicity and/or inability to cure under aqueous conditions. The production of a clinically acceptable PMMA-based acrylic bone cement containing a microencapsulated non-toxic healing agent is a logical starting point.

2-octyl cyanoacrylate (OCA) tissue adhesive is water-reactive, FDA-approved, and currently employed in sutureless surgeries and external wound closure systems[47, 145] and is therefore a strong candidate for the biocompatible monomer healing agent in a self-healing biomaterial. By selecting OCA as the healing agent of interest, the aforementioned self-healing material design is simplified because no catalyst will need

to be embedded within the material matrix; the released cyanoacrylate would be polymerized by ambient moisture permeating the bone cement matrix from the surrounding tissue.

Polyurethane (PUR) is widely used in biomaterials due to its blood compatibility and its ability to be engineered to have a wide range of mechanical properties through the selection of various soft and hard segments[150-153]. Polyurethane capsules have previously been generated via interfacial polymerization of a variety of isocyanates and polyols using numerous emulsion characteristics. Encapsulated agents include pesticides[154, 155], oils and organic solvents[156-161], drugs and proteins such as ibuprofen, ovalbumin, and isoniazid[162-164], and various dyes[152]. Microcapsules of toluene-2,4-diisocyanate (TDI)-based polyurethane have been shown to be both robust and capable of containing a water-reactive monomer for self-healing applications[165], which we found attractive.

In the current study we present the first phase of the development of a self-healing PMMA bone cement: the encapsulation of OCA within PUR microcapsules. The average capsule size and size distribution, capsule shell thickness, content and reactivity of encapsulated agent, and shelf life of these capsules were studied and preliminary experiments have been performed to incorporate these capsules into a bone cement matrix to assess their process survivability for future testing of a biocompatible self-healing composite.

2.3 Experimental section

2.3.1 Materials

Unless otherwise specified, materials were obtained from commercial suppliers and used without further purification. OCA was generously donated by Ethicon, Inc., Raleigh, NC 27616. Acetone, methyl ethyl ketone (MEK), diethyl ketone (DEK), methyl isobutyl ketone (MIBK), and cyclohexanone (Sigma Aldrich) were used as solvents and TDI and 1,4-butanediol (1,4-BD) (Sigma Aldrich) were used to synthesize the polyurethane prepolymer (pPUR) following the protocol outlined by Yang et al[165]. Pluronic F-68 (Sigma Aldrich) was used as a surfactant. Para-toluenesulfonic acid monohydrate (Sigma Aldrich, PTSA) was added to the organic phase as a monomer stabilizer. Commercially available bone cement (Biomet Cobalt G-HV High Contrast bone cement) was used in the preliminary bone cement matrix experiments.

2.3.2 Preparation of polyurethane prepolymer

A TDI prepolymer was prepared for use in the microencapsulation procedure by scaling up the protocol reported by Yang et al[165]. Briefly, TDI (109.25 g) was dissolved in cyclohexanone (750 mL) in a 3-necked round bottom flask. The mixture was suspended in an oil bath at 80 ºC and agitated with a magnetic stirrer. 1,4-BD (20.315 mL) was slowly added to the stirring TDI/cyclohexanone solution at a rate of 2 mL/min

and then the flask was purged with N_2 and allowed to react for 24 h. Following this reaction time, the mixture was distilled at 100 ºC under vacuum for 4-5 h to remove the excess cyclohexanone, water, and TDI from the system. A viscous yellow polyurethane prepolymer remained in the flask following the completion of this process. Gel permeation chromatography analyses were performed with a Varian Prostar Model 210 pump, a Varian Prostar Model 320 UV/Vis detector set to 254 nm detection, a Wyatt Dawn EOS multi-angle light scatterer, Wyatt QELS (quasi-electric light scattering), Wyatt Optilab DSP Interferometric Refractometer (RI), and a series of two Agilent Technology PL gel columns (7.5 X 300mm, 1 79911GP-503 (10^3 Å) and 1 79911GP-504 (10^4 Å)) in tetrahydrofuran at 22 ºC. Molecular weights were calculated using a dn/dc value of 0.108 mL/g calculated from solutions of known concentration using the dn/dc calibration mode of the Wyatt Technology ASTRA software version 5.3.2.16. The polydispersity index of the prepolymer was found to be 1.23, which was comparable to the value of 1.33 reported by Yang et al[165].

2.3.3 Preparation of microcapsules

At room temperature, Pluronic F-68 surfactant (1.84 g) was dissolved in deionized water (90 mL) in a 250 mL beaker. The solution was agitated for 1 h with a digital mixer (VWR PowerMax Elite Dual-Speed Mixer) before beginning the

encapsulation procedure. The aqueous phase was suspended in a hot water bath and heated to 40 ºC prior to the addition of the organic phase and chain extender.

To prepare the organic solutions, the pPUR (3 g) was dissolved in MEK (10 mL) at room temperature. OCA (4 mL) was dissolved in MIBK (8 mL) separate from the pPUR solution. PTSA (1%) was dissolved in the MIBK phase to further stabilize the OCA monomer. The pPUR and OCA solutions were added simultaneously to the aqueous phase but not mixed prior to this addition. After the organic and aqueous phases were combined, 1,4-BD (3 mL) chain extender was added dropwise to the stirring mixture via a syringe to form the segmented PUR shell material consisting of hard TDI-based segments and soft 1,4-BD segments. After a reaction time of 2 h, the agitator was switched off, the suspension of microcapsules rinsed with deionized water, and vacuum filtered.

2.3.4 Characterization of microcapsules

2.3.4.1 Capsule morphology, size, and shell thickness

A vacuum sputter coater (Denton Desk IV) was used to deposit a 10 nm layer of gold onto the microcapsule samples for scanning electron microscope (SEM) imaging. The surface morphology of the capsules was examined and average capsule diameters and shell thicknesses were also measured.

2.3.4.2. Characterization of capsule content and reactivity

Following the vacuum filtering and drying of the capsules, samples were taken and examined under a stereoscope (Bausch & Lomb). Capsules were sliced open with a scalpel and release of their liquid contents observed. Capsules were then crushed between two glass coverslips to qualitatively assess their bonding ability.

Thermogravimetric analysis (TA Instruments Q500 v6.7, TGA) was used to quantitatively analyze the capsule contents as well as the shelf life of the capsules. Small amounts (< 10 mg) of each sample were heated from 25 to 650 ºC at a rate of 10 ºC/min under N_2 environment until all of the material was vaporized. Comparisons were made between the decomposition rates of pure PUR shell, pure OCA healing agent, pure MIBK solvent, and capsules containing healing agent fabricated under various conditions to approximate the content of the capsules. Samples were also tested after various storage times to assess capsule shelf life.

2.3.4.3 Compression testing of individual microcapsules

The compressive strength of single microcapsules was measured using a dynamic mechanical analyzer (TA Instruments RSA-G2 solid analyzer, DMA). This approach was adapted from a procedure described elsewhere[165, 166] that employed a single capsule compression apparatus to examine the mechanical response of microcapsules. A single capsule was placed on the lower DMA compression plate and

the presence of a single capsule on the testing plate was verified by performing sample loading under a stereoscope. Displacement of the upper DMA plate was applied at a constant rate of 5 μm/s until shell compressive failure was observed.

2.3.4.4 Adhesion testing of crushed microcapsules

Microcapsules containing OCA were crushed between two aluminum plates (8 mm diameter) using a Tinius Olsen 1000 Universal Testing Machine. The contents were allowed to cure at room temperature for 1.5 h, thus gluing the plates together. The detachment force necessary to break the bond between the upper and lower plates was recorded. The adhesive forces measured for Loctite® Super Glue (ethyl 2-cyanoacrylate), monomer OCA, monomer OCA dissolved in MIBK, crushed empty capsules, and crushed empty capsules manually mixed with OCA were used as negative and positive controls.

2.3.4.5 Incorporation of capsules into a PMMA matrix

Biomet Cobalt G-HV High Contrast bone cement kits were obtained from the Duke University Medical Center. The powder component of the bone cement (10 g) was mixed with the liquid monomer (4.7 g) according to the manufacturer's instructions. PUR capsules (1 g) were added to the PMMA dough and vigorously stirred to disperse the capsules within the matrix material. The cement dough was shaped into small disks

and cured for 1 h. Small samples of the resulting composites were broken from the polymerized disks and analyzed under a stereoscope as well as via SEM to visualize the embedded capsules and estimate the fraction that remained intact.

2.4 Results

2.4.1 Reaction conditions

2.4.1.1 Organic solvents

Numerous solvents have been used in PUR microcapsule formation to encapsulate drugs, pesticides, oils, organic solvents, and various dyes[159, 160, 165, 167]. Several organic solvents were considered for the organic phase. The majority of these solvents were eliminated either because they failed to dissolve the pPUR (octanol, valeric acid, hexane, cyclohexane, butanol, toluene, dichloromethane, ethyl acetate, xylene, and ethyl ether) and/or had toxicity concerns (chlorobenzene, cyclohexanone, and tetrahydrofuran). Acetone and acetic acid were eliminated for being too miscible with water. Following these broad solvent eliminations, only MEK, DEK, and MIBK remained from the original group of potential solvents. MIBK was selected as the solvent for OCA and PTSA because its solubility in water is lower than that of MEK and DEK. However, the pPUR was not soluble in DEK or MIBK; therefore, MEK was selected as the solvent for pPUR.

2.4.1.2 Surfactants

Several emulsifying surfactants were also considered[162-164]. Tergitol NP-10, Myrj 52, Brij 52, Tween 20, Tween 65, sodium dodecyl sulfate, and poly(styrene-co-maleic anhydride) were eliminated because they were unable to create a stable emulsion, resulting in a solid mass of polymer. Poly(vinyl alcohol) resulted in the formation of capsules, but was eliminated because it appeared to react with the OCA monomer. Gum arabic was eliminated because it resulted in the formation of both capsules and solid spheres. Pluronic F-68 was selected because it consistently yielded spherical capsules of uniform size, density, and smooth surface morphology.

2.4.1.3 Temperature

Reactions carried out at room temperature (25 ºC) and 40 ºC produced capsules with similar spherical morphology and smooth capsule characteristics, however, increased temperature resulted in decreased average diameter and narrower capsule size distribution (342 ± 99 μm at 25 ºC versus 220 ± 74 μm at 40 ºC at 500 rpm agitation rate). Reactions performed at 70 ºC yielded a polymer mass within the reaction vessel rather than capsules. A reaction temperature of 40 ºC was selected because smaller capsules are more ideal when considering the effects of their inclusion on the mechanical properties of the matrix. Furthermore, the increased temperature should serve to enhance the rate of interfacial polymerization.

2.4.1.4 Controlling OCA reactivity

The reactivity of the OCA was reduced by adding 1% PTSA to the organic phase. PTSA dissociates into H^+ and a tosylate anion that is stable with the OCA monomer and should not initiate anionic polymerization. The addition of PTSA eliminated the formation of residual polymer seen on the blades of the agitator, enhanced the adhesion of capsules crushed between two glass slides, and resulted in capsules that were 15-25% smaller than those made without PTSA.

To minimize interactions between the OCA and the pPUR prior to encapsulation, separate organic pPUR and OCA solutions were prepared and added to the aqueous phase simultaneously at the same rate using 25 mL pipets. This mode of addition resulted in increased uniformity of the size, shape, and surface morphology of resulting capsules.

2.4.2 Effect of agitation rate

The average diameters of the microcapsules were measured for a range of agitation rates (impellor speed of 350-1100 rpm) while all other reaction conditions were held constant. Figure 2.1A is a double-y plot of microcapsule diameter and shell thickness as a function of agitation rate. Similar results were also reported for urea-formaldehyde capsules containing dicyclopentadiene[168] and PUR capsules containing isophorone diisocyanate[165]. Increasing agitation rate from 350 to 1100 rpm decreased

the average capsule diameter from 222 ± 56 μm to 74 ± 19 μm, and decreased the capsule shell thickness from 6.3 ± 2.6 μm to 1.6 ± 0.5 μm, although both appeared to reach asymptotes with increasing agitation rate (numbers given as average ± one standard deviation of at least 200 diameter and 15 shell thickness measurements). Figure 2.1B is an SEM image of microcapsules made at 700 rpm. The ratio of shell thickness to shell diameter also remained remarkably consistent from 350 to 1100 rpm, ranging from 0.01 to 0.02.

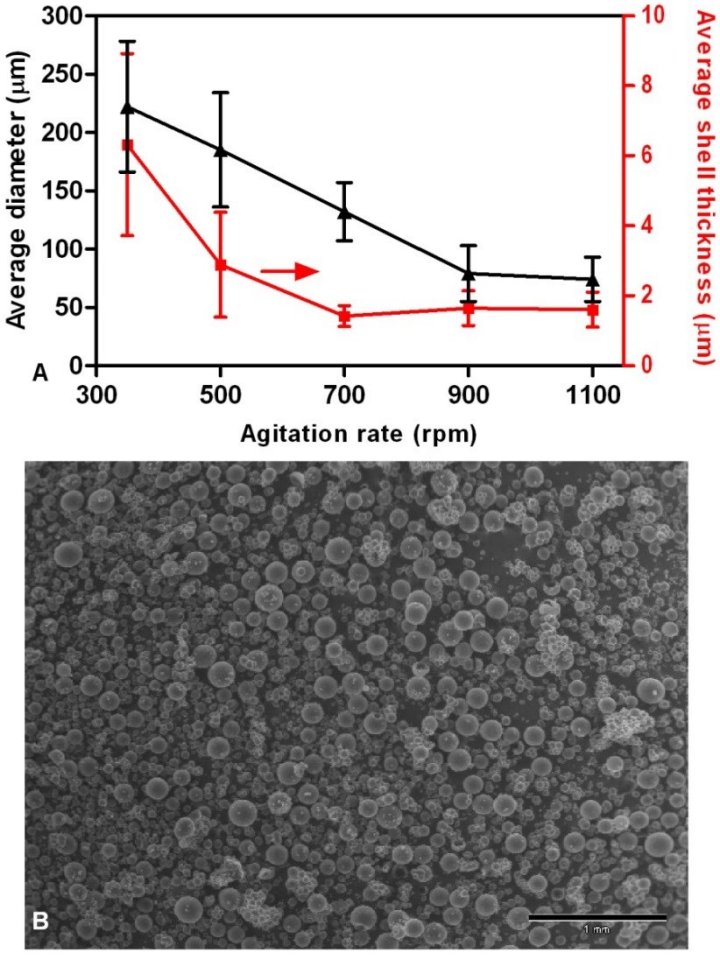

Figure 2.1: (A) Increasing agitation rate results in decreasing average capsule diameter and average shell thickness; (B) smooth surface morphology of microcapsules made at 700 rpm is clearly visible under SEM.

2.4.3 Capsule thermal properties

TGA was used to determine the composition of the OCA-containing PUR microcapsules by comparing the thermal properties of the intact microcapsules made at various agitation rates with samples of the pure OCA monomer, pure MIBK solvent, and pure PUR shell wall material. Figures 2.2A and 2.2B present the weight loss and derivative of weight loss for these samples at increasing temperatures. MIBK and OCA showed sharp vaporization curves, with samples completely vaporized by 78 ºC and 255 ºC respectively. The pure PUR shell wall material and OCA-containing microcapsules demonstrated more prolonged and multi-phased vaporization curves. The pure shell material rapidly loses about 50% of its weight between 200 ºC and 325 ºC while the remainder was lost more gradually between 325 ºC and 650 ºC. These two distinct phases may be attributed to the degradation of the PUR soft (1,4-BD) and hard (TDI) segments respectively.

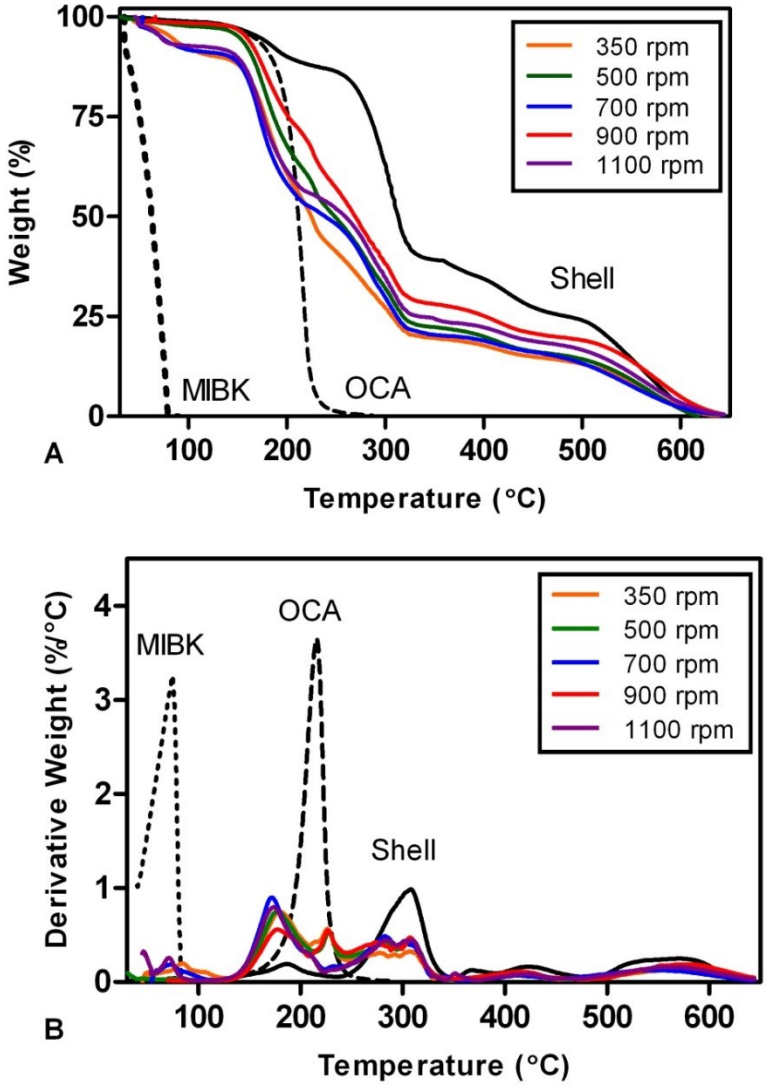

Figure 2.2: TGA results provide thermal degradation behaviors of capsules made under various conditions. The weight loss curves of capsules as well as pure samples of MIBK, OCA, and PUR shell material are shown in (A). Derivatives of the TGA data for capsules, MIBK, OCA, and PUR shell material are presented in (B). All experiments were conducted at a heating rate of 10 ºC/min under N_2.

The TGA graphs of the weight loss and derivative weight loss of OCA-containing microcapsules fabricated at agitation rates ranging from 350 to 1100 rpm are also shown in Figures 2.2A and 2.2B. Note that these traces exhibit the same multi-phasic behavior of the pure shell material, but are initiated at lower temperatures due to the presence of core OCA material. The weight percentages of the core and shell components in the various capsule types were estimated based on analysis of the TGA data as described previously[165]. Figure 2.3 shows the weight percentages of MIBK, OCA, and PUR shell for the intact capsules as a function of agitation rate. The OCA content in the core decreased from 58% in capsules made at 350 rpm to 46% in capsules made at 1100 rpm while the shell content increased correspondingly from 37% to 47%. Note: the presence of MIBK was consistently less than 7% in capsules made at all agitation rates.

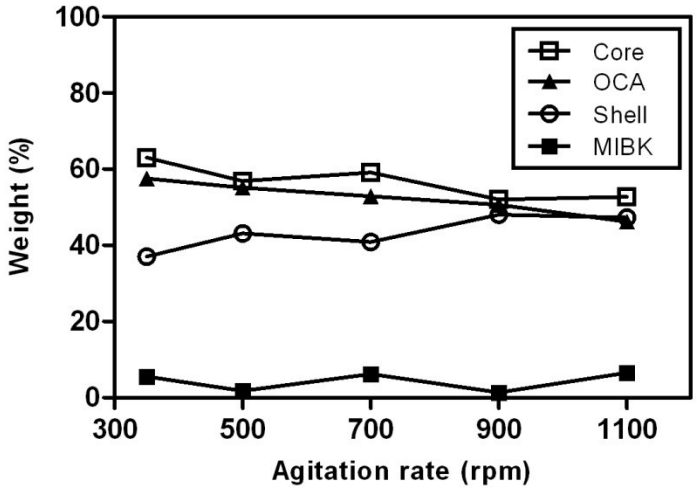

Figure 2.3: TGA data analysis was used to determine the various weight fractions of components of the microcapsules.

Figure 2.4 shows the TGA curves of OCA-containing microcapsules made at 700 rpm that were stored at room temperature for up to 8 weeks in sealed glass scintillation vials. A 4.9% reduction in the core content was observed over a 14 day storage period with a total reduction of 6.6% seen following 56 days of storage.

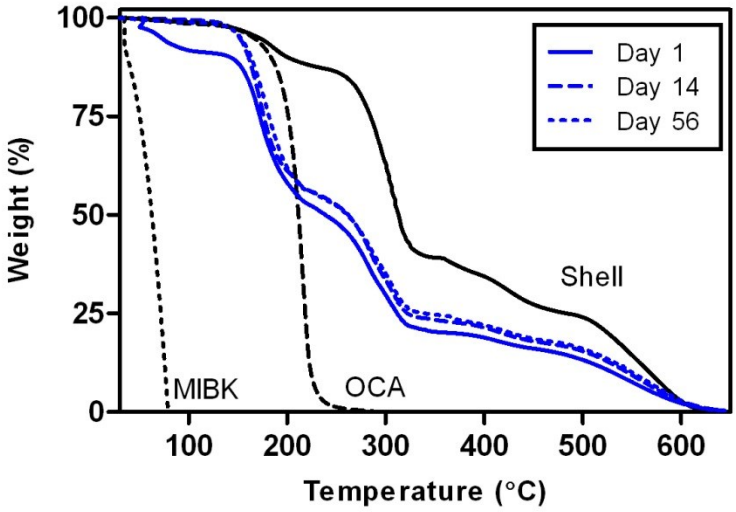

Figure 2.4: TGA weight loss curves of microcapsules made at 700 rpm following 56 days of storage.

2.4.4 Capsule mechanical properties

Stress-strain curves of individual OCA-filled microcapsules compressed at constant rate of 5 μm/s are shown in Figure 2.5. For all samples, the load increased monotonically in response to a constant compression rate until reaching failure at a maximum load. The inset is an SEM image of a typical compression-failed microcapsule post-fracture. The largest and thickest-walled microcapsules showed the greatest malleability, and the thinnest-shelled capsules demonstrated the lowest compressive strength.

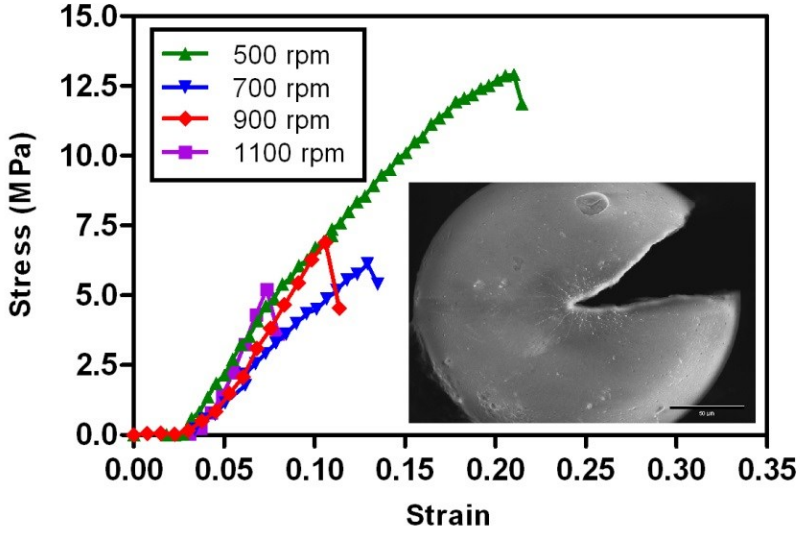

Figure 2.5: Stress-strain curves of microcapsules fabricated at various agitation rates. All compressions performed at a rate of 5 μm/s. Following capsule shell failure, the capsule was removed from the lower DMA compression plate, transferred to carbon tape on an SEM stage, gold-coated, and then imaged. (Inset) An SEM image of a capsules post-DMA testing where the failure plane is clearly visible; the original capsule diameter was 180 μm.

Normalizing the DMA data shown in Figure 2.5 to microcapsule equatorial cross-sectional area yields the compressive strengths listed in Table 2.1. As both the shell and liquid contents contribute to the mechanical properties of the capsules, variations in the percent fill of the capsules could play a significant role in the maximum loads that can be borne by those capsules and account for some of the observed variability. An increase in microcapsule stiffness with increasing compression rate used during testing was also observed (data not shown), possibly due to viscous contributions from the fluid-filled core. A decrease in the strain at failure was also observed in capsules fabricated at higher agitation rates.

Table 2.1: Mechanical properties of single capsules (data presented as average ± one standard deviation)

Agitation rate (rpm)	t (μm)	σ_{max} (MPa)	ε at failure (%)
500	2.88 ± 1.5	13.63 ± 1.44	20.8 ± 0.2
700	1.42 ± 0.3	6.71 ± 0.79	10.4 ± 3.1
900	1.65 ± 0.5	9.38 ± 1.95	10.6 ± 0.9
1100	1.60 ± 0.5	8.33 ± 2.25	8.1 ± 0.8

To quantify the adhesive properties of the encapsulated healing agent, capsules fabricated at 700 rpm were crushed between two aluminum plates. The detachment force necessary to separate the bonded upper and lower plates is presented in Table 2.2 for microcapsules along with values for the pure adhesive positive controls and empty capsule negative controls. Crushed empty microcapsules showed no detachment force, while crushed OCA-containing microcapsules exhibited nearly the same detachment force as crushed empty capsules manually mixed with adhesive, but considerably less detachment force than the adhesives alone.

Table 2.2: Detachment forces required to separate aluminum plates bonded by various cyanoacrylate (data presented as average ± one standard deviation)

Material	Detachment force (N)
Adhesives	
Loctite® Super Glue	546 ± 112
Pure OCA	108 ± 18
OCA dissolved in MIBK	40.8 ± 1.7
Crushed microcapsules	
Empty microcapsules	0 ± 0
Empty microcapsules + Loctite® Super Glue	7.6 ± 1.4
Empty microcapsules + OCA	5.1 ± 0.4
OCA-containing microcapsules	4.4 ± 0.8

2.4.5 Incorporation of capsules into the PMMA matrix

OCA-filled microcapsules fabricated at 500 rpm were added to Biomet Cobalt G-HV High Contrast bone cement and mixed, cast, cured, and fractured as described above. Figure 2.6A shows an SEM image of intact microcapsules distributed throughout the PMMA matrix. The crack plane of a PMMA specimen containing 30 wt% capsules is shown in Figure 2.6B; capsules fractured by the damage event are clearly visible in this plane as well as in Figure 2.6C, a magnified SEM image of a ruptured microcapsule. A scan of fractured planes indicates that roughly 40% of the capsules remained intact following the damage event.

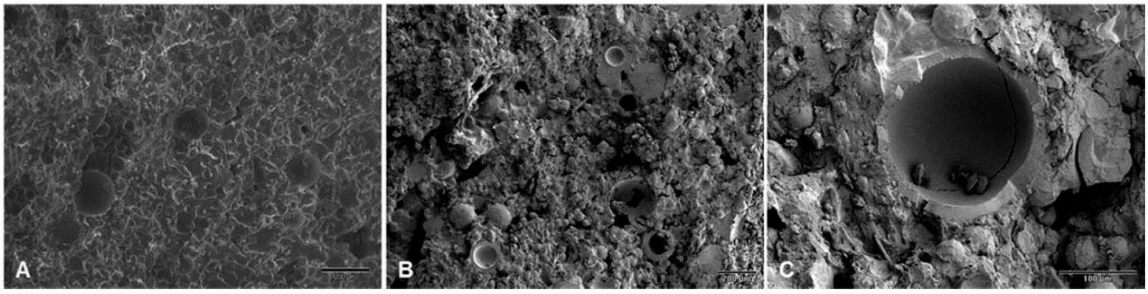

Figure 2.6: (A) An SEM image of PMMA bone cement containing intact microcapsules, (B) a PMMA fracture plane in which ruptured capsules are visible, and (C) a magnified image of a fractured microcapsule within the damage plane of the matrix.

2.5 Discussion

The OCA-containing PUR capsules described here represent a new embedded catalyst-free self-healing system with biomedical applications. The optimization of the encapsulation protocol relied on the identification of the proper emulsion conditions with respect to variables such as solvent, surfactant, and temperature. The primary concerns were improper solvent miscibility, insufficient stability of the o/w interface, interaction between the OCA and other emulsion components, and reaction temperature. While a number of options were considered and investigated, the final conditions using MEK and MIBK as solvents, Pluronic-F68 as the surfactant, and a reaction temperature of 40 ºC were selected.

The average diameter of the microcapsules was influenced by various factors including the fluid mechanics associated with the mixing apparatus, viscosity of the emulsion, the characteristics of the surfactant used, the agitation rate, and the temperature of the emulsion[165]. As the agitation rate was increased, the oil phase was emulsified into smaller droplets upon its introduction to the aqueous phase. Variability in capsule contents was observed though most can be attributed to variations in solvent content. Capsules were all tested day 1 post-fabrication and were thoroughly dried before all TGA procedures were performed so losses in weight at less than 78 ºC are most likely due to loss of MIBK rather than loss of surface moisture; the change in weight between 78 and 100 ºC was minimal in capsules made at all agitation rates,

suggesting little to no water is present in or on the capsules at day 1. Differences in the shell content of the capsules determined from TGA (Figure 2.3) correlated with the small variations in the ratio of shell thickness to capsule diameter for capsules made at higher agitation rates; i.e. the slightly higher t/d values for capsules made at 900 and 1100 rpm (0.02 versus 0.01) indicate that a larger weight percent of those capsules is composed of shell material.

It is interesting to note that at 110 ºC, the upper end of the PMMA polymerization exotherm[169], there is little mass loss seen in capsules with low MIBK content (500 and 900 rpm), indicating that capsules will survive the temperatures associated with matrix polymerization (Figure 2.2A). This observation was later supported by the successful incorporation of the capsules into a PMMA matrix (Figure 2.6). However, temperature is not the only factor that will come into play when assessing the process survivability of the capsules[47] and these observations merely confirm the feasibility of the material design concept.

To be implemented successfully, these capsules must retain their self-healing capability for a significant percentage of the lifetime of the implant. Even though TGA data showed a 4.9% decrease in core content over 2 weeks of storage time, this could be partially attributed to the diffusion and subsequent evaporation of MIBK through the capsule shell. At day 14, only 0.4% of capsule weight was lost prior to 78 ºC, bolstering the hypothesis that solvent evaporation is the main cause in the decrease of capsule core

content during that time frame. Testing of the capsules after 56 days dry storage indicates minimal change in the capsules over that time as a majority of the MIBK evaporated during the first 2 weeks of storage. The rightward shift in the TGA curve over time could be explained by slow polymerization of the encapsulated OCA monomer by infiltrating moisture. In a previous study, Yang et al. reported a loss in core contents of 7.9 and 8.6 wt% of PUR capsules containing isophorone diisocyanate following 3 and 6 months storage[165]. The decreases presented here are comparable to these rates of mass loss. Future TGA analysis will be performed to determine if the loss of core material continues to be marginal over longer storage times. Shelf life studies following capsule storage in water, an environment more relevant for this application, are also underway.

Other groups have reported single microcapsule compression testing using a modified load frame[165, 166] to gather information on the mechanical properties of the shell material. In the current study, compression testing showed the larger microcapsules to be more malleable; the compressive stress also decreased with decreasing shell thickness. The strain at failure decreased with increasing agitation rate and increasing PUR content, suggesting the OCA core contributes to the malleability of the capsules. Loads born by smaller microcapsules made at 900 and 1100 rpm were very similar (Figure 2.5) as expected given the similarities between the average diameters and shell thicknesses of microcapsules made at these rates.

Bulk polyurethane elastomers typically show MPa strengths and stiffnesses[170]; however, there is some uncertainty in the literature about how to calculate single microcapsule strength and stiffness. When normalized to equatorial shell cross-sectional area only, as reported previously[165], our microcapsules showed GPa strengths and stiffnesses, which are extremely high for an elastomer such as 1,4-BD-extended TDI. When normalized to the full equatorial cross-sectional area of the shell plus the core, the microspheres showed both MPa strengths and stiffnesses that are consistent with bulk elastomers. This makes sense since both the OCA core material and the shell contribute to microcapsule mechanical properties.

Detachment force studies were conducted to provide a quantitative measure of the adhesive capability of crushed OCA-containing microcapsules. Pure OCA tissue adhesive exhibited a detachment force of approximately 100 N that was 20% that of pure Loctite® Super Glue, indicating that OCA is a weaker adhesive. Dissolving OCA in MIBK, as used in the encapsulation process, weakened the average detachment force to approximately 40 N. Crushed OCA-containing microcapsules and crushed empty microcapsules mixed with OCA or Loctite® Super Glue exhibited detachment forces of 4-8 N. As expected, crushed empty microcapsules exhibited no detachment force.

The OCA-containing microcapsules clearly possessed bonding capability, albeit much weaker than the pure adhesive. Samples of crushed OCA-containing microcapsules removed from between the aluminum plates were composite patties of

bonded microcapsule fragments. This same patty formation was observed with crushed empty microcapsules manually mixed with OCA or Loctite® Super Glue; however, crushing of empty capsules resulted in an unbonded powder of broken PUR shell fragments. This indicates that the released or added adhesive was more effective in forming a composite of shell fragments and polymerized OCA than it was in bonding the aluminum plates together. It should be noted, however, that compression testing and detachment force testing are considerably different measures of microcapsule functionality and not necessarily a good indicator of how microcapsules may perform in halting the progression of microcracks within the PMMA matrix.

The next phases of this project will focus on (1) optimizing the microcapsule preparation protocol and investigating the effects of capsule inclusion on the bulk mechanical properties of PMMA, (2) characterizing the fracture toughness and self-healing functionality of the system, and (3) investigating the biocompatibility of the microcapsule-embedded bone cement compared with commercial formulations.

2.6 Conclusions

This chapter summarizes the first report of encapsulated OCA with adhesive capability, which supports the feasibility of our self-healing biomaterial design. OCA-containing PUR microcapsules possessing regular, spherical morphology were created via interfacial polymerization of a TDI-based polyurethane prepolymer with a small

chain diol. Capsules with average diameters ranging from approximately 75-220 μm were made at agitation rates of 350-1100 rpm. Average capsule diameter and shell thickness both decreased with increasing agitation rate; however, a consistent wall thickness to diameter ratio of 0.01-0.02 was observed throughout. Core content comprised more than half of the microcapsule volume at all agitation rates with little weight loss after 8 weeks of storage. Individual capsule compression tests showed that larger microcapsules were more malleable and microcapsule strength was influenced by shell thickness. Crushed OCA-containing capsules possessed bonding capability that was diminished due to the presence of capsule debris that interfered with the ability of the glue to bond between the two testing surfaces.

2.7 Chapter acknowledgements

The authors would like to thank Ethicon, Inc. for the generous donation of 2-octyl cyanoacrylate, use of their TGA, and conversations with Dr. William Daunch, Dr. Ibraheem Badejo, Andrés Rivera, and Errol Purkett. The authors also gratefully recognize the contributions of Duke University colleagues Dr. Stephen Craig, Dr. James Ogle, and Zachary Kean for polymer synthesis, Ashley Black Ramirez for GPC analysis, and Matthew Novak for assistance with TGA data analysis. This research was supported by NIH grants T32-GM8555 (ABWB) and R21 EB 013874-01 (WMR).

3. Chapter 3: Mechanical testing of acrylic bone cement embedded with microencapsulated 2-octyl cyanoacrylate

Sections of the text and figures included in Chapter 3 were recently accepted for publication in the Journal of Biomedical Materials Research Part B: Applied Biomaterials. The full citation for the article is: Brochu Alice BW, Evans GA, Reichert WM. 2013. Mechanical and cytotoxicity testing of acrylic bone cement embedded with microencapsulated 2-octyl cyanoacrylate. J Biomed Mater Res Part B 2013. This article does not yet have a publication date; however, John Wiley & Sons Ltd. does not require permission for authors to reuse their own articles, but an optional grant of license will be obtained as soon as one is available. Please note that this manuscript described the work for Specific Aims 2 and 4 and was in to two chapters for this dissertation to maintain parallel structure with the Specific Aims.

3.1 Chapter synopsis

The water-reactive tissue adhesive 2-octyl cyanoacrylate (OCA) was microencapsulated in polyurethane shells and incorporated into Palacos R bone cement. The tensile and compressive properties of the composite material were investigated in accordance with commercial standards and fracture toughness of the capsule-embedded bone cement was measured using the tapered double-cantilever beam (TDCB) geometry. Incorporating up to 5 wt% capsules had little effect on the compressive and tensile

properties of the composite, but greater than 5 wt% capsules reduced these values below commercial standards. Fracture toughness was increased by 13% through the incorporation of 3 wt% capsules and eventually decreased below the toughness of the capsule-free controls at capsule contents of 15 wt% and higher; fracture toughness remained within the literature-reported range for all capsule contents tested. Overall, the addition of lower wt% of OCA-containing microcapsules to commercial bone cement was found to moderately increase static mechanical properties of the material.

3.2 Introduction

Self-healing materials (SHM) are a rapidly emerging class of materials that prevent failure through the autonomous repair of microdamage *in situ*. One of the most broadly reported SHMs is the matrix repolymerization scheme pioneered by White and Sottos et al. in which a polymer matrix is co-embedded with catalyst and microcapsules containing a reactive healing agent[47, 63, 65, 71-73, 171]. Upon encountering a propagating microcrack, the microcapsule shell ruptures and releases the healing agent into the crack plane, exposing it to the catalyst embedded in the matrix. *In situ* curing of the healing agent ensues, halting crack propagation.

Numerous implants fail due to fatigue, wear, and environmental cracking following the accumulation of microdamage[27, 47, 172-175], marking these biomaterials as potential candidates for the introduction of self-healing biomaterials; however, there has

been very little discussion of extending SHM into biomaterials. Consequently, none of the existing SHM systems currently under development employ materials and reagents acceptable for *in vivo* load-bearing applications. Furthermore, no SHM have been tested under conditions that simulate the *in vivo* environment.

Due to its long history of use, ease of fabrication, and susceptibility to fatigue, acrylic bone cement is an attractive candidate for the first self-healing biomaterial based on the matrix repolymerization approach to self-healing[47, 77, 84, 171]. Acrylic bone cement is a space-filling matrix that forms mechanical interlocks between the metallic stem of a total joint replacement and the surrounding boney tissue[10], serving to transfer loads from the prosthesis to the bone[11]. Bone cement is a two-component thermoset consisting of a low molecular weight poly(methyl methacrylate) (PMMA) powder containing an initiator (e.g. benzoyl peroxide), and liquid MMA monomer. *In situ* mixing the two components initiates polymerization to yield a workable dough that is applied to the implant and hardens into a solid mass after the stem is inserted[8, 171].

The total loading experienced by bone cement *in vivo* is a mixture of compressive, bending, tensile, shear, and torsional forces[90] and as such, procedures to determine the mechanical properties involve the application of various static or dynamic stresses. Bone cements must adhere to static mechanical standards for tensile, compression, and fracture toughness testing before it is deemed suitable to investigate more biomimetic cyclic testing[90].

Although the overall project aim is to develop a bone cement capable of self-repair in response to damage, any new material proposed must also meet the standards required for the static mechanical properties of commercial formulations. We recently reported the microencapsulation of OCA in polyurethane shells as well as the successful distribution and fracture of the capsules embedded in a commercial bone cement matrix[171]. Among candidate cyanoacrylates, OCA is an attractive healing agent for a self-healing biomaterial because it is widely used clinically[145, 176] and because its use would eliminate the need for the incorporation of a potentially toxic catalyst into the matrix; the catalyst for OCA polymerization would be ambient moisture from the surrounding tissue.

The current study presents the first mechanical characterization of a biomaterial formulation consisting of OCA-containing microcapsules embedded in commercial PMMA bone cement. Incorporating up to 5 wt% capsules had little effect on the compressive and tensile properties of the composite, but greater than 5 wt% capsules reduced these values below commercial standards. Fracture toughness was increased by 13% through the incorporation of 3 wt% capsules and eventually decreased below the toughness of the capsule-free controls at capsule contents of 15 wt% and higher. Overall the addition of lower wt% of OCA-containing microcapsules to commercial bone cement was found to moderately increase static mechanical properties of the material.

3.3. Experimental section

3.3.1 Reagents

Unless otherwise specified, materials were obtained from commercial suppliers and used without further purification. OCA was generously donated by Ethicon, Inc., Raleigh, NC 27616. Methyl ethyl ketone (MEK), methyl isobutyl ketone (MIBK), and cyclohexanone (Sigma Aldrich) were used as solvents and 2,4-toluene diisocyanate (TDI) and 1,4-butanediol (1,4-BD) (Sigma Aldrich) were used to synthesize the polyurethane prepolymer (pPUR) following the protocol outlined by Yang et al. and reported by the authors previously[165, 171]. Pluronic F-68 (Sigma Aldrich) was used as a surfactant. Para-toluenesulfonic acid (Sigma Aldrich, PTSA) was added to the organic phase as a stabilizer for the OCA monomer. Commercially-available Palacos R PMMA bone cement (Zimmer) was used for all experiments reported herein.

3.3.2 Microcapsule preparation

Microcapsules were prepared and characterized as described previously[171]. Briefly, at room temperature, Pluronic F-68 surfactant (1.84 g) was dissolved in deionized water (90 mL) in a 250 mL beaker. The solution was agitated for 1 h with a digital mixer (VWR PowerMax Elite Dual-Speed Mixer) before beginning the encapsulation procedure. The aqueous phase was suspended in a hot water bath and heated to 50 ºC prior to the addition of the organic phase and chain extender.

OCA (4 mL) was dissolved in MIBK (8 mL) and pPUR (3 g) was dissolved in MEK (10 mL) separately at room temperature. PTSA (1%) was added to the OCA-MIBK solution to further stabilize the OCA monomer. The pPUR- and OCA-containing solutions were then added simultaneously to the aqueous phase but not mixed prior to this addition. After the organic and aqueous phases were combined, the 1,4-BD (3 mL) chain extender was added dropwise to the stirring mixture via a syringe to form the segmented PUR shell material consisting of hard TDI-based segments and soft 1,4-BD segments. After a reaction time of 2 h at an agitation rate of 700 rpm, the mixer was switched off and the suspension of microcapsules rinsed with deionized water and vacuum filtered. Capsules were air-dried prior to use in the following experiments[171].

3.3.3 Preparation of capsule-containing bone cement samples

The powder and liquid components of the bone cement were mixed according to the manufacturer's instructions[177], OCA-containing capsules were added to the slurry, and the resultant material was added to molds to form the desired specimen shape. Samples were cured in the molds for at least 1 h, released, and smoothed with 240 mesh silicon carbide to conform to the specified geometrical requirements. The wt% of OCA-containing capsules in the bone cement composites ranged from 0-40 wt% where the wt% of total particulates (OCA capsules plus PMMA powder) was held constant at 67 wt% in all specimens.

3.3.3.1 Tensile testing of capsule-embedded bone cement

Following ASTM D638, bone cement specimens were cured in "dog bone"-shaped silicone rubber molds for 1 h and then smoothed, producing specimens with midsection dimensions of 13 ± 0.5 mm by 3.2 ± 0.4 mm (Figure 3.1A). 24 h post-manufacturing, specimens were subjected to uniaxial tensile testing at a cross-head speed of 5 ± 1 mm/min until failure using a Tinius Olsen 1000 Ultimate Testing Machine. All tests were performed in air at RT. The ultimate tensile strength (UTS) was calculated as the force at failure divided by the cross-sectional area measured for each sample.

3.3.3.2 Compression testing of capsule-embedded bone cement

Following ASTM F451, bone cement specimens were cured in a polytetrafluoroethylene mold for 1 h and smoothed, yielding cylindrical specimens with a diameter of 6 ± 0.1 mm and height of 12 ± 0.1 mm (Figure 3.1B). 24 h post-fabrication, specimens were subjected to uniaxial compression testing at a cross-head speed of 20 mm/min using a Tinius Olsen 1000 Ultimate Testing Machine. All tests were performed in air at RT. The ultimate compressive strength (UCS) was calculated as the peak load divided by the pre-test cross-sectional area measured for the specimen.

3.3.3.3 Fracture toughness testing of capsule-embedded bone cement

Fracture toughness, K, of capsule-embedded PMMA samples was determined using tapered double-cantilever beam (TDCB) specimens as described previously for other self-healing systems[65, 85, 89, 178] (Figure 3.1C). Prior to mechanical testing, a razor blade was used to create a pre-crack in the grooved centerline region of the TDCB specimen, and specimen was loaded into a Test Resources Q series machine. The specimen was subjected to vertical displacement at 5 μm/s until the peak critical load, P_c, was reached and crack propagation was initiated.

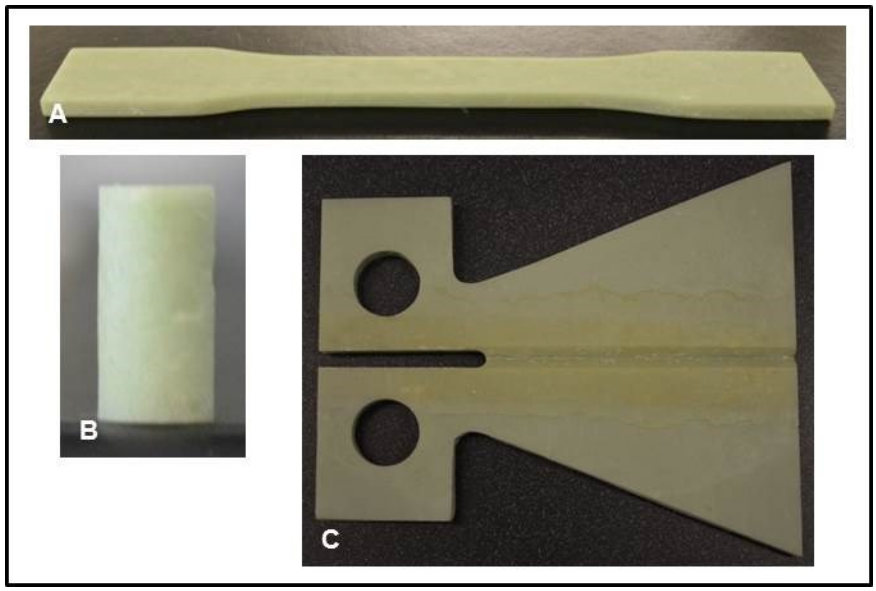

Figure 3.1: Palacos R PMMA samples for (A) tension, (B) compression, and (C) fracture toughness testing.

3.4 Results

3.4.1 Capsule morphology

Capsules fabricated at an agitation rate of 700 rpm were shown to have uniformly spherical morphology with average diameter and shell thickness of 121 ± 24 μm and 3 ± 0.9 μm, respectively, consistent with measurements obtained previously[171]. Capsules made at this agitation rate were used for all experiments.

3.4.2 Tensile testing of capsule-embedded bone cement

Capsule-free (unfilled) Palacos R bone cement used in the current study had a UTS of 41.2 ± 1.5 MPa (average ± SEM, n=5) and a Young's modulus of 1.85 ± 0.04 GPa (average ± SEM, n=5), both of which fall within the reported literature range of 25-70 MPa[11, 90, 107] and 1.36-3.07 GPa[11, 107, 109, 110], respectively. The UTS of the capsule-embedded (filled) specimens decreased monotonically with increasing wt% capsules (Figure 3.2A), whereas the Young's modulus of capsule-containing samples appeared to drop more sharply up to 5 wt% and then decreased more slowly thereafter (Figure 3.2B). The UTS of cements filled with 5 wt% was 29.1± 1.1 MPa (average ± SEM, n=5), which lies above the lower limit of the literature-reported values; however, at this capsule content, the Young's modulus for the material (1.13 ± 0.04 GPa, average ± SEM, n=5) was outside the range of values reported in the literature.

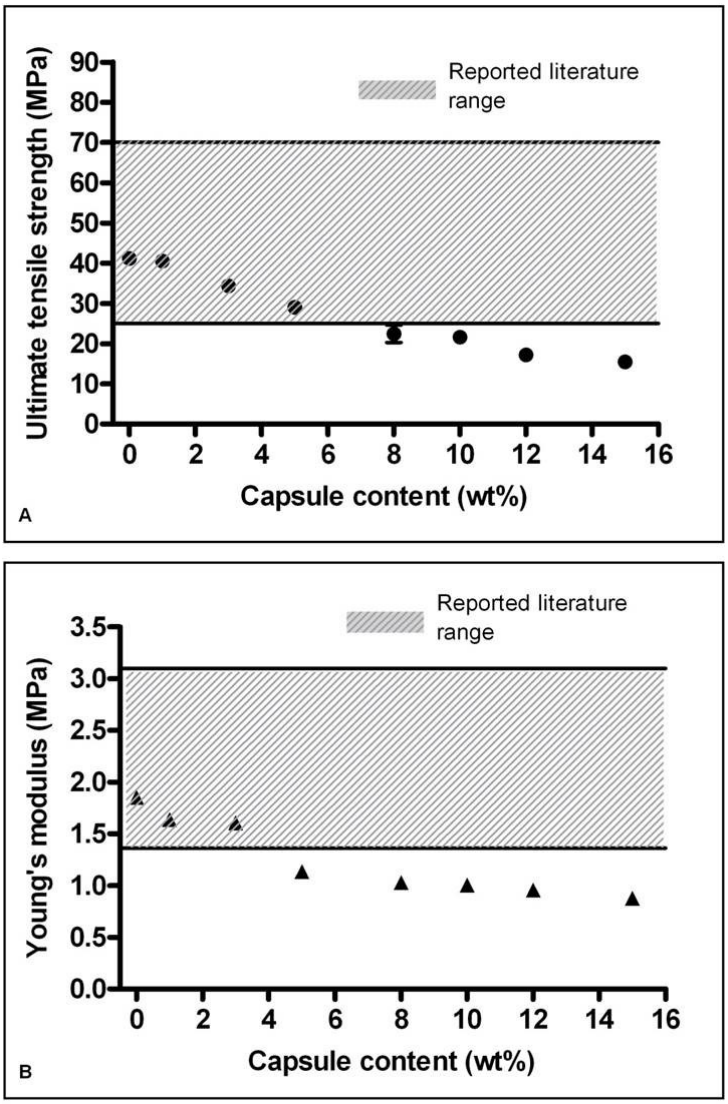

Figure 3.2: Relationship between capsule content and (A) ultimate tensile strength and (B) Young's modulus (average ± SEM, n=5).

3.4.3 Compression testing of capsule-embedded bone cement

Compressive tests of bone cement specimens filled with 5 wt% or fewer capsules all exceeded the minimum standard for the compressive strength of 70 MPa[90] (Figure 3.3A); whereas specimens filled with 10 wt% or higher capsules all had compressive strengths that declined steadily below this standard. Additionally, specimens containing 10 wt% or fewer capsules deformed plastically upon failure whereas specimens with higher capsule content fragmented upon failure (Figures 3.3B and C).

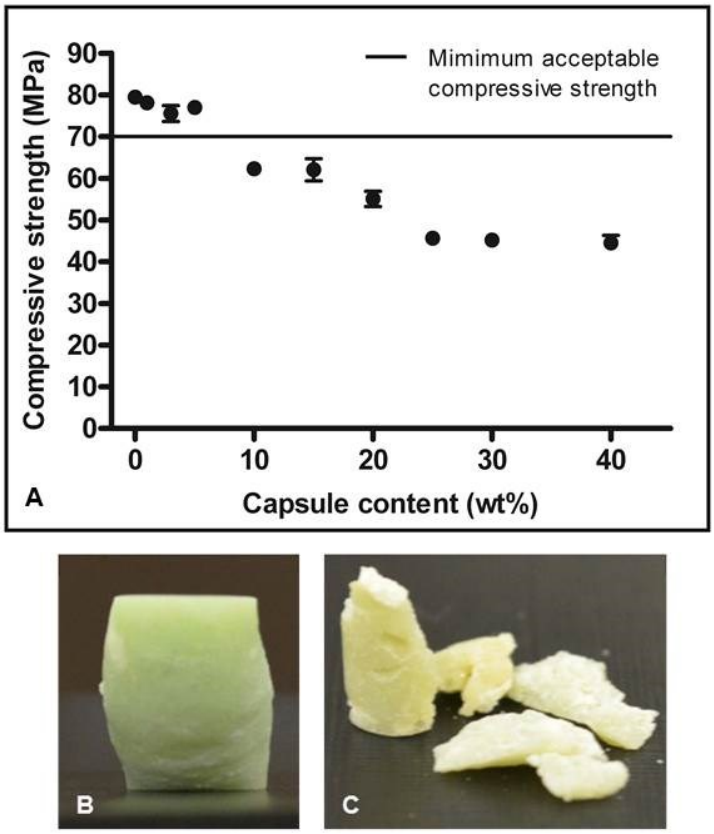

Figure 3.3: (A) Relationship between capsule content and the ultimate compressive strength of bone cement (average ± SEM, n=3 with 5 replicates per group). Photographs of samples containing (B) 0 wt% and (C) 40 wt% capsules post-compression testing.

3.4.4 Fracture toughness testing of capsule-embedded bone cement

Figure 3.4A compares the load-vertical displacement curves for unfilled bone cement (dashed line) and bone cement filled with 3 wt% capsules (solid line). The unfilled specimen exhibited instantaneous crack growth to complete failure upon reaching the peak critical load (~197 N), whereas the specimen filled with 3 wt% capsules exhibited slow and progressive crack growth beyond the peak critical load (~211 N) prior to the initiation of rapid propagation leading to complete failure.

Fracture toughness, K, varies based on numerous factors, including the molecular weight of the PMMA, sterilization methods, mixing techniques, storage conditions, and specimen geometry. The fracture toughness of unfilled specimens was found to be 2.11 ± 0.09 MPa $m^{1/2}$ and the effects of capsule inclusion on K are shown in Figure 3.4B. The addition of 3 wt% capsules resulted in a modest 13% increase in average K while samples filled with 5 wt% and 10 wt% capsules yielded K values approximately equal to that of unfilled control samples. Increasing capsule content to 15 and 20 wt% resulted in decreases of 26% and 45% in K, respectively when compared with unfilled controls, but remained within the literature-reported range of 0.88-2.58 MPa $m^{1/2}$ [11, 95-98].

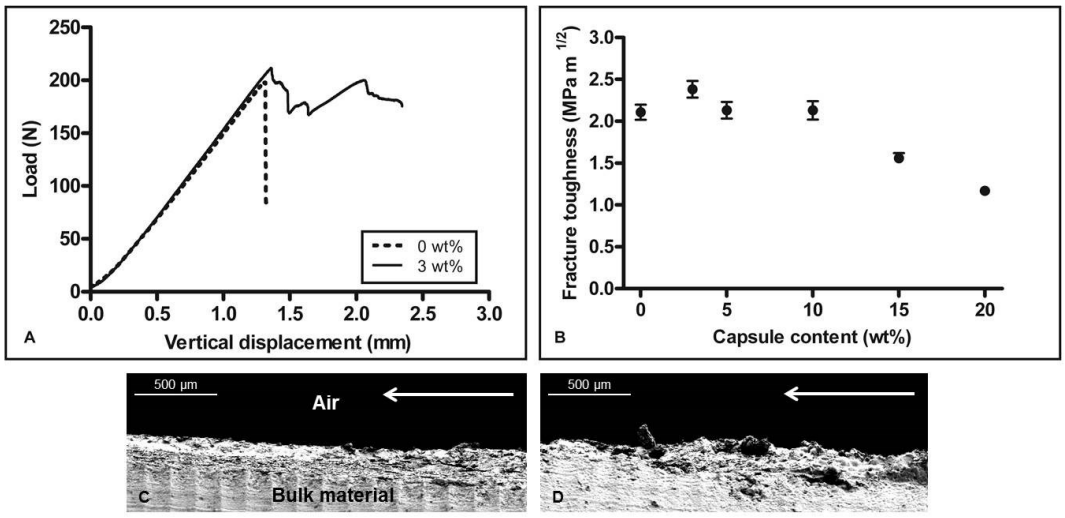

Figure 3.4: Load with increasing vertical displacement is shown in (A) for samples containing 0 and 3 wt% capsules. The effect of capsule content on fracture toughness is presented in (B) (average ± SEM, n=5). Fracture plane roughness and sub-surface microcracking are observed in SEM images of the side views of TDCB samples containing (C) 0 wt% and (D) 3 wt% capsules. Direction of crack propagation is indicated by arrows.

SEM images of the crack planes of unfilled (Figure 3.4C) and filled (3 wt%, Figure 3.4D) specimens revealed a marked increase in the roughness of the crack plane with increasing capsule content. In capsule-containing specimens, regions of slow, progressive crack growth exhibited sub-fracture plane microcracking that was less evident in capsule-free control specimens.

3.5 Discussion

This work describes the static mechanical testing of an acrylic bone cement matrix embedded with OCA-containing microcapsules using well-established ASTM and ISO mechanical standards for acrylic bone cements. Each test was designed to examine how capsule incorporation affected the integrity of the bone cement relative to the unfilled control.

Overall, composites containing up to 5 wt% capsules had compressive strengths above the commercially acceptable minimum and tensile strengths and stiffnesses within the reported ranges for commercial acrylic bone cements. Incorporation of higher wt% capsules did however result in mechanical weakening. Under compression, the composite began to fragment at high capsule contents (>25 wt%, Figure 3.3C) and could be attributed to the increased void space introduced by the capsules or possibly by altering the PMMA powder:MMA monomer ratio that is well-known to influence polymerization rate, setting time, and mechanical properties of PMMA[111]. Compression

testing of samples with powder:monomer ratios modified to correspond with those in filled specimens found the UCS decreased as the ratio became less than 2:1; a 20% reduction in UCS with the ratio adjusted to that of samples containing 40 wt% capsules (data not shown). This indicates that while varying the ratio contributes to the observed decrease in UCS, it is not the only factor dictating the mechanical property. The decrease in UTS could be attributed to a reduction in the cross-sectional area occupied by bone cement matrix in samples containing higher capsule contents or to poor shell/matrix interfacial bonding.

The weakening of a composite matrix through the addition of particulates typically occurs when the particulate-matrix interfacial adhesion is poor and increasing the particulate content provides a path for crack propagation. These observations are consistent with the general trend of limiting the incorporation of encapsulated healing agent to 5-10 wt% in self-healing polymeric composites[178]. Evidence of capsule pull-out following tensile tests as well as the fragmenting of the matrix under compression observed at high capsule contents suggests poor interfacial bonding between the PUR shell material and the PMMA matrix. In addition to chemical modification of the shell, alterations to the physical properties of the capsule, such as changing the shell material[168] or adding a coating[167, 179], could be investigated to further promote adhesion via increased surface roughness and material interactions.

The fracture toughness was relatively unaffected by capsule incorporation up to 10 wt% capsules, after which it also declined. For a specimen containing 3 wt% capsules (solid line in Figure 3.4A), the load increased linearly with increased displacement identically to the unfilled specimen (dashed line in Figure 3.4A) until reaching a load of approximately 200 N, after which the crack in the unfilled specimen propagated immediately to failure while the crack in the 3 wt% sample advanced in short unstable jumps, as reflected by the jagged load-displacement curve. This difference is also reflected in the distinctly different morphologies of the crack planes of the two specimens (Figures 3.4C and D). Previous examinations of self-healing composites observed similar stick-slip crack propagation in virgin load-displacement curves[64, 180].

The addition of 3 wt% OCA-containing capsules only slightly increased the fracture toughness when compared with capsule-free bone cement. In contrast, the addition of microencapsulated dicyclopentadiene to an epoxy matrix was previously demonstrated to increase fracture toughness up to 127%[178]. As the acrylic bone cement is already a highly filled composite of 60-70 wt% PMMA particles in a PMMA matrix, the fracture toughness of the bone cement here (2.11 ± 0.09 MPa $m^{1/2}$) was already nearly four times higher than that of neat EPON 828 epoxy[178] (0.55 ± 0.04 MPa $m^{1/2}$). Consequently, the addition of 3 wt% capsules does not appear to have a significant toughening effect on the bone cement composite.

Finally, it is important to note that the testing described here examines OCA-containing capsule-filled acrylic bone cement strictly within the context of ASTM and ISO commercial standards for the static mechanical properties of acrylic bone cement; therefore these results do not speak to the self-healing capacity of the system. Dynamic testing of the self-healing capacity of the system will be presented in a subsequent manuscript.

3.6 Conclusions

The effects of capsule incorporation on the compressive, tensile, and fracture toughness properties of bone cement showed that inclusion of greater than 5 wt% capsules resulted in the decrease of UCS and UTS below the commercially-required levels; the fracture toughness was improved with the incorporation of 3 wt% capsules but declined as content was increased above 15 wt%. These findings suggest that an optimal capsule content could be incorporated into PMMA bone cement while maintaining its static mechanical properties and support the future promise of this system.

3.7 Chapter acknowledgements

The authors would like to thank Ethicon, Inc. for the generous donation of 2-octyl cyanoacrylate. The authors also gratefully recognize the contributions of Duke

University colleagues Dr. Marcus Henderson, Steven Owen, and Sonia George with respect to TDCB testing protocols and specimen mold fabrication in addition to Dr. Stephen Craig and Zachary Kean for polymer synthesis and Matthew Novak for assistance with statistical analyses. This research was supported by NIH grants T32-GM8555 (ABWB) and R21 EB 013874-01 (WMR).

4. Chapter 4: Functional lifetime of acrylic bone cement containing microencapsulated 2-octyl cyanoacrylate

The manuscript describing the work presented in Chapter 4 is currently in preparation and will be submitted for publication shortly.

4.1 Chapter synopsis

An FDA-approved, water-reactive tissue adhesive, 2-octyl cyanoacrylate (OCA) was encapsulated within polyurethane shells and incorporated into Palacos R poly(methyl methacrylate) (PMMA) bone cement to assess the bending strength and fatigue lifetime of the capsule-embedded materials. The bending strength, bending modulus, and fatigue lifetime of the materials were investigated in accordance with ISO standards. To identify effects specific to encapsulated OCA, PMMA samples without capsules and PMMA samples embedded with OCA-containing and OCA-free capsules were prepared for bending and fatigue testing. To investigate capsule susceptibility to moisture intrusion, individual capsule compressive strength was examined over 50 d of storage in air at room temperature (RT), Ringer's solution at RT, and Ringer's solution at 37 ºC. The bending strength of OCA-containing specimens was maintained above the minimum commercial limit at capsule contents below 5 wt% while the minimum bending modulus was exceeded regardless of capsule content. At low applied cyclic loads, the index of fatigue performance of OCA-containing bone cement stored in air at

RT was increased 2.5 and 1.8 times when compared to specimens containing OCA-free capsules and specimens without capsules, respectively. However, following 4 weeks of storage in Ringer's solution at 37 ºC, the lifetime extension observed in OCA-containing samples was lost. Studies of individual capsule compressive strength revealed increased strength with increasing storage time; storage in Ringer's solution at 37 ºC produced the most rapid increase in individual capsule compressive strength, suggesting the storage conditions affected the mechanical properties and on the capsule contents.

4.2 Introduction

Self-healing materials (SHM) are designed to halt and repair microdamage accumulated through repetitive loading. One of the most broadly reported self-healing schemes is that pioneered by White and Sottos et al. in which a polymer matrix is co-embedded with a catalyst and microcapsules containing a reactive healing agent. Once encountered by a propagating microcrack, the capsule shell is ruptured and releases its healing agent into the crack plane where it is exposed to a catalyst embedded in the matrix. *In situ* curing of the healing agent ensues, halting crack propagation[47, 63-65, 71-73, 171]. A majority of the systems proposed to date are for civil, mechanical, aerospace, and electrical engineering applications.

Although the SHM field has been steadily growing over the past 10 years, little discussion of extension into biomaterials has taken place and current systems do not

utilize materials that are acceptable for *in vivo* applications[47, 171]. Numerous implants fail following the accumulation of damage and are potential candidates for the introduction of self-healing to biomaterials. However, as there are stringent requirements for materials used in clinical applications, any SHM proposed for a biomedical application would need to be assessed from mechanical, biocompatibility, and self-healing perspectives.

Bone cements are two-component materials consisting of a low molecular weight poly(methyl methacrylate) (PMMA) powder containing an initiator (e.g. benzoyl peroxide), and liquid MMA monomer containing an activator for the initiator. *In situ* mixing of the liquid and powder initiates polymerization to yield a workable dough that is applied to the metallic stem of a TJR implant and cures to form a solid mass after the stem is inserted into the bone[8, 171]. PMMA bone cement has a long history of use in total joint replacement (TJR) surgeries, does not require post-polymerization modifications, and there is significant need for improvement of the material. Bone cement is a brittle material that is weak in tension and strong in compression and is susceptible to crack initiation and subsequent propagation resulting from the loading patterns experienced *in vivo*. For these reasons, the development of a self-healing PMMA bone cement is an attractive option for the first self-healing biomaterial designed with the aforementioned embedded capsule and catalyst approach[47, 84].

As bone cement is considerably weaker than bone[11] and comes with its own set of challenges, researchers have proposed composite designs to improve the mechanical properties of the material; dispersed particulates and fibers have been investigated to increase the toughness, impact strength, and wear resistance of the PMMA by absorbing a greater fraction of the load, inhibiting pathways for crack propagation, and resisting void formation. However, in spite of a long history of development in load-bearing applications, very few composite devices have progressed to widespread clinical use[47].

Previous research by the authors has demonstrated encapsulation of a water-reactive tissue adhesive, 2-octyl cyanoacrylate (OCA), in polyurethane shells to be investigated for applications in a self-healing bone cement[171]. The successful incorporation of these capsules into a commercial bone cement matrix was also confirmed; tension, compression, and fracture toughness analyses suggested that 5 wt% was the maximum capsule content that could be used in the material while still adhering to commercial requirements and literature values[181]. Furthermore, the addition of OCA-containing capsules to the matrix was not found to affect the viability and proliferation of MG63 human osteosarcoma cells treated with extract from these materials[181].

While promising, the previous work examined OCA-containing capsule-filled acrylic bone cement strictly within the context of ASTM and ISO commercial standards for the static mechanical properties of acrylic bone cement. Therefore, those results did

not speak to the self-healing capacity of the system. Previous assessments of healing efficiency successfully utilized tapered double cantilever beam (TDCB) specimens to investigate fracture toughness and healing efficiency[65, 74-76, 87-89]. Typically, the healing efficiency of a SHM is determined by testing the "virgin" specimen until a crack propagates through the center of the material; the separate pieces are reapposed to allow the healing agent to react and bond the surfaces together and the "healed" specimen is then tested again.

Most studies using the TDCB geometry to investigate healing efficiency have induced crack propagation through a single, continuously applied load[65, 74-76]. However, given that SHM are intended to prevent accumulated damage, their healing efficiency under cyclic loading has also been investigated[86-89]. While TDCB tests currently provide valuable information about the healing efficiency of some systems, they introduce very large defects that are not representative of damage likely to be sustained by a TJR *in vivo*. Also, given the water-reactive nature of the OCA healing agent proposed for this application, the time taken to induce crack propagation in the TDCB specimen may result in the polymerization of any released OCA by moisture in the air. A more clinically-relevant and informative procedure would involve assessing the healing capabilities of a self-healing bone cement system under *in vivo* conditions to repair microdamage.

Here we present analyses of the functional lifetime of both individual capsules as well as fatigue analyses of capsule-free and capsule-embedded bone cements in air at RT and in Ringer's solution at 37 ºC. These properties, in addition to the bending strength of the material, are investigated to demonstrate the self-healing functionality of this OCA/PMMA bone cement SHM system. Similar to the compressive and tensile properties reported previously[181], bending strength decreased with increasing capsule content; however, bending modulus was relatively unaffected by capsule inclusion up to 15 wt%. At low applied cyclic loads, the index of fatigue performance of OCA-containing bone cement stored in air at RT was increased 2.5 and 1.8 times when compared to specimens containing OCA-free capsules and specimens without capsules, respectively. However, following 4 weeks of storage in Ringer's solution at 37 ºC, the lifetime extension observed in OCA-containing samples was lost. Studies of individual capsule compressive strength revealed increased strength with increasing storage time; storage in Ringer's solution at 37 ºC produced the most rapid increase in individual capsule compressive strength, suggesting the storage conditions affected the mechanical properties and on the capsule contents.

4.3 Experimental section

4.3.1 Reagents

Materials were obtained from commercial suppliers and used without further purification. OCA was generously donated by Ethicon, Inc., Raleigh, NC 27616. Methyl ethyl ketone (MEK), methyl isobutyl ketone (MIBK), and cyclohexanone (Sigma Aldrich) were used as solvents and 2,4-toluene diisocyanate (TDI) and 1,4-butanediol (1,4-BD) (Sigma Aldrich) were used to synthesize the polyurethane prepolymer (pPUR) following the protocol outlined by Yang et al. and reported by the authors previously[165, 171]. Pluronic F-68 (Sigma Aldrich) was used as a surfactant. Para-toluenesulfonic acid (Sigma Aldrich, PTSA) was added to the organic phase as a stabilizer for the OCA monomer. Ringer's solution was prepared with reagent-grade water (Sigma), sodium chloride, potassium chloride, and calcium chloride (Sigma Aldrich). Commercially-available Palacos R PMMA bone cement (Zimmer) was used for all experiments reported herein.

4.3.2 Microcapsule preparation

Microcapsules were prepared and characterized as described previously[171]. Briefly, at room temperature, Pluronic F-68 surfactant (1.84 g) was dissolved in deionized water (90 mL) in a 250 mL beaker. The solution was agitated for 1 h with a digital mixer (VWR PowerMax Elite Dual-Speed Mixer) before beginning the

encapsulation procedure. The aqueous phase was suspended in a hot water bath and heated to 50 ºC prior to the addition of the organic phase and chain extender.

OCA (4 mL) was dissolved in MIBK (8 mL) and pPUR (3 g) was dissolved in MEK (10 mL) separately at room temperature. PTSA (1%) was added to the OCA-MIBK solution to further stabilize the OCA monomer. The pPUR- and OCA-containing solutions were then added simultaneously to the aqueous phase but not mixed prior to this addition. After the organic and aqueous phases were combined, the 1,4-BD (3 mL) chain extender was added dropwise to the stirring mixture via a syringe to form the segmented PUR shell material consisting of hard TDI-based segments and soft 1,4-BD segments. After a reaction time of 2 h at an agitation rate of 700 rpm, the mixer was switched off and the suspension of microcapsules rinsed with deionized water and vacuum filtered. Capsules were air-dried prior to use in the following experiments[171]. To manufacture OCA-free control capsules, the OCA was replaced with additional MIBK (4 mL) and the agitation rate reduced to 450 rpm; all other aspects of the encapsulation procedure were performed identically.

4.3.3 Preparation of capsule-containing bone cement samples

The powder component was mixed with the liquid component according to the manufacturer's instructions[177], OCA-containing capsules were added to the slurry, and the resultant material was added to molds to form the desired specimen shape. Samples

were cured in the molds for at least 1 h, released, and smoothed with 240 mesh silicon carbide to conform to the specified geometrical requirements. The wt% of OCA-containing capsules in the bone cement composites ranged from 0-40 wt% where the wt% of total particulates (OCA capsules plus PMMA powder) was held constant at 67 wt% in all specimens.

4.3.3.1 Bending testing of capsule-embedded bone cement

Following ISO 5833, rectangular bone cement samples were cured in silicone rubber molds for 1 h and then smoothed, producing specimens with dimensions of 10 ± 0.1 mm by 3.3 ± 0.1 mm by 75 ± 0.1 mm. 24 h post-manufacturing, specimens were subjected to 4-point bending at a crosshead speed of 5 ± 1 mm/min until failure using a Test Resources 840LE2 Electrodynamic tension-compression-flexural fatigue machine. All tests were performed in air at RT. The bending strength, B, was calculated using Equation 1:

$$B = \frac{3Fa}{bh^2} \tag{1}$$

where F is the force at break (in N), b is the average measured width of the specimen (10 mm), h is the average measured thickness (3.3 mm), and a is the distance between the inner and outer loading points (20 mm).

Equation 2 was used to determine the bending modulus, E:

$$E = \frac{\Delta F a}{4 f b h^3}(3l^2 - 4a^2) \quad (2)$$

where f is the difference in the deflection under the loads of 15 and 30 N (in mm), b is the average measured width of the sample (10 mm), h is the average thickness (3.3 mm), l is the distance between the outer loading points (60 mm), ΔF is the load range over which the deflection was measured (15 N), and a is the distance between the inner and outer loading points (20 mm). The commercial requirements for B and E as described in ISO 5833 are 50 and 1800 MPa, respectively.

4.3.3.2 Fatigue testing of capsule-embedded bone cement

Specimens were prepared as described for bending testing. Samples were either tested 1 d after manufacturing or after 4 weeks of storage in Ringer's solution at 37 ºC[99, 100]. The samples were cycled to failure under load control using a Test Resources 840LE2 Electrodynamic tension-compression-flexural fatigue machine. The bending strength of capsule-free samples was used as the reference strength; during fatigue analyses, various upper stress levels ranging from 50-90% of the reference value were selected for testing and 10 samples were cyclically-loaded to each of these maximum stress levels[106]. A loading ratio R, $\sigma_{min}/\sigma_{max}$, of 0.05 and a frequency of 5 Hz were used to mimic normal gait[34, 99, 100, 105].

Just as capsule-free control samples were tested to certain percentages of their reference strength, specimens containing encapsulated OCA were cyclically-loaded at

maximum stress levels that were 50-90% of their reference strength using R=0.05 and a frequency of 5 Hz. Based on previous studies of the static mechanical properties of capsule-containing PMMA samples[181], specimens containing 5 wt% capsules were used for all fatigue experiments of capsule-embedded samples. To determine if an encapsulated OCA system went beyond passive toughening to actively slow and repair damage, samples containing 5 wt% of OCA-free capsules were tested under the same conditions.

The probability-of-failure, P(N_f), was obtained using the equation P(N_f) = (M-0.3)/(G+0.4), where M and G are the failure order number and the total number of specimens tested, respectively[105, 182]. The failure order number is defined as the number assigned to an N_f value to denote its position within a list of G values arranged in ascending order of magnitude; M=1,2,3…G. For a given stress level, the N_f results were fitted to the linearized form of the 3-parameter Weibull equation, as shown in Equation 3:

$$\ln\ln[\frac{1}{(1-P(N_f))}] = b\ln(N_f - N_0) - b\ln(N_a - N_0) \quad (3)$$

where N_0 is the minimum or guaranteed fatigue life, N_a is the characteristic fatigue life, and b is the Weibull slope. N_0 was determined from the vertical asymptote of the plot of ln(N_f) versus ln ln[1/(1-P(N_f))][43, 105, 183]; this is the number of cycles below which all

specimens have a 100% probability of survival. The Weibull slope, b, is a measure of the spread of the data, and N_a, the characteristic fatigue life, is the number of cycles below which lie 63.2% of the N_f results. Both of these parameters are determined from the linear fit of the plot of $\ln(N_f\text{-}N_0)$ versus $\ln \ln[1/(1\text{-}P(N_f))]$[43, 105, 183]. The Weibull mean, N_{WM}, also called the index of fatigue performance, was calculated as shown in Equation 4:

$$N_{WM} = N_a \sqrt{b} \tag{4}$$

4.3.4 Capsule susceptibility to moisture intrusion

OCA-containing capsules were stored in glass scintillation vials in air at RT for 50 days or soaked in Ringer's solution at RT or 37 ºC for the same duration. Small samples of capsules were removed from each vial at various time points, dried, and subjected to compression testing using a dynamic mechanical analyzer (TA Instruments RSA-G2 solid analyzer, DMA) as described previously[171]. Displacement of the upper DMA plate was applied at 5 μm/s until shell compressive failure was observed. Capsule compressive strength was determined by dividing the maximum compressive load by the pre-test equatorial cross-sectional area measured for each capsule. A vacuum sputter coater (Denton Desk IV) was used to deposit a 10 nm layer of gold onto post-compression samples for scanning electron microscope (FEI XL30 SEM-FEG, SEM) imaging to examine capsule morphology with increasing storage time.

4.3.5 Statistical analyses

Independent two-sample t-tests were used to compare the average individual capsule compressive strength of samples taken from each treatment at a given time point. The level of statistical significance was set at $p < 0.05$.

4.4 Results

4.4.1 Capsule morphology

Capsules fabricated at an agitation rate of 700 rpm were shown to have uniform spherical morphology with average diameter and shell thickness of 132 ± 29 μm and 2 ± 0.8 μm, respectively, consistent with measurements obtained previously[171, 181]. Capsules made at this agitation rate were used for all experiments with OCA-containing specimens. OCA-free capsules made at 450 rpm were also shown to have spherical morphology with average diameter and shell thickness of 89 ± 15 μm and 3 ± 0.7 μm, respectively, resembling those containing OCA.

4.4.2 Bending testing of capsule-embedded bone cement

Capsule-free Palacos R bone cement used in the current study had a bending strength (*B*) of 74.9 ± 1.2 MPa (average ± SEM, n=5) and a bending modulus (*E*) of 3047 ± 56 MPa (average ± SEM, n=5); these values are well above those of 50 MPa and 1800 MPa required for *B* and *E* of commercial bone cements and are similar to those reported in the literature for Palacos R[90, 99]. *B* decreased monotonically with increasing OCA-containing capsule content; however, *E* remained fairly constant regardless of capsule content (Figures 4.1A and 4.1B). The average bending strengths of samples containing fewer than 5 wt% capsules lie above the commercial minimum and the bending modulus requirement was met at all capsule contents tested. Similar results were found when testing samples containing OCA-free capsules; *B* was maintained at all contents lower than 10 wt% while *E* always exceeded the commercial minimum.

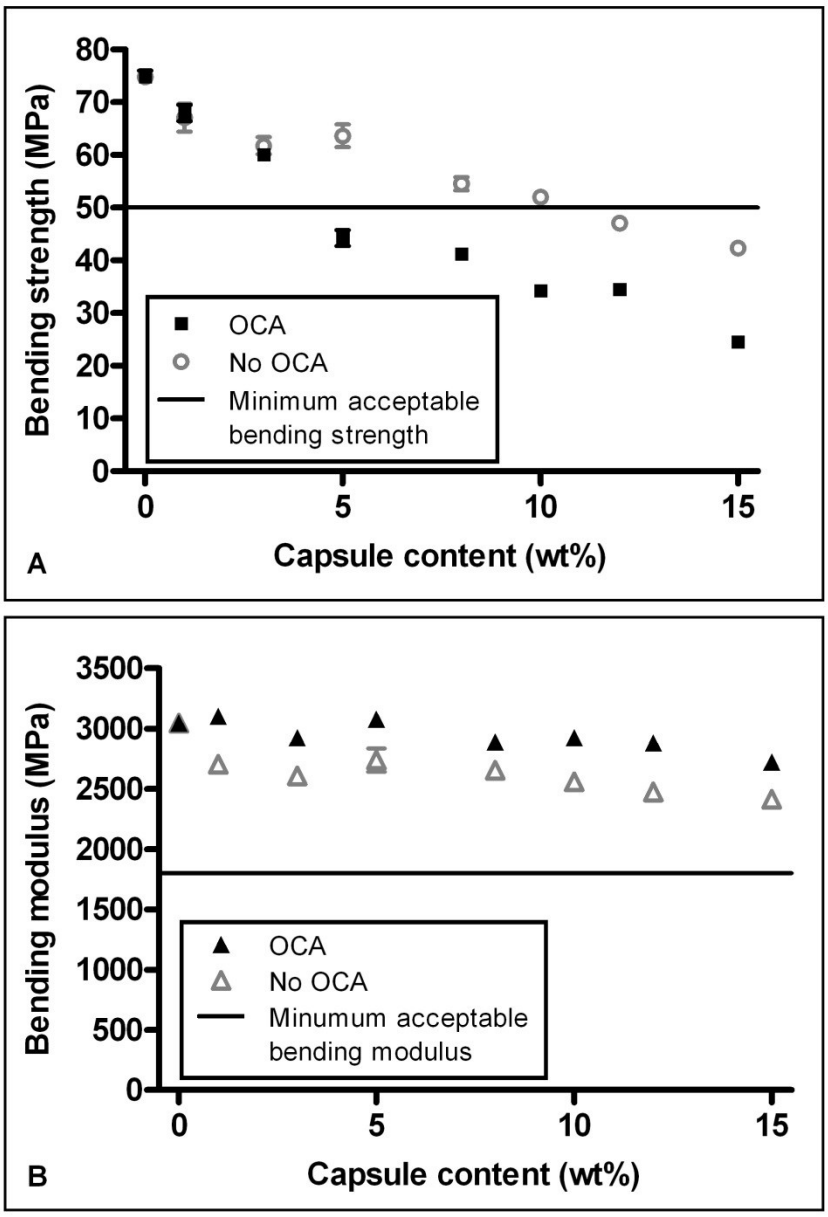

Figure 4.1: Relationship between capsule content and (A) bending strength and (B) bending modulus (average ± SEM, n=5) for specimens embedded with OCA-containing and OCA-free capsules.

4.4.3 Fatigue testing of capsule-embedded bone cement

The reference bending strengths and fatigue lives of the various specimen types are summarized in Figure 4.2A. The reference strengths, as determined by bending testing to failure, were 74.9 ± 1.2, 63.7 ± 2.2, and 44.2 ± 1.5 MPa for capsule-free specimens and those embedded with 5 wt% OCA-free capsules and 5 wt% OCA-containing samples, respectively (Figure 4.2A). Fatigue testing 1 d post-manufacturing at maximum cyclic stress levels of 50, 70, 80, and 90% of the reference stress was performed to generate the S-N relationships presented in Figure 4.2B.

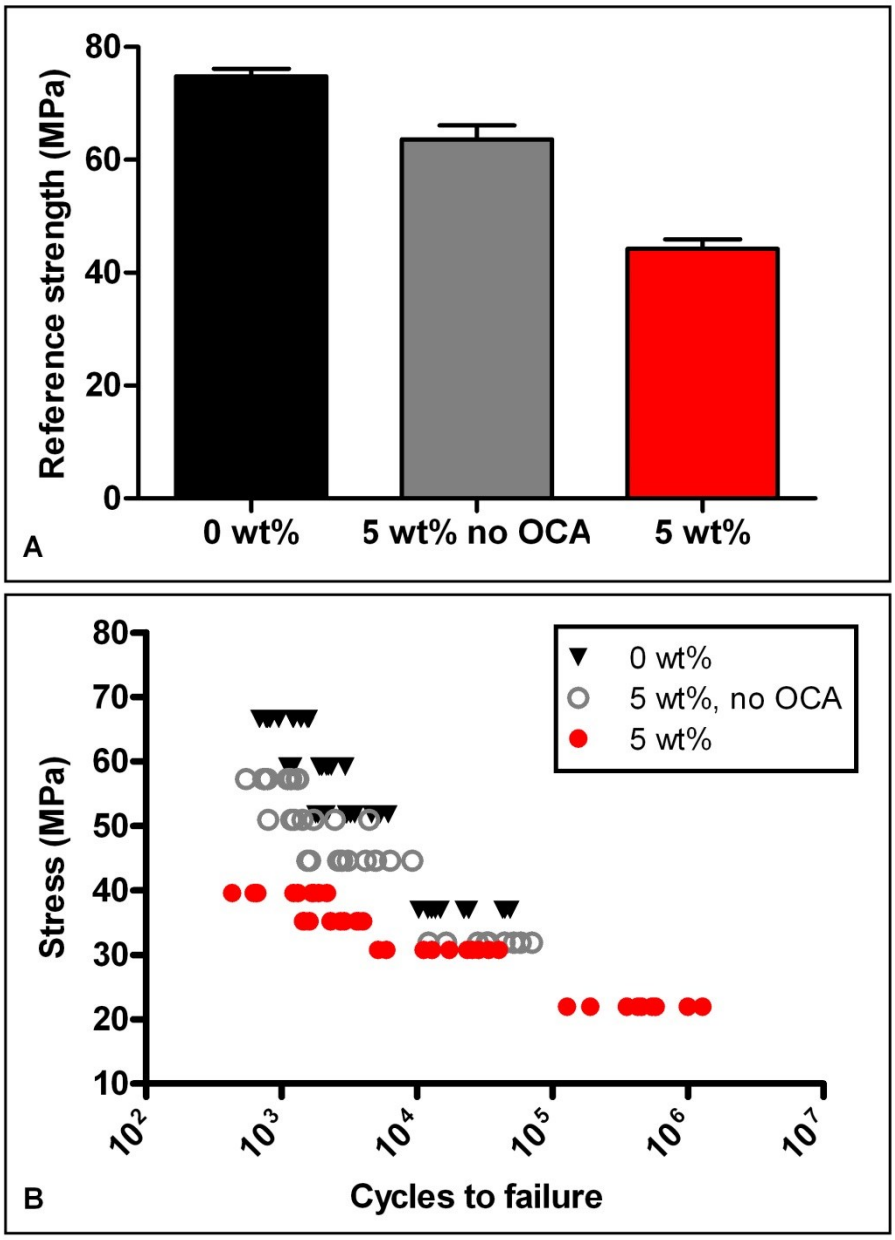

Figure 4.2: The reference bending strengths for each sample type are depicted in (A) (n=10). The fatigue test results as applied stress versus the number of cycles to failure for samples tested after 1 d storage in air are summarized in (B).

Fatigue life was increased with decreasing upper cycling load regardless of specimen type; however, differences between the reference bending strengths complicated the comparisons across sample type (Figure 4.2B). Although the reference strength of OCA-containing samples was lower than those of the other specimen types, the samples underwent more cycles prior to failure at lower load levels. Extrapolation of the S-N data suggested that at upper cycling loads less than 40 N (~22 MPa), OCA-containing specimens would outperform the others, regardless of reference strength. Samples of each type were cyclically loaded at a maximum force of 40 N at a frequency of 5 Hz with R=0.05; the results of fatigue testing at this lower load condition are presented in Figure 4.3.

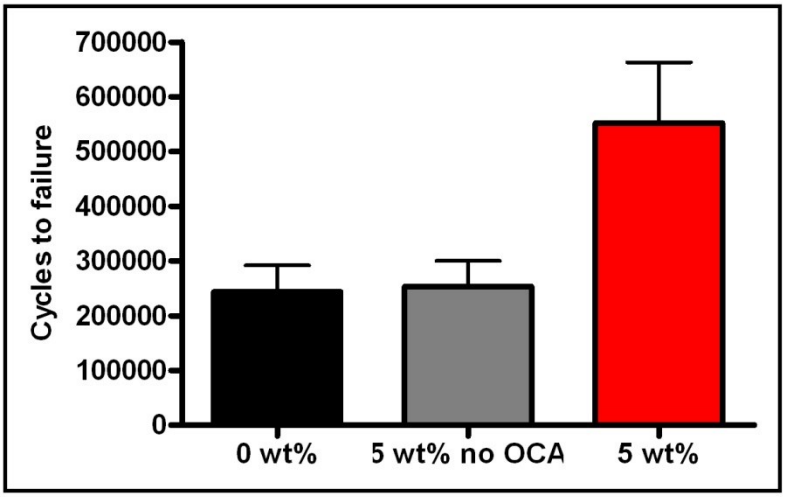

Figure 4.3: Number of cycles to failure in samples tested to a maximum load of 40 N (n=10). OCA-containing specimens underwent approximately two times as many cycles prior to failure at this lower load level.

The numbers of cycles to failure were found to be significantly increased in samples containing OCA-filled capsules when tested to 40 N when compared with capsule-free controls and samples containing 5 wt% capsules without OCA. Table 4.1 summarizes the properties of the fatigue samples tested to upper cycling loads of 40 N in air.

Table 4.1: Mechanical properties of capsule-filled and capsule-free bone cements tested in air

Condition	Capsule free	Capsules with OCA	Capsules without OCA
B (MPa)	74.9 ± 1.2	44.2 ± 1.5	63.7 ± 2.2
E (MPa)	3047 ± 56	3078 ± 14	2902 ± 41
Characteristic fatigue life, N_a (cycles)	410658	532698	284916
Minimum fatigue life, N_0 (cycles)	64786	84966	134427
Weibull slope, b	0.5685	0.6025	0.5848
Weibull mean, N_{WM}	309632	544661	217882

Following 4 weeks of storage in Ringer's solution at 37 ºC, the *B* of unfilled bone cement was relatively unchanged, increasing slightly, but not significantly, to 75.3 ± 1.4 MPa; the *B* of samples filled with 5 wt% OCA-containing capsules increased to 51.6 ± 1.6 MPa while *B* of specimens containing OCA-free capsules decreased slightly to 60.5 ± 0.5 MPa (Figure 4.4A). Over the same period, the average *E* of unfilled bone cement decreased from 3047 ± 56 MPa to 2806 ± 36 MPa while the *E* of samples filled with 5 wt% OCA-containing capsules decreased from 3078 ± 14 MPa to 2689 ± 38 MPa and *E* of samples filled with 5 wt% OCA-free capsules decreased from 2902 ± 41 MPa to 2566 ± 26 MPa. However, all average values for *E* are substantially higher than the 1800 MPa minimum commercial limit regardless of storage condition.

Fatigue testing was conducted at stress levels 50, 70, 80, and 90% of the specimen reference strengths to generate the S-N relationships shown in Figure 4.4B. As observed in samples tested in air 1 d after fabrication, fatigue lifetime was extended as the maximum applied stresses decreased. While the average number of cycles to failure was found to be slightly increased in capsule-free samples when compared to their counterparts that were not stored in Ringer's solution (Figures 4.2B and 4.4B), the number of cycles to failure was reduced following storage in Ringer's solution in specimens containing either type of capsules (Figures 4.2B and 4.4B). Extrapolation of the S-N data revealed that there was no load level at which OCA-containing specimens would outperform the others.

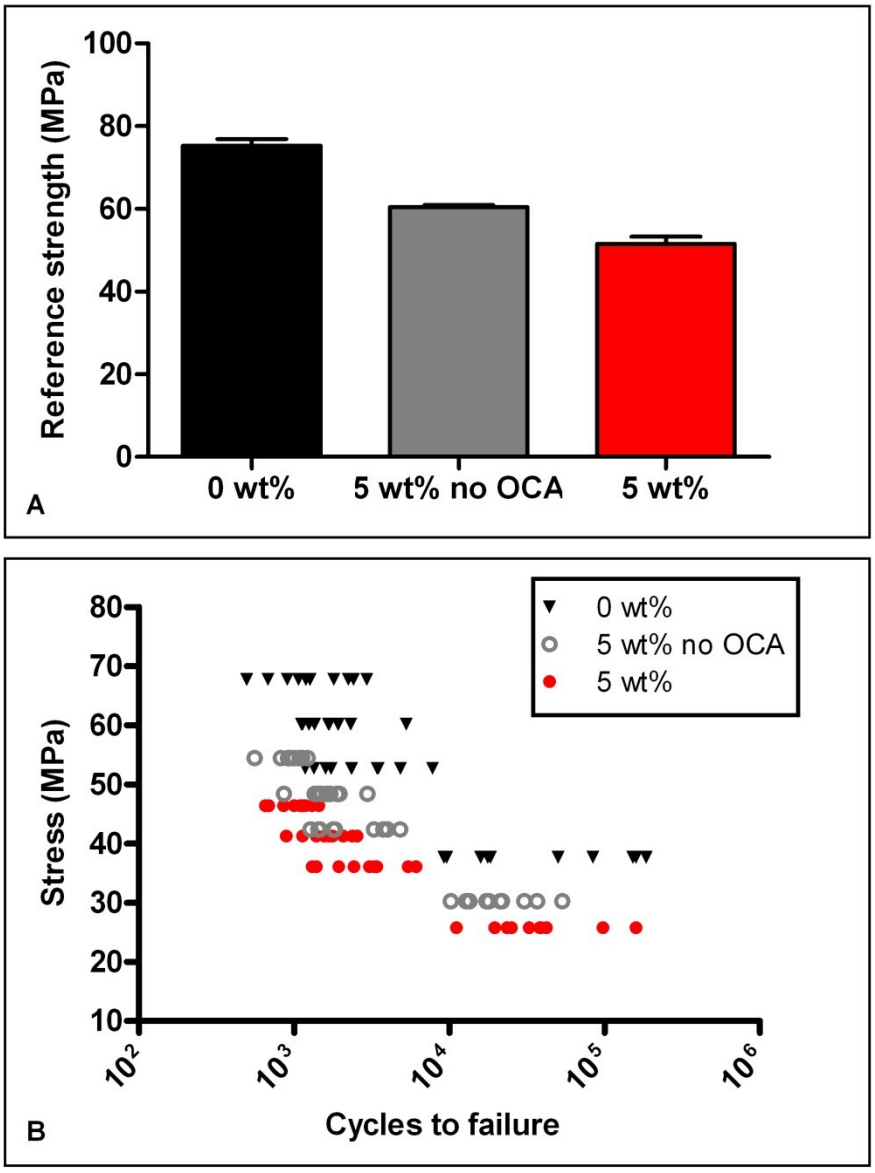

Figure 4.4: The reference bending strengths for each sample type are depicted in (A) (n=10). The fatigue test results as applied stress versus the number of cycles to failure for samples tested after 4 weeks storage in Ringer's solution at 37 ºC are summarized in (B).

4.4.4 Capsule susceptibility to moisture intrusion

Figure 4.5 summarizes the effects of storage time on the compressive strength of individual capsules stored in air at RT and in Ringer's solution at RT and 37 ºC over a period of 50 days. In all cases, capsule compressive strength increased with days in storage; the rate of strengthening was most rapid for capsules stored at 37 ºC in Ringer's solution, followed by Ringer's solution at RT, and then in air at RT. Capsules reached apparent upper limits of ~16-17 MPa for capsules stored in Ringer's solution at 37 ºC, and ~14 MPa for capsules stored at RT in either air or Ringer's solution. The average individual capsule compressive strengths for capsule stored in each condition were only significantly different at days 5 and 15 between capsules stored at RT and those in Ringer's solution at 37 ºC

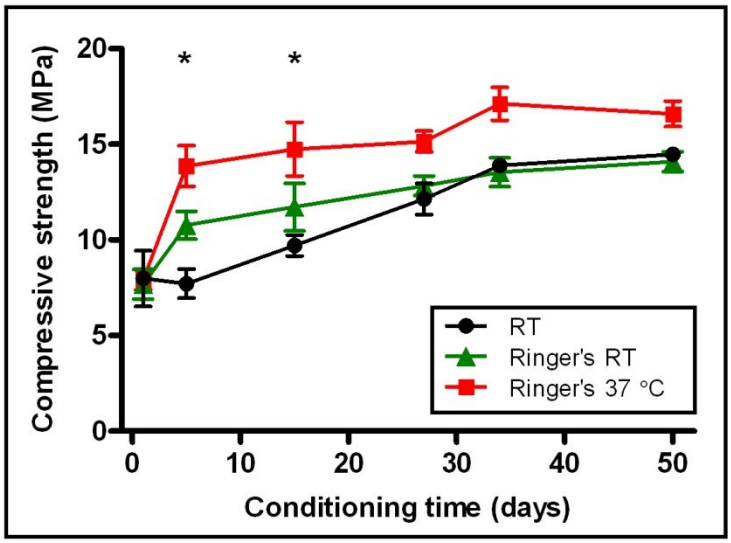

Figure 4.5: Compressive strength of individual capsules over storage time. Capsules were stored in air at RT and Ringer's solution at RT or 37 ºC (average ± SEM, n=3 with 3 replicates per group). Asterisks indicate significance between the RT and Ringer's 37 ºC samples.

SEM images of capsules fractured after 15 days of storage time clearly showed increased capsule shell thickness in the sample stored at 37 ºC in Ringer's solution (Figure 4.6A) when compared to the specimen stored in air at RT (Figure 4.6B).

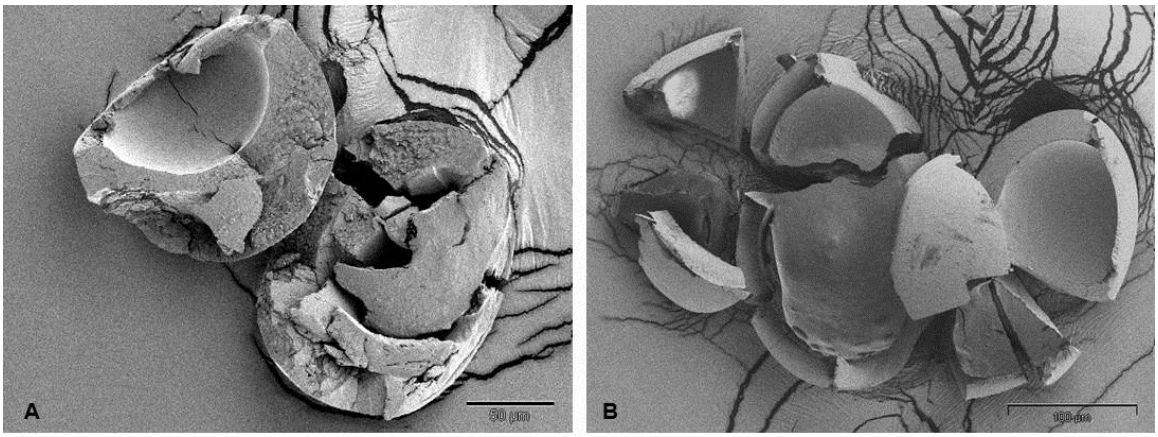

Figure 4.6: SEM images of capsule morphology with exposure to (A) Ringer's solution at 37 ºC and (B) air at RT for 15 days of storage time. Note the increased shell thickness of the capsule stored in Ringer's solution when compared with the capsule stored in air.

4.5 Discussion

One of the primary challenges associated with the development of SHMs is identifying a proper balance between decreasing the mechanical strength of the material while increasing its self-healing capacity; this was observed here as the addition of capsules gradually decreased the static bending strength of the PMMA. For OCA-containing specimens, the required bending strength *B* was maintained at capsule contents of less than 5 wt%; this was expected as 5 wt% was also the maximum limit for compression and tension properties[181] and bending is a combination of these two forces. In specimens embedded with OCA-free capsules, *B* was maintained at capsule contents of less than 10 wt%; this difference in maximum allowable wt% of capsules is attributed to the slightly decreased size of the OCA-free capsules when compared to the OCA-containing capsules. The bending specimens were all smoothed prior to testing, but any surface defects serve as initiation sites for crack propagation. Capsules at or near the surface of the material could act as initiation sites and contribute to the decrease in bending strength observed in samples containing either type of capsule; with increasing capsule content, the number of defects at or near the surface increased, resulting in more initiation sites and subsequently a decreased *B*. Even though the bending strength of the PMMA is decreased through capsule inclusion (Figure 4.1A), these strengths are still much higher than the physiologically-relevant values at which the material will ultimately be used.

Interestingly, the bending modulus *E* remained remarkably consistent regardless of capsule content in samples embedded with OCA-containing and OCA-free capsules. Based on Equation 2, the deflection *f* is the only variable that could change between the sample types and/or with increasing capsule content; consistent *f* regardless of increasing capsule wt% suggests that while increasing capsule content increased the crack initiation, crack propagation rates were unchanged. Crack propagation rates in OCA-free capsules may be influenced by the size of the capsules as well as differences in the mechanical properties of the individual capsules, leading to the slightly lower *E* observed in samples with OCA-free capsules (Figure 4.1B).

Higher cycling stresses resulted in a decreased number of cycles prior to failure regardless of sample type or reference bending strength (Figure 4.2). Differences between the reference strengths make comparisons difficult across sample type; however, at lower applied cyclic stresses, specimens containing encapsulated OCA underwent more cycles prior to failure than the other sample types (Figure 4.3). For the system's intended application, behavior at lower stress levels is more indicative of the *in vivo* environment; a SHM of this design is not intended to repair damage that occurs near the upper limits of the PMMA's mechanical properties.

The addition of particulates to PMMA has previously been found to retard fatigue failure through increasing the fracture toughness, impact strength, and wear resistance of the material by absorbing a greater fraction of the load, inhibiting pathways

for crack propagation, and resisting void formation. The fatigue life in samples containing OCA-free capsules and no capsules were approximately equal at the lowest load level tested (Figure 4.3); as it was hypothesized that additives would contribute to lifetime extension, these findings support previous data suggesting the need for improvement in the interfacial bonding between the capsule shell and PMMA matrix[181]. From this fatigue data, it can be inferred that other factors are contributing to the increased number of cycles to failure observed in OCA-containing samples.

Brown et al. reported that when healing agent was released into the crack plane of a cyclically-loaded TDCB specimen, it polymerized to form a polymer wedge, generating a crack tip shielding mechanism[87, 88]. This shielding wedge resulted in temporary crack arrest and extended the fatigue lifetime by 20 times. Hydrodynamic pressure crack-tip shielding due to viscous flow has also been found to retard crack growth[87], indicating that the initiation of healing agent polymerization could act to slow crack growth before full polymerization and subsequent polymer wedge formation. The forces required to squeeze a viscous fluid from the crack plane during unloading provided crack-tip shielding. Testing with TDCB specimens introduces macrocracks far larger than those intended to be repaired by these SHMs in their usage environments, but it is hypothesized that similar mechanisms are contributing to the increased fatigue lifetime observed in PMMA samples containing encapsulated OCA.

Analyses using the linearized 3-parameter Weibull model indicated that both the characteristic life (N_a) and guaranteed fatigue life (N_0) were increased in OCA-containing specimens when compared to the other specimen types (Table 4.1). The Weibull slope is an indicator of the likelihood of specimen failure; distributions with higher slopes indicate samples that are approaching failure. Additionally, the slope describes the variability or degree or scatter in the cycles to failure data[183]; an increased slope indicates a reduction in scatter, meaning that the samples fail at more consistent cycle numbers. A decrease in the Weibull slope, as seen with the lower stress levels tested here, indicates a broader range of N_f; this is to be expected when the PMMA is tested at lower stresses and the crack propagation behavior dominates over the crack initiation behavior[30]. The Weibull mean (N_{WM}), or index of fatigue performance, describes the overall fatigue performance as a function of both the magnitude of the fatigue life and the variability of the cycles to failure[184]; specimens containing encapsulated OCA had a Weibull mean that was more than double those of specimens without capsules and with OCA-free capsules (Table 4.1).

Given the multitude of variables involved with fatigue testing, such as the sample preparation methods and geometry, the testing procedure, the storage and testing conditions, etc. it is difficult to make meaningful cross-study comparisons to determine how capsules specifically improve fracture toughness and fatigue lifetime of bone cement when compared with other additives. Furthermore, to our knowledge, no

previous studies investigating how the incorporation of encapsulated materials into bone cement affects fatigue life have been undertaken. However, this work represents a new avenue of PMMA research and confirms the potential of a self-healing biomaterial based on PMMA and OCA.

For more physiologically-relevant information, PMMA specimens were stored in Ringer's solution for 4 weeks to allow for 95% saturation of the material to mimic the behavior of the material *in vivo*[99, 100]. Capsule-free samples soaked in Ringer's displayed moderately increased lifetimes over their counterparts stored in air at RT (Figures 4.2B and 4.4B); this is supported by numerous studies investigating the effects of storage conditions on the properties of bone cement[90, 185]. Other researchers have previously reported extended fatigue life in samples soaked in saline during testing at room temperature[185] which was attributed to the plasticizing effect of the saline at the crack tip[185, 186].

Capsule-containing samples displayed reduced fatigue lifetime following storage in Ringer's at 37 ºC when compared with their counterparts stored in air at RT. While the fatigue life of OCA-free samples was reduced only slightly after storage, OCA-containing specimens displayed a marked reduction in fatigue life following storage in Ringer's solution for 4 weeks (Figures 4.2B and 4.4B). The slight reduction in fatigue life in OCA-free specimens is attributed to the infiltration of Ringer's solution between the capsule and PMMA matrix, further reducing adhesion between the two and

encouraging propagation around rather than through the capsule. Testing with OCA-containing specimens suggests that the encapsulated OCA gradually polymerizes over storage time in Ringer's solution at 37 ºC, thus reducing its healing capacity and resulting in a material with similar fatigue characteristics as one containing OCA-free capsules.

Investigation of the effects of storage conditions on capsule compressive strength reveal clear trends suggesting capsule strength was increased following exposure to physiological conditions; it is hypothesized that polymerization of the core OCA material resulting from water infiltration increased capsule shell thickness (Figure 4.6). Significant differences in compressive strength were only observed between capsules stored at RT and in Ringer's 37 ºC after 5 and 15 d of storage, suggesting that the capsules are most susceptible to moisture right after fabrication. The strengthening of capsules exposed only to moisture from the surrounding air also indicates that capsule hermeticity must be improved for this system's functionality to be maintained for periods of time prior to material implantation.

These results in combination with the fatigue studies on post-Ringer's specimens indicate the need to further shield the core material to extend the reactive lifetime of the encapsulated OCA. Individual capsules stored in air at RT reached maximum strength after 50 days of storage and exhibited increased compressive strength following only 15 d of storage time, suggesting the shelf life of the capsules could be improved. While the

rate of moisture infiltration may have been altered somewhat by the presence of the PMMA matrix, various capsule modifications could minimize water infiltration and extend capsule shelf life. Increasing the hydrophobicity of the shell material may be a promising approach to reducing water infiltration and extending the reactive lifetime of the OCA. Ongoing work is focused on modifying the PUR soft segments to increase shell hydrophobicity. Improvements to capsule/matrix adhesion could simultaneously increase the maximum allowable wt% of capsules to increase fatigue lifetime while reducing moisture infiltration to extend the functionality of the encapsulated agent.

In addition to maximizing adhesion at the shell/PMMA interface while minimizing water infiltration, visualization of healing agent release in the crack plane would enable better understanding healing agent release in response to fatigue damage. Encapsulation of dyed OCA is currently in progress to be used for this application. Given the modes of bone cement failure *in vivo*, more complex loading strategies should be employed to investigate the ability of this system to minimize crack initiation at the cement/bone and cement/stem interfaces, the response of the material following variable amplitude loading, as well as a reduction in wear debris generation.

4.6 Conclusions

Capsule inclusion above 5 wt% resulted in the decrease of B below the commercially-required levels while E was maintained at all capsule contents tested.

OCA-containing bone cement displayed superior fatigue properties at physiologically-relevant load levels when compared with control specimens and those containing OCA-free capsules. However, following storage of PMMA samples in Ringer's solution at 37 ^{o}C for 4 weeks, the reparative function of encapsulated OCA was diminished. Individual capsules demonstrated susceptibility to moisture intrusion, as indicated by increasing capsule compressive strength resulting from increased shell thickness after 50 d of storage under various conditions. These results support the need to investigate methods of reducing permeability of the capsule shell but also support the future promise of a self-healing bone cement based on OCA and PMMA.

4.7 Chapter acknowledgements

The authors would like to thank Ethicon, Inc. for the generous donation of 2-octyl cyanoacrylate. The authors also gratefully recognize the contributions of Duke University colleague Steven Owen for specimen mold fabrication in addition to Dr. Stephen Craig and Zachary Kean for polymer synthesis and Dr. Steve Wallace and Matthew Novak for assistance with statistical analyses. This research was supported by NIH grant R21 EB 013874-01 (WMR).

5. Chapter 5: Cytotoxicity testing of acrylic bone cement embedded with microencapsulated 2-octyl cyanoacrylate

Portions of the text and figures included in Chapter 5 were recently accepted for publication in the Journal of Biomedical Materials Research Part B: Applied Biomaterials. The full citation for the article is: Brochu Alice BW, Evans GA, Reichert WM. 2013. Mechanical and cytotoxicity testing of acrylic bone cement embedded with microencapsulated 2-octyl cyanoacrylate. J Biomed Mater Res Part B 2013. This article does not yet have a publication date; however, John Wiley & Sons Ltd. does not require permission for authors to reuse their own articles, but an optional grant of license will be obtained as soon as one is available. Please note that this manuscript described the work for Specific Aims 2 and 4 and was in to two chapters for this dissertation to maintain parallel structure with the Specific Aims.

5.1 Chapter synopsis

2-octyl cyanoacrylate (OCA), an FDA-approved, water-reactive tissue adhesive, was microencapsulated in polyurethane shells and incorporated into Palacos R bone cement. Extracts from Palacos R bone cement, capsule-embedded Palacos R bone cement, and OCA were prepared in complete culture medium. Viability and proliferation of MG63 human osteosarcoma cells cultured with these extracts were investigated over 24-72 h; viability was determined with live/dead staining and

proliferation was assessed using EdU staining. The effects on cell proliferation and viability in response to extracts prepared from capsule-embedded and commercial bone cements were not significantly different from each other, whereas extracts from OCA were moderately toxic to cells.

5.2 Introduction

Poly(methyl methacrylate) (PMMA) bone cement is commonly used to anchor the metallic stem of a total joint replacement to native bone and serves to uniformly transfer the body weight from the implant to the tissue. Bone cements are generally two-component materials consisting of a low molecular weight PMMA powder containing an initiator (e.g. benzoyl peroxide), and liquid MMA monomer containing an activator for the initiator. *In situ* mixing these materials initiates polymerization to yield a workable dough that is applied to the implant and cures to form a solid mass after the stem is inserted to provide stability to the implant *in vivo*[8, 171].

In addition to the comprehensive testing procedures required to determine the mechanical properties of bone cement, these materials are also subject to cytotoxicity and tissue compatibility standards. Primary toxicity concerns associated with PMMA-based bone cements include localized cell death due to the exothermic reaction of the MMA and leaching of residual monomer from the matrix[113]. An estimated 3-5% of the MMA remains 15 minutes post-polymerization and is reduced to about 1-2% over time

as the residues are eliminated through the bloodstream[114, 115]. *N*,*N*-dimethyl-*p*-toluidine, which is present in small amounts (≤ 2% of the liquid component) and initiates MMA polymerization when it reacts with benzoyl peroxide present in the powder component, is very toxic at low concentrations and is able to inhibit protein synthesis and cause chromosomal mutations[114].

Previous groups have investigated strategies to reduce the toxicity of bone cement; these primarily include the use of other monomers, such as ethyl hexylacrylate[113, 187, 188], 2-ethylhexyl methacrylate, and trimethylolpropane trimethacrylate[189], to reduce the toxicity of any residual monomer and/or decrease the curing temperature to minimize cytotoxicity and heat-induced tissue necrosis. Use of these materials have also been proposed to improve bone cement's bioactivity and mechanical strength[187, 188].

The current study presents the first characterization of the cytotoxicity of a biomaterial formulation consisting of OCA-containing microcapsules embedded in commercial PMMA bone cement. Extracts from Palacos R bone cement, capsule-embedded Palacos R bone cement, and OCA were prepared in complete culture medium. Those prepared from the capsule-embedded and commercial bone cements had little effect on cell proliferation and viability and were not significantly different from each other, whereas extracts prepared from OCA alone were moderately toxic to cells. Overall the addition of 10 wt% of OCA-containing microcapsules to the

commercial bone cement was found to have in insignificant effect on the toxicity of the material.

5.3 Experimental section

5.3.1 Reagents

Unless otherwise specified, materials were obtained from commercial suppliers and used without further purification. OCA was generously donated by Ethicon, Inc., Raleigh, NC 27616. Methyl ethyl ketone (MEK), methyl isobutyl ketone (MIBK), and cyclohexanone (Sigma Aldrich) were used as solvents and 2,4-toluene diisocyanate (TDI) and 1,4-butanediol (1,4-BD) (Sigma Aldrich) were used to synthesize the polyurethane prepolymer (pPUR) following the protocol outlined by Yang et al. and reported by the authors previously[165, 171]. Pluronic F-68 (Sigma Aldrich) was used as a surfactant. Para-toluenesulfonic acid (Sigma Aldrich, PTSA) was added to the organic phase as a stabilizer for the OCA monomer. Commercially-available Palacos R PMMA bone cement (Zimmer) was used for all experiments reported herein. Loctite® Super Glue and copper sheets were also purchased and used as received.

Minimum Essential Medium Eagle (Sigma), heat-inactivated fetal bovine serum, sodium pyruvate, non-essential amino acids, and penicillin-streptomycin (Gibco) were used for cell culture. Calcein AM, Hoechst 33342, Click-iT EdU Alexa Fluor 488 kit

(Invitrogen), and Dulbecco's Phosphate Buffered Saline (Gibco, DPBS) were used in cell staining procedures.

5.3.2 Microcapsule preparation

Microcapsules were prepared and characterized as described previously[171]. Briefly, at room temperature, Pluronic F-68 surfactant (1.84 g) was dissolved in deionized water (90 mL) in a 250 mL beaker. The solution was agitated for 1 h with a digital mixer (VWR PowerMax Elite Dual-Speed Mixer) before beginning the encapsulation procedure. The aqueous phase was suspended in a hot water bath and heated to 50 ºC prior to the addition of the organic phase and chain extender.

OCA (4 mL) was dissolved in MIBK (8 mL) and pPUR (3 g) was dissolved in MEK (10 mL) separately at room temperature. PTSA (1%) was added to the OCA-MIBK solution to further stabilize the OCA monomer. The pPUR- and OCA-containing solutions were then added simultaneously to the aqueous phase but not mixed prior to this addition. After the organic and aqueous phases were combined, the 1,4-BD (3 mL) chain extender was added dropwise to the stirring mixture via a syringe to form the segmented PUR shell material consisting of hard TDI-based segments and soft 1,4-BD segments. After a reaction time of 2 h at an agitation rate of 700 rpm, the mixer was switched off and the suspension of microcapsules rinsed with deionized water and vacuum filtered. Capsules were air-dried prior to use in the following experiments[171].

5.3.3 Biocompatibility of capsule-containing bone cement

5.3.3.1 Preparation of bone cement and OCA extracts

The powder component was mixed with the liquid component according to the manufacturer's instructions[177], OCA-containing capsules were added to the slurry, and the resultant material was added to rectangular silicone rubber molds to form the desired extraction specimens (Figure 5.1A). Samples containing 0 or 10 wt% OCA-containing capsules were prepared; the total particulates (OCA-containing capsules plus PMMA powder) in the composites were held constant at 67 wt%. Samples were cured in the molds for 1 h, released, cured at RT for an additional 23 h and then autoclaved at 120 ºC for 30 minutes. Each sample was then immersed in a 50 mL conical tube containing sterile complete culture medium and incubated for 24 h at 37 ºC[113] (Figure 5.1B). A ratio of 0.2 g bone cement to 1 mL extract medium was maintained[190].

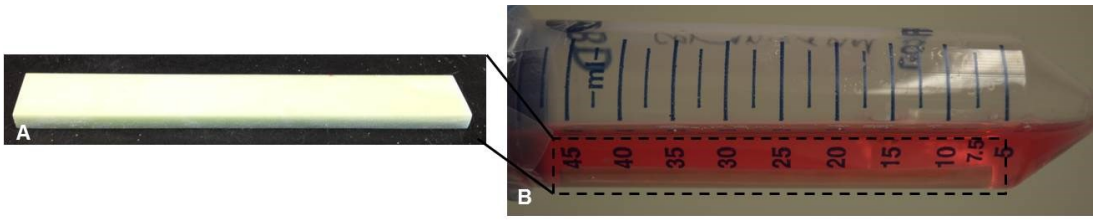

Figure 5.1: (A) Rectangular specimens were prepared and (B) extracted into complete culture medium in a 50 mL conical tube.

To prepare OCA extracts, 15 μL OCA was added to 5 mL culture medium and incubated at 37 ºC for 24 h in a 15 mL conical tube[191, 192]; the OCA polymerized immediately upon contact with the culture medium. As the OCA was not received sterile, the media was then filtered prior to use in these experiments. Loctite® Super Glue (ethyl cyanoacrylate) and copper sheets[113] were selected as liquid and solid positive controls for these studies. To prepare the Super Glue extracts, 15 μL of Super Glue was added to 5 mL culture medium and incubated at 37 ºC for 24 h in a 15 mL conical tube; the Super Glue polymerized immediately upon contact with the culture medium. Copper samples were immersed in a 15 mL conical tube and incubated at 37 ºC for 72 h; a ratio of 0.2 g copper to 1 mL extract medium was maintained[190]. Extracts from the Super Glue and copper were both filtered prior to addition to cells.

5.3.3.2 Cell viability and proliferation

MG63 human osteosarcoma cells have been used in numerous biocompatibility studies[113, 114, 117-120] because they share several features with normal human osteoblasts, including secretion of insulin-like growth factor, binding proteins, matrix metalloproteinases, and osteocalcin. Similar to undifferentiated osteoblasts, MG63 cells also synthesize collagen types I and III and have a low basal expression of alkaline phosphatase that is increased in response to 1,25-dihydroxyvitamin D_3[120, 193].

MG63 human osteosarcoma cells were cultured in Minimum Essential Medium Eagle supplemented with 10% heat-inactivated fetal bovine serum, and 1% each of sodium pyruvate (100 mM), non-essential amino acids (100x), and penicillin-streptomycin (10,000 units/mL penicillin and 10,000 μg/mL streptomycin). The cells were routinely passaged and incubated at 37 ºC in a humidified environment of 5% CO_2 in air.

Cells were passaged and plated in 96-well plates at a density of 2000 cells/well and allowed to attach for 24 h. After 24 h, the growth media was replaced by the same volume of treatment media. Media was also changed in the control wells so that cells in all wells were exposed to a media change 24 h after plating. For all experiments, cells in 3 different wells received each treatment and the experiments were performed 4 times with new extract media prepared from different material samples for each trial.

To investigate the effects of bone cement extract, four treatment groups were studied: an undiluted extract from capsule-free PMMA; undiluted extract from capsule-embedded PMMA (10 wt% capsules); and extract from capsule-embedded PMMA (10 wt% capsules) diluted to 50 and 25% using fresh media[113]. To investigate the effects of OCA extract, three treatment groups were studied: OCA extract diluted to 50, 25, and 10% using fresh media[191]. A negative control of cells not treated with any material extract and positive controls of cells treated with extract prepared from Loctite® Super Glue and copper sheets were also investigated.

Cell viability was assessed by a combination of staining with calcein AM and Hoechst 33342. After 72 h culture, the various treatment media were removed and cells rinsed twice with DPBS containing calcium chloride and magnesium chloride (1X), then incubated at 37 ºC in calcein AM in DPBS (0.75 μL/1.5 mL) for 20 minutes. The DPBS containing calcein AM was removed and the cells were rinsed twice with DPBS and incubated an additional 20 min at 37 ºC in DPBS containing Hoechst 33342 (1.5 μL/1.5 mL). The DPBS containing Hoechst 33342 was removed and the cells were rinsed twice with DPBS, and then imaged using a Nikon Eclipse TE2000-U inverted fluorescence microscope and NIS Elements software (Nikon). Images were analyzed with ImageJ.

Cell proliferation was investigated with EdU staining following the manufacturer's instructions included with the Click-iT EdU Alexa Fluor 488 kit. The stain was performed following 24, 48, and 72 h of culture with the treatment extracts to examine potential effects of extract dilution and exposure time on proliferation. The plates were imaged using a Nikon Eclipse TE2000-U inverted fluorescence microscope and NIS Elements software (Nikon). Images were analyzed with ImageJ.

5.3.4 Statistical analyses

Statistical analyses were performed to compare the results of treatment cultures with respect to the negative and positive controls using a one-way analysis of variance

with the significance of individual differences established by Tukey post-hoc test. In all cases the level of statistical significance was set at $p < 0.05$.

5.4 Results

5.4.1 Capsule morphology

Capsules fabricated at an agitation rate of 700 rpm were shown to have uniformly spherical morphology with average diameter and shell thickness of 121 ± 24 μm and 3 ± 0.9 μm, respectively, consistent with measurements obtained previously[171, 181]. Capsules made at this agitation rate were used for all experiments.

5.4.2 Cytotoxicity testing of OCA and capsule-embedded bone cement

5.4.2.1 MG63 viability

The cytotoxic effects of leachates extracted from unfilled bone cement, bone cement filled with 10 wt% capsules, and OCA tissue adhesive were assessed after 72 h exposure using calcein AM staining to detect live cells and Hoechst 33342 staining to detect all cells. Cells cultured in media containing no material extract served as negative controls. Loctite® Super Glue (ethyl cyanoacrylate) and copper sheets[113] were used as positive controls. Microscope images revealed that while cells in the treatment groups were still surviving at 72 h, the viable cells covered area less of the well when compared with controls that received no extract (Figures 5.2 and 5.3). Viability was assessed as the

total area covered by live cells in the treatment groups compared to coverage by live cells observed in control samples not treated with any extract[194].

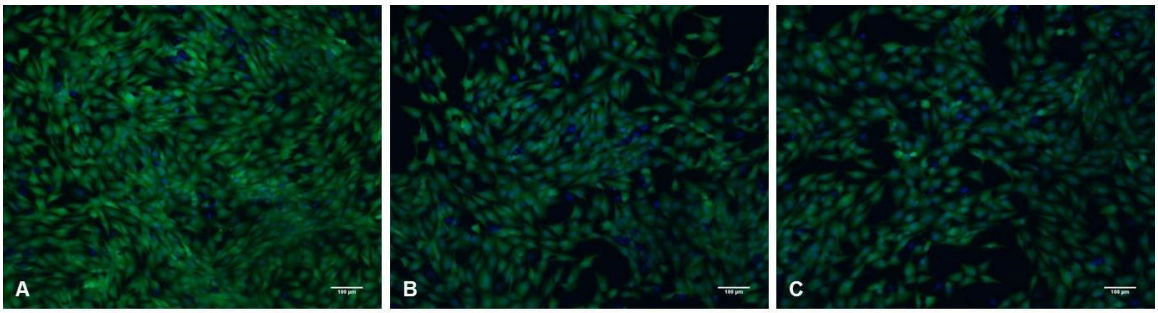

Figure 5.2: Viability of MG63 cells following 72 h exposure to (A) control media, (B) undiluted extract prepared from unfilled and (C) filled bone cements. Green – calcein; blue – Hoechst 33342.

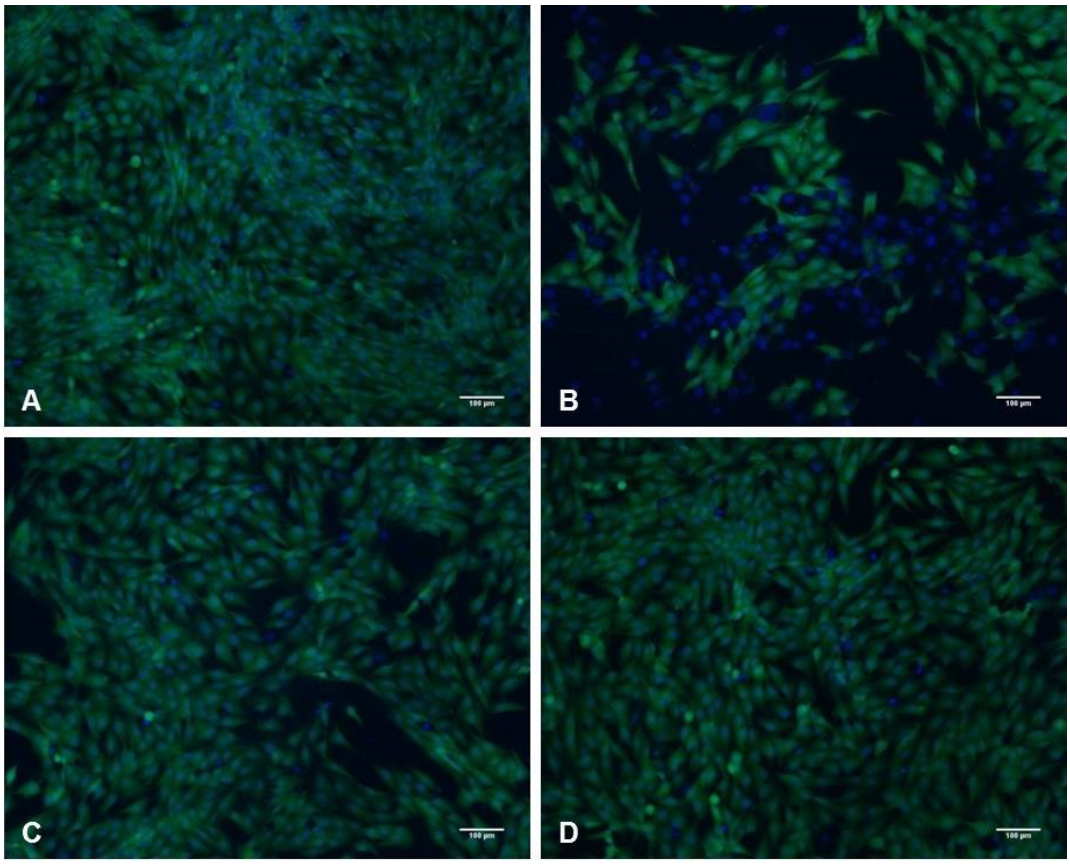

Figure 5.3: Viability of MG63 cells following 72 h exposure to (A) control media and media containing OCA extract diluted to (B) 50%, (C) 25%, and (D)10% using fresh medium. Green – calcein; blue – Hoechst 33342.

Extracts from all bone cement specimens exhibited significantly reduced cell viability compared to the negative control but not with respect to each other; a slight but not significant dose-dependent response was also observed (Figure 5.4A). In contrast, extracts from OCA-containing medium showed a significant reduction in coverage by live cells for all dilutions with respect to control samples and a significant dose-dependent dilution effect was observed (Figure 5.4B). No live cells were present following 72 h culture with extract from either the copper or Super Glue positive controls.

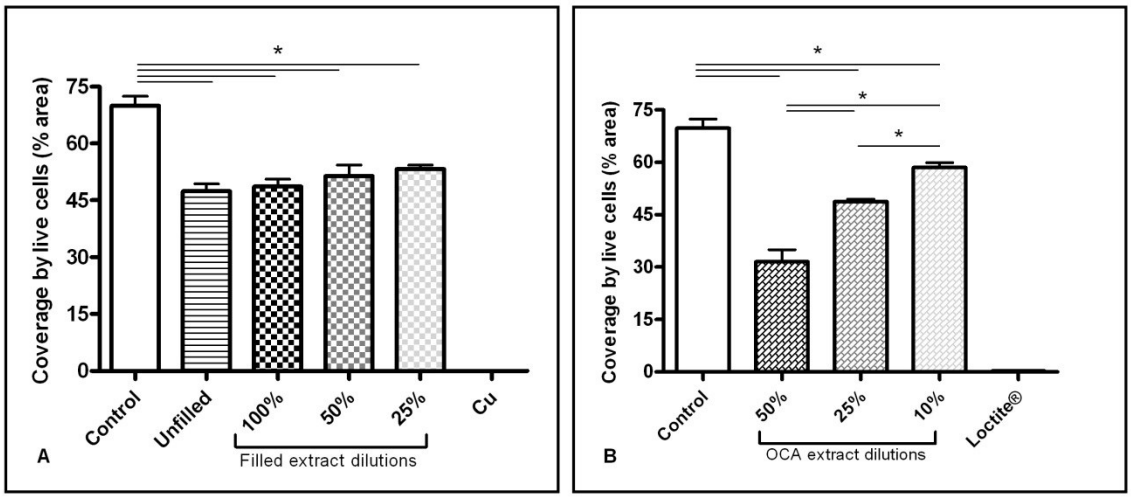

Figure 5.4: Viability of MG63 human osteosarcoma cells after 72 h exposure to (A) PMMA bone cement and (B) OCA extracts (average ± SEM, n=4). Coverage by live cells in the positive controls, Cu and Loctite®, were significantly different from all treatment groups though significance is not indicated on the figures.

5.4.2.2 MG63 proliferation

The effects of bone cement and OCA extracts on MG63 cell proliferation over 24, 48, and 72 h are shown in Figures 5.5-5.8. Compared to extract-free negative controls, cell proliferation was significantly reduced upon exposure to undiluted extracts from unfilled and filled bone cement and to 50% diluted extracts from OCA at all time points, but proliferation trended upwards with increased dilution of the extracts.

Overall, microscope images revealed that cell proliferation in undiluted extracts from unfilled and capsule filled bone cements were nearly indistinguishable (Figure 5.5), indicating that the addition of capsules to the bone cement did not significantly affect proliferation of cells at 24, 48, or 72 h (Figures 5.8A-C). However, the dose-dependent dilution effect for capsule-filled bone cement was significant only at 48 h between undiluted extracts and extract diluted to 25%.

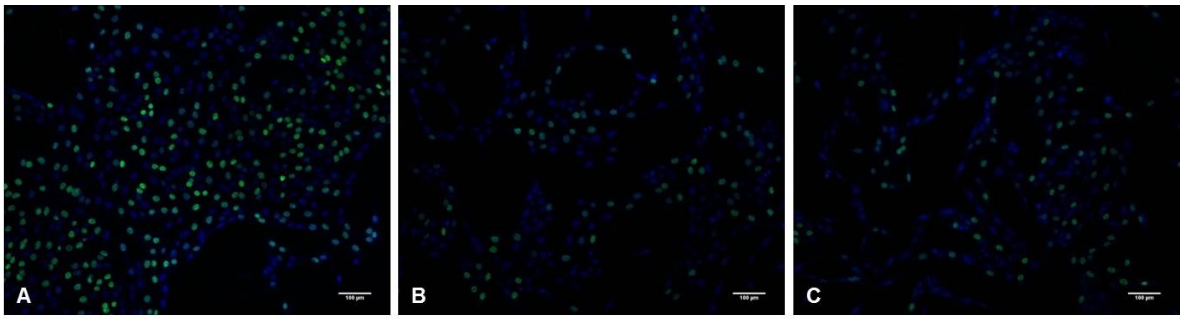

Figure 5.5: Proliferation of MG63 cells after 24 h exposure to (A) control media and undiluted extracts prepared from (B) unfilled and (C) filled bone cements. Green – EdU; blue – Hoechst 33342.

In contrast, extract obtained from OCA had a more substantial effect on curtailing cell proliferation, thus requiring that 50% dilution be the least diluted extract tested (Figure 5.6).

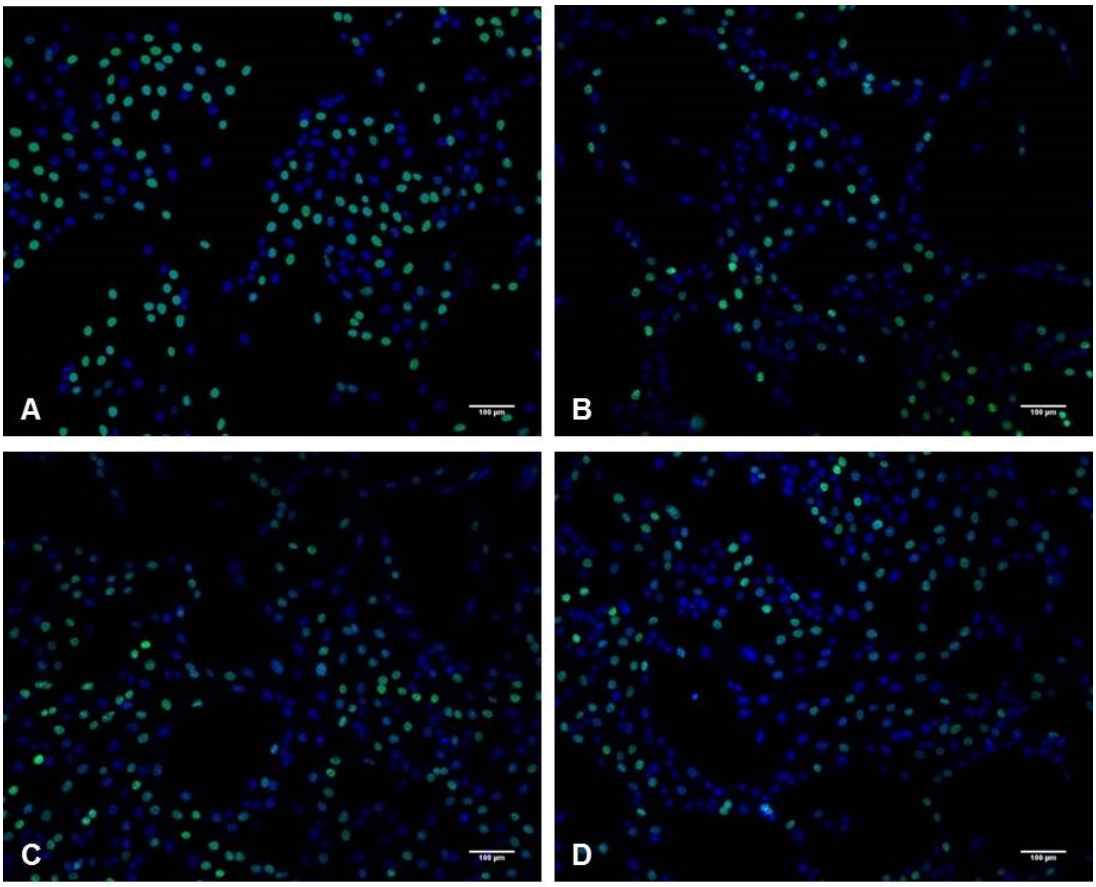

Figure 5.6: Proliferation of MG63 cells following 24 h exposure to (A) control media and media containing OCA extract diluted to (B) 50%, (C) 25%, and (D) 10% using fresh medium. Green – EdU; blue – Hoechst 33342.

A significant decrease in the proliferation of cells exposed to OCA extract-containing medium diluted to 50% was observed at each time point with respect to the negative control, with the largest decrease observed after 48 h (Figure 5.7).

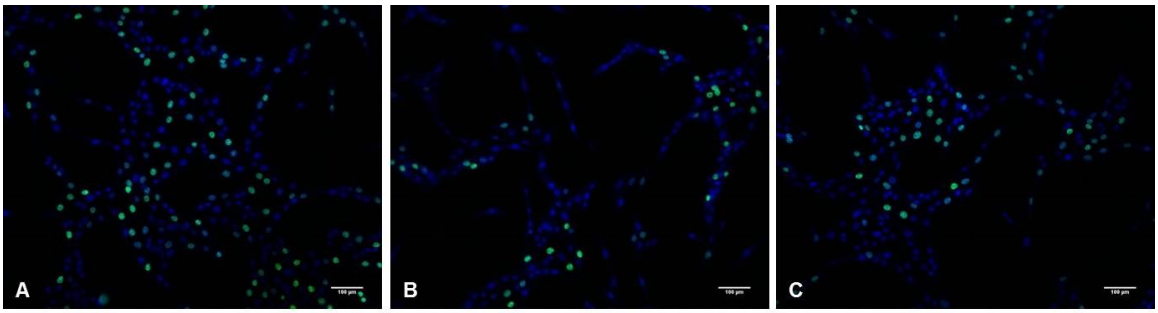

Figure 5.7: Proliferation of MG63 cells exposed to OCA extract media diluted to 50% for (A) 24 h, (B) 48 h, and (C) 72 h. Note the recovery of proliferation between 48 and 72 h, suggesting the effects of OCA on MG63 cell proliferation may be transient. Green – EdU; blue – Hoechst 33342.

The dose-dependent dilution effect for OCA extract was significant between all dilutions at 48 h and between 50% and 10% at 72 h (Figures 5.8D-F). Treatment with extract from Super Glue and copper sheets eliminated proliferation at every time point. Additionally, cells in all groups exhibited decreased proliferation over time.

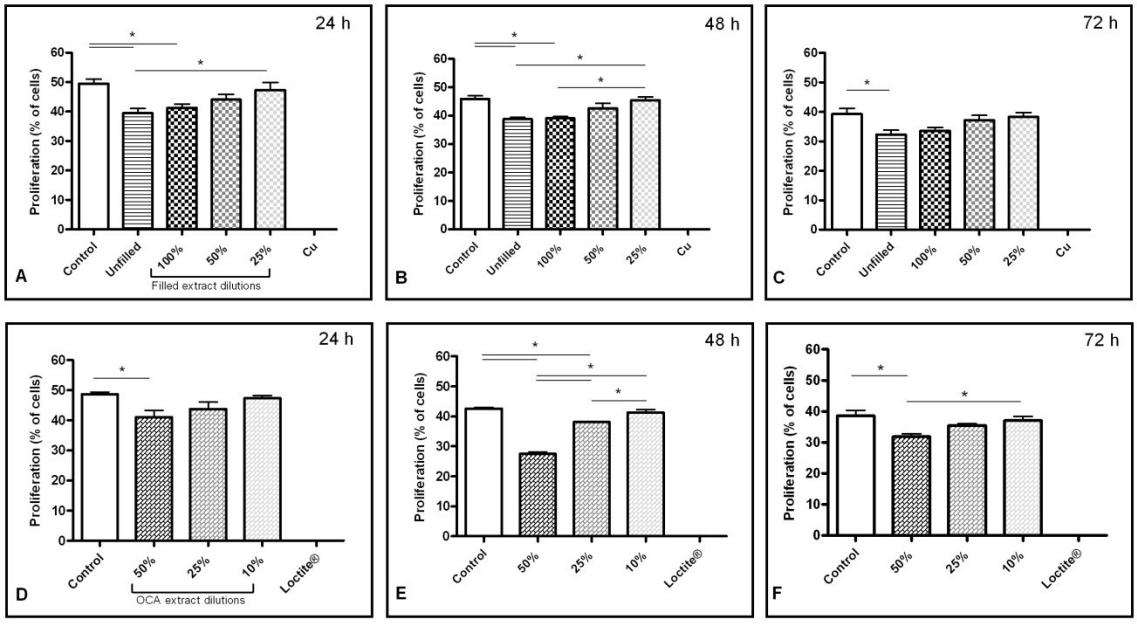

Figure 5.8: Proliferation of MG63 human osteosarcoma cells in response to growth in extract from (A,B,C) bone cement and (D,E,F) OCA after (A,D) 24 h, (B,E) 48 h, and (C,F) 72 h (average ± SEM, n=4). Proliferation of cells in the positive controls, Cu and Loctite®, were significantly different from all treatment groups though significance is not indicated on the figures.

5.5 Discussion

This work is an assessment of basic biocompatibility measures for the first bone cement based on a self-healing material. Each test was designed to examine how capsule incorporation affected the cytotoxicity of the bone cement relative to the unfilled control as well as how cells responded to the healing agent alone.

Numerous investigations of the cytotoxicity of various bone cement formulations have been reported[113, 114, 117, 195-197]. As the toxicity associated with bone cement has been primarily attributed to the MMA monomer and its activator[113-115], both of which are unchanged in the capsule-embedded formulation, the similar cellular responses observed between the filled and unfilled bone cements were anticipated (Figures 5.2, 5.4A, 5.5, and 5.8A-C).

Similar to the results presented here, previous studies found the proliferation of MG63 cells to be reduced as the exposure time to bone cement extracts was increased[114]. However, these results also indicate the addition of capsules did not significantly affect cell proliferation or viability in response to PMMA bone cement. It is also accepted that the toxic effects of bone cement on cells and tissue primarily occurs before and during polymerization *in vivo*[114, 198]; potential evaporation of residual MMA during the curing and autoclaving procedures may have reduced its presence in the bone cement extracts. As MMA is a major toxicity concern associated with bone cement[113-115] the added opportunities for its removal influenced the *in vitro* survival and continued proliferation

of cells. These *in vitro* analyses do not fully reflect what happens to the cells as the PMMA cures *in vivo* but do support the potential promise of the system.

There are also numerous studies dedicated to analyses of toxicity of cyanoacrylate adhesives for clinical applications[191, 192, 199, 200], albeit not in the context of a self-healing material. Cyanoacrylate adhesives degrade into formaldehyde and cyanoacetate, which may cause tissue irritation[192, 199-203]. Shorter chain cyanoacrylate adhesives such as the Loctite® positive control used here are known to be more toxic than longer alkyl chain adhesives such as OCA[192, 199-204].

Proliferation and viability testing of OCA extracts (Figures 5.3, 5.4B, 5.6, 5.7 and 5.7D-F) clearly showed the OCA had a toxic effect on the MG63 cells in culture, and extracts from the Loctite® positive control killed virtually all of the cells. Similar to the work of others with various cyanoacrylates, these results showed both time- and dose-dependent effects on cell proliferation and viability[192, 200]. While OCA extract diluted to 50% and 25% significantly decreased proliferation with respect to the negative control, there was no significant decrease in proliferation of cells treated with 10% OCA extract, suggesting the effects of the extract were mediated through the dilution of the extract. Therefore, it is hypothesized that some effects of both PMMA and OCA on surrounding cells may be mediated through clearance (e.g. dilution) of the released leachates *in vivo*. Furthermore, as the OCA is intended polymerize within the PMMA matrix upon contact with moisture, limited exposure to cells is anticipated.

Although cell death was visualized with viability staining, in areas where the cells grew in large aggregates it was difficult to identify single cells to get an accurate measure of cell number and determine which cell nuclei were associated with each cytoplasmic calcein stain indicating a live cell. Therefore, viability was determined as the total area covered by live cells in the treatment groups compared to coverage by live cells observed in control samples[194]. Quantifying viability as a measure of cell coverage allowed for slight changes in cell morphology to be taken into account (Figure 5.3B), but depends on the effects of extract on cell proliferation. As some cells were still living after treatment with various extracts but their number and area coverage was diminished, the inhibition of proliferation may be a more sensitive marker for biocompatibility than viability stains; reduced proliferation could account for the significantly reduced coverage by live cells observed in more concentrated extracts[194].

5.6 Conclusions

The effects of extract from a capsule-embedded bone cement on the proliferation and viability of MG63 human osteosarcoma cells indicated the addition of capsules did not significantly affect the viability and proliferation of the cells in response to the PMMA. The effects of both capsule-embedded bone cement and OCA extracts were found to be mediated somewhat through dilution of the extract. Even though an extensive and comprehensive cytotoxicity analysis was not the goal of these

experiments, these findings support the future promise of this system and indicate its toxicity is similar to existing commercial formulations.

5.7 Chapter acknowledgements

The authors would like to thank Ethicon, Inc. for the generous donation of 2-octyl cyanoacrylate. The authors also gratefully recognize the contribution of Duke University colleague Steven Owen with respect to specimen mold fabrication in addition to Dr. Stephen Craig and Zachary Kean for polymer synthesis and Matthew Novak for assistance with statistical analyses. This research was supported by NIH grants T32-GM8555 (ABWB) and R21 EB 013874-01 (WMR).

6. Chapter 6: Dissertation summary and future work

6.1 Dissertation summary

This project was motivated by the clinical need to improve the functional lifetime of cemented TJRs. The following hypotheses were tested: (1) reactive OCA can be successfully encapsulated and the resulting capsules thoroughly characterized; (2) the static mechanical properties of the PMMA composite can be improved or maintained through inclusion of an optimal wt% of OCA-containing capsules; (3) PMMA containing encapsulated OCA has a prolonged lifetime when compared with a capsule-free PMMA control as measured by the number of cycles to failure; and (4) the addition of capsules to the PMMA does not significantly alter the biocompatibility of the material. The specific aims of the project were to: (1) use interfacial polymerization techniques to encapsulate reactive OCA healing agent and characterize the properties of the resulting capsules; (2) determine the effects of capsule content on the tensile, compressive, and fracture toughness properties of PMMA to identify an optimal maximum allowable wt%; (3) examine the fatigue lifetime of capsule-embedded and capsule-free commercial samples to assess the functionality of the self-healing system; and (4) investigate the viability and proliferation of MG63 human osteosarcoma cells when treated with extracts from capsule-containing bone cement as a preliminary assessment of biocompatibility.

In Chapter 2, the optimization of the encapsulation of OCA within PUR capsules and subsequent capsule characterization was presented. Interfacial polymerization of PUR and 1,4-BD in an oil-in-water emulsion was used to encapsulate OCA. Average capsule diameter and shell thickness were dictated by agitation rate though the ratio of thickness/diameter remained fairly consistent, ranging from 0.01-0.02 regardless of the rate used during capsule fabrication. TGA analyses revealed the multiphasic thermal degradation behavior of OCA-containing capsules; from this data, it was determined that the OCA content of the capsules ranged from 46-58% depending on the agitation rate used. The compressive strength of individual capsules made at different speeds ranged from 8.3 to 13.6 MPa; this variability was attributed to variations in percent fill of the capsules as well as the shell thickness in capsules fabricated a different agitation rates, with thicker shells observed at slower agitation rates. To investigate the functionality of the encapsulated OCA, capsules were crushed between two plates and the detachment force necessary to separate the bonded plates was recorded. Finally, capsules were incorporated into a PMMA matrix as a preliminary assessment of process survivability. Results from Chapter 2 supported the hypothesis that reactive OCA could be encapsulated and the resulting capsules thoroughly characterized; the results also supported progression to mechanical testing of capsule-embedded specimens.

Various mechanical properties of PMMA specimens embedded with encapsulated OCA were determined and presented in Chapter 3. The tensile and

compressive properties of the PMMA/capsule composite were maintained at capsule contents up to 5 wt%; above this content, the required strengths were no longer sustained. Compression samples containing 10 wt% or fewer capsules deformed plastically upon failure whereas specimens with higher capsule contents (≥ 25 wt%) fragmented upon failure. Fracture toughness was increased slightly by the inclusion of 3 wt% capsules and remained within the range of literature-reported values for fracture toughness of PMMA at all capsule contents tested (0-15 wt%). Increased fracture toughness suggests the ability of capsules to slow crack propagation rates to contribute to material lifetime extension. The results in Chapter 3 confirmed the hypothesis that the static mechanical properties of a PMMA composite could be maintained or improved through the inclusion of an optimal wt% of OCA-containing capsules, in this case, up to 5 wt%.

In Chapter 4, studies investigating the functional lifetime of capsules, the bending strength of capsule-containing specimens, and the effects of capsules on PMMA fatigue lifetime were presented. Capsules demonstrated some susceptibility to moisture intrusion as evidenced by the increase in shell thickness and subsequently in individual capsule compressive strength. Similar to UTS and UCS, bending strength was decreased with increased capsule wt% while the bending modulus remained largely unchanged regardless of the capsule content. Following storage in Ringer's solution at 37 ºC, the bending strengths of unfilled specimens was virtually unchanged while *B* of samples

filled with 5 wt% encapsulated OCA was increased by 17%. The bending moduli of unfilled and filled specimens were reduced slightly following storage in Ringer's; *E* decreased by 7.9% and 12.6%, respectively for unfilled and filled samples. This decrease is attributed to reduced deflection undergone by samples prior to failure post-storage in Ringer's solution.

Fatigue lifetime was increased in samples containing capsules when compared with unfilled controls; the effect of the OCA was confirmed through cyclic testing of PMMA specimens containing OCA-free capsules. At low applied cyclic loads, the index of fatigue performance of OCA-containing bone cement stored in air at RT was increased 2.5 and 1.8 times when compared to specimens containing OCA-free capsules and specimens without capsules, respectively. However, when samples were tested following storage in Ringer's solution, there was a pronounced effect on the fatigue lifetime of samples filled with encapsulated OCA while the number of cycles to failure of unfilled samples stored in Ringer's was increased. It was also determined that at cyclic loading to an upper force of ≤ 40 N without storage in Ringer's solution, the OCA-containing samples could undergo an increased number of cycles to failure with respect to the other specimen types. The results of the experiments performed in Chapter 4 support the hypothesis that PMMA containing encapsulated OCA has a prolonged functional lifetime as measured by the cycles to failure but that the capsules may be

susceptible to moisture infiltration, and therefore have a diminished functional lifetime, in their intended *in vivo* environment.

Biocompatibility analyses of the components of the self-healing system were presented in Chapter 5. Extracts from all bone cement samples were found to significantly reduce the viability of MG63 human osteosarcoma cells when compared to the negative control but not with respect to each other; additionally, a slight but not significant dose-dependent response was observed through extract dilution. In contrast, extracts from OCA alone showed a significant reduction in coverage by live cells for all dilutions with respect to control samples as well as a significant dose-dependent dilution effect. Compared to extract-free controls, cell proliferation was significantly reduced upon exposure to undiluted extracts from capsule-free and capsule containing controls; however, overall MG63 proliferation in undiluted extracts from capsule free and capsule embedded bone cements were nearly indistinguishable. This indicates that the addition of capsules did not significantly affect proliferation after 24, 48, or 72 h. A dose-dependent dilution effect for capsule-containing specimens was significant only at 48 h between undiluted extract and extract diluted to 25%.

OCA was observed to have a more substantial effect on curtailing proliferation, thus requiring that a 50% dilution to be the least diluted extract tested; widespread cell death was observed in studies performed with undiluted OCA extract. Proliferation was significantly decreased in cells exposed to OCA extract diluted to 50% with respect

to the negative control at every time point and the largest decrease was observed after 48 h. Modest recovery after 72 h suggests that proliferation may not be permanently reduced by this extract. There was also a significant dose-dependent effect for OCA extract for all dilutions at 48 h and between 50% and 10% at 72 h. The results in Chapter 5 confirmed that the addition of capsules to the PMMA did not significantly alter the proliferation and viability of cells exposed to the bone cement. While OCA displayed some cytotoxic effects, they were decreased through extract dilution, suggesting that clearance *in vivo* may mediate any cell toxicity.

Overall the results presented in this dissertation support the feasibility of a self-healing bone cement system based on OCA. Specifically, we found that functional OCA could be encapsulated within PUR shells and successfully incorporated into PMMA bone cement. Lower wt% of capsules was found to maintain the tensile, compressive, fracture toughness, and bending properties of the PMMA. The inclusion of 5 wt% of OCA-containing capsules in the matrix increased the number of cycles to failure when compared to unfilled specimens and those filled with OCA-free capsules while maintaining material biocompatibility. It was also determined that OCA-containing samples had superior fatigue performance at lower loads more relevant to those observed *in vivo*. Storage of capsules in Ringer's solution 37 ºC resulted in increased individual microcapsule compressive strength; Ringer's solution moderately affected the bending strength and modulus, and increased the number of cycles to failure in unfilled

specimens. In OCA-filled samples, the number of cycles to failure was decreased following storage in Ringer's solution for 4 weeks, suggesting capsules are susceptible to moisture infiltration and subsequent OCA polymerization.

6.2 Future work to complete current studies

In Chapter 3, the fracture toughness of TDCB samples of capsule-free and capsule-embedded PMMA was determined and presented in Figure 3.4. In the work presented in Chapter 4, samples of PMMA containing OCA-free capsules were used to assess the effects of the capsules themselves on the fatigue properties of the material. The fracture toughness of samples of PMMA containing OCA-free capsules could also be determined to complete this study.

Similarly, moisture infiltration into OCA-free capsules could also be investigated to help investigate the effects of Ringer's on the encapsulated OCA and on the PUR shell itself. The increase in capsule compressive strength observed in Figure 4.1 was attributed to polymerization of the core OCA contents and swelling of the PUR shell itself; similar analyses with OCA-free capsules could provide information that would support or negate the hypothesis that the PUR swelling in the Ringer's solution over time contributed to increased shell thickness. Additionally, fatigue testing of PMMA samples filled with OCA-free capsules following storage in Ringer's solution at 37 ºC for 4 weeks is also in progress.

To gain a better understanding of the mechanisms of OCA release in response to fatigue damage, dye visualization studies could aid in determining capsule distribution and healing agent release in response to damage. Given the lower wt% of capsules used in these experiments and the opacity of the PMMA, dyes with high contrast in the green Palacos R material, such as Oil Red, Sudan Black B, and D&C Violet, are all currently under investigation for this application (work not shown). It is hypothesized that the inclusion of dye would not alter the mechanical or release properties of the capsules, but visualization of the released contents would enable assessments of the effectiveness of the system. Information on capsule distribution as well as quantification of healing agent release would provide valuable insights into the limits of the system.

6.3 Implications of this research

This work represents the first introduction of a matrix repolymerization-based SHM to a biomedical application. As discussed in Chapter 1, over 1 million TJR procedures are estimated to be performed in 2013, with the numbers projected to increase significantly as the population ages and patients require TJRs at younger and more active ages. All primary and revision procedures have the potential to fail as a result of accumulated material microdamage; any action taken to extend the functional lifetime of cemented implants could translate to years of improved patient quality of life, as well as reduced hospital costs.

The promising fatigue lifetime results presented in Chapter 4 support the progression of testing into more biomimetic *in vitro* analyses and to assessments of *in vivo* biocompatibility and functionality. The presence of encapsulated OCA increased PMMA fatigue life more than the addition of capsules alone (Figures 4.4, 4.5, and 4.8), suggesting that encapsulation of various liquids and oils, even those not meant to react upon release, could be used to increase the fatigue life of other composites used across numerous engineering applications.

In the most straightforward sense, this project demonstrates the encapsulation of cyanoacrylate that retains its functionality post-encapsulation. This technique, or modified versions of it, could have applications across many engineering disciplines, particularly those in which toxicity of the system is less important than the water reactivity of the encapsulated agent. The removal of this constraint could allow for more effective encapsulation procedures through the use of more toxic, though less water miscible, solvents and shell materials.

The potential benefits from and enormous growth in the area of self-healing biomaterials are evident. Although bone cement was selected as the focus of this dissertation, numerous other implants fail following years of cyclic usage and new designs for such implants should also be considered for additional self-healing applications. These implants include artificial heart valves, load-bearing surfaces of TJRs, dental implants, orthopedic nails and screws, and vertebral disc replacements,

among others[47]. By being the first to enter this nascent field, we hope to encourage other biomedical engineers to utilize SHM strategies for existing applications and to inspire current self-healing researchers to identify uses for their techniques within biomaterials.

6.4 Future directions for the self-healing bone cement project

This project was intended to investigate the feasibility of a SHM based on OCA and PMMA bone cement. While the results within this dissertation are promising, at this stage, there are numerous directions in which the project could go to develop a bone cement that could be clinically-implemented to reduce the likelihood of TJR failure and the need for revision procedures. Future work should focus on improving the functional lifetime of the encapsulated material and gaining a more comprehensive understanding of the mechanisms of OCA release and repair within the PMMA. More complex fatigue testing strategies will need to be investigated in addition to in-depth and clinically-relevant assessments of the material's *in vitro* and *in vivo* biocompatibility.

The results in Chapter 3 indicate that bonding at the capsule/matrix interface could be improved; capsule pull-out and crack propagation around (rather than through) capsules were observed in some specimens. As presented in Chapter 4, the capsules also demonstrated susceptibility to moisture intrusion, thus limiting their storage and functional lifetimes. Capsule mechanical strength increased following

exposure to physiological conditions and was attributed to polymerization of the core OCA material and swelling of the PUR shell material, each of which is undesirable for long-term stability and functionality of this self-healing system. Potential solutions to these problems may require the selection of a new capsule material or modification of the current PUR material to increase adhesion between the capsule shell and PMMA matrix and to increase capsule hydrophobicity to minimize water infiltration.

Preliminary studies were performed to functionalize the PUR shell to improve capsule adhesion to the matrix and increase capsule hydrophobicity. An alkene bond was introduced into the small diol used as the chain extender during capsule fabrication (Figure 6.1).

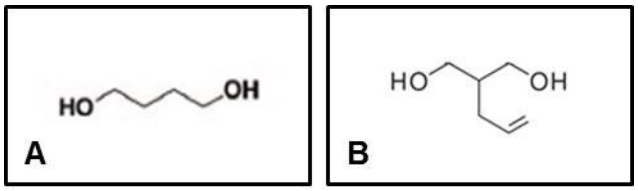

Figure 6.1: The structure of the 1,4-BD chain extender currently used in encapsulation procedures is shown in (A) while the structure of a proposed potential chain extender, 2-allyl-1,3-propanediol, is shown in (B).

Alkene bonds can be used to react with any number of chemistries to tailor the surface properties of the capsules but is not anticipated to react with the OCA monomer during encapsulation or over long storage periods. The modified diol, 2-allyl-1,3-propanediol (PD), has been successfully utilized in the encapsulation procedure. As a proof-of-concept study to determine whether or not this modified diol could be used to increase PUR hydrophobicity, thin films were made by reacting the pPUR with a chain extender of either 1,4-BD or PD during a spin-coating process. The films were covered in a 1:1 solution of 1*H*,1*H*,2*H*,2*H*-perfluorodecanethiol:isopropyl alcohol and exposed to UV (254 nm) light for 60 min; this particular thiol was selected because its high hydrophobicity allowed for easy detection via contact angle measurements. Following the thiol reaction, the films were rinsed with isopropyl alcohol and F-toluene. A goniometer was used to measure contact angle of films made with various combinations of the chain extenders treated with the thiol (Table 6.1).

Table 6.1: Effect of thiol functionalization on contact angle of PUR films

Sample type	Functionalization	Contact angle
PUR + 1,4-BD	None	77.3 ± 0.3
PUR + PD	None	76.4 ± 1.3
PUR + 1,4-BD	Perfluorodecanethiol	78.1 ± 0.6
PUR + PD	Perfluorodecanethiol	96.7 ± 2.2

This data suggests that fabricating films with different the chain extenders did not significantly affect the PUR hydrophobicity, as indicated by the contact angles of 77.3 ± 0.3 and 76.4 ± 1.3. Furthermore, the thiol was observed only to react with the alkene present on films made with PD while the contact angle was relatively unchanged in films made with 1,4-BD treated with the thiol from the untreated controls.

While a promising future direction for this project, infinitely many factors could be changed to tailor the properties of the PUR + PD, including: the concentration of the thiol solution, the type of thiol used, the UV exposure time, the solvents used for rinsing, etc. Additionally, the PUR used in these experiments was fabricated using 1,4-BD as the soft segment; varying the ratio of 1,4-BD to PD in the pPUR itself could also play a role in the functionalization of the PUR material. Other thiols, such as 6-mercapto-1-hexanol and (3-mercaptopropyl)trimethoxysilane could be investigated for their hydrophobicity and potential interactions with the PMMA matrix. However, there are significant challenges to this approach, most notably, the ability to evenly functionalize the rounded surfaces of capsules.

In addition to chemical modifications of the PUR already used for the OCA encapsulation, alterations to the physical properties of the capsule, such as changing the shell material[168] or adding a coating[167, 179], could be investigated to further promote adhesion via increased surface roughness. Polyethylene and silica could be investigated as potential capsule materials given that MMA does not affect these materials and

therefore the capsules could be exposed to the monomer for a longer period of time, improving the mixability and workability of the capsule-containing PMMA. This would simplify the sample preparation procedure and reduce the potential for voids and defects in the final capsule-embedded samples. It may also be worthwhile to investigate other solvents to improve encapsulation. In Chapter 2, data was presented indicating that solvent comprised less than 7% solvent[171]; given the small volume of solvent that remains in the final capsules, perhaps the use of a more toxic solvent would improve encapsulation efficiency without increasing the overall material toxicity. Use of such solvents could expand the number of materials able to be used for the encapsulation procedure. Previous work has also indicated the potential of encapsulations based on oil-in-oil-in water emulsions utilizing paraffin oil for the encapsulation of OCA[205]; this work could be continued in the future to determine the system's efficacy once embedded into a PMMA matrix.

Any strategies to improve shell/matrix adhesion may allow for incorporation of more capsules while sustaining the commercially-required static mechanical properties. Greater increases in fracture toughness could also be achieved from these modifications. Because the healing capabilities of these systems are limited by the supply of healing agent, the incorporation of more capsules would serve to further increase the functional lifetime of the SHM. Improvement to the capsule/matrix adhesion is crucial to improving the static mechanical properties and perhaps to obtaining more efficient

healing. Additionally, if interfacial bonding is improved, it may be possible to optimize the size and wt% of capsules used in the matrix to maximize the volume of available healing agent.

The fatigue studies described in Chapter 4 are promising and indicate that the presence of OCA, not merely the addition of capsules, is contributing to lifetime extension, particularly at clinically-relevant loads. If adhesion between the capsule and matrix could be improved, the effects may become even more pronounced. The results presented here support the extension of fatigue testing to more complex models that mimic the loading of TJRs *in vivo*. Variable amplitude loading strategies have previously been used to mimic the loads experienced by joints during normal activity, such as walking, standing, sitting, and climbing stairs[206]; such strategies could also be investigated for this project to more accurately reflect both the loading *in vivo* as well as the periods of rest that might be conducive to matrix repair. Interfacial wear has been shown to be responsible for considerable generation of PMMA wear debris[6, 38, 135, 137, 207]; therefore, testing that specifically examines the ability of this SHM to repair fatigue damage generated from bonding defects at the cement/stem and cement/bone interfaces would provide valuable information about clinically-relevant failure modes. Additionally, testing of samples soaked in Ringer's solution for 4 weeks indicated that fatigue life was increased in unfilled specimens and decreased in samples containing encapsulated OCA; future work should investigate strategies to protect the capsule core

contents. Other work could focus on expanding the testing to be performed while samples are immersed in Ringer's solution at 37 ºC, as this would also influence the fatigue properties and would more accurately reflect the behavior of the material *in vivo*.

Although an encouraging initial study, the biocompatibility analyses presented in Chapter 5 should be expanded in order to make definitive claims about the suitability of this self-healing composite *in vivo*. Given the toxicity observed with OCA extract, future studies should focus on growth of cells in extract medium obtained from fatigued samples in which encapsulated OCA has presumably been released into the PMMA to reflect the material's composition *in vivo*; cells should also be grown in direct contact with the materials. Use of primary cells, like human osteoblasts and osteoclasts, would provide more relevant *in vitro* information than that obtained from the immortalized MG63 human osteosarcoma line[129, 208, 209]. Furthermore, *in vitro* analyses of cells grown in direct contact with the material rather than with its extract could better indicate the responses to be expected *in vivo*. Given the osteolysis associated with wear debris and subsequent TJR failure, experiments designed to quantify wear debris generation from unfilled and filled specimens could determine if the self-healing approach actually noticeably reduces material loss by minimizing crack propagation. Investigations of macrophage response, particularly the production of key cytokines (TNF-alpha, IL-1, and IL-6) associated with osteolysis[37, 56, 210], to wear debris generated from capsule-

embedded bone cement would provide valuable information about the potential for reducing osteolysis *in vivo*.

Finally, an animal model is necessary to look at *in vivo* responses in terms of the biocompatibility of the material as well as its functionality[56, 141-144]. It is possible that cell response could be different if the material were undergoing *in situ* loading; for example, OCA release and subsequent polymerization may have different effects on cells than those resulting just from contact with the static material or extracts from the static material. Results presented in Chapter 5 suggest that exposure to OCA released during material loading may result in cell death[181], although the OCA should polymerize inside the PMMA matrix, minimizing direct contact with cells and the interstitial fluid. Even though PMMA toxicity in humans is well-documented, an appropriate (i.e. load-bearing) animal model should be identified to examine the material's functionality and subsequent cytotoxicity *in vivo.*

I believe that the work presented in this dissertation is promising and supports the feasibility of developing a self-healing PMMA bone cement/OCA SHM that could significantly extend the functional lifetime of TJRs and minimize the number of revision procedures that are required. There are still many exciting avenues to pursue that could yield even more information about this material design and potentially lead to an improved and more robust system.

Appendix A: Glossary of Terms

Abbreviation	Term
1,4-BD	1,4-butanediol
ASTM	American Society for Testing and Materials
B	Bending strength
b	Weibull slope
BrdU	5-bromo-2′-deoxyuridine
DBTL	Di-*n*-butyltin dilaurate
DCPD	Dicyclopentadiene
DEK	Diethyl ketone
DETA	Diethylenetriamine
E	Bending modulus
EdU	5-ethynyl-2′-deoxyuridine
Epon 682	Diglycidyl ether of bisphenol-F
Epon 828	Diglycidyl ether of bisphenol-A
FITC	Fluorescein isothiocyanate
HOPDMS	Hydoxyl end-functionalized polydimethylsiloxane
ISO	International Organization for Standardization
K	Fracture toughness
KH-816	Cycloalipathic amine
MEK	Methyl ethyl ketone
MIBK	Methyl isobutyl ketone
MMA	Methyl methacrylate
MTS	3-(4,5-dimethylthiazol-2-yl)-5-(3-carboxymethoxyphenyl)-2-(4-sulfophenyl)-2H-tetrazolium
MTT	3-(4,5-dimethylthiazolyl-2)-2,5-diphenyltetrazolium bromide
η	Healing efficiency
N_0	Guaranteed/minimum fatigue life
N_a	Characteristic fatigue life
N_f	Number of cycles to failure
N_{WM}	Weibull mean
OA	Osteoarthritis
OCA	2-octyl cyanoacrylate
P_c	Critical fracture load
PD	2-allyl-1,3-propanediol
PDES	Polydiethoxysilane
PMMA	Poly(methyl methacrylate)

Abbreviation	Term
PI	Propidium iodide
PTSA	Para-toluenesulfonic acid
PUR	Polyurethane
RANK/RANKL	Receptor activator of nuclear factor - κB/ligand
RT	Room temperature
pPUR	Polyurethane prepolymer
SHM	Self-healing material
TDCB	Tapered double-cantilever beam
TDI	Toluene-2,4-diisocyanate
TJR	Total joint replacement
TNF	Tumor necrosis factor
UCS	Ultimate compressive strength
UF	Urea formaldehyde
UHMWPE	Ultra high molecular weight polyethylene
UTS	Ultimate tensile strength
WTDCB	Width tapered double-cantilever beam
YD-115	Butyl diglycidyl ether of bisphenol-A

Appendix B

Permission to reuse portions of "Self-healing biomaterials" included in Chapter 1.

JOHN WILEY AND SONS LICENSE TERMS AND CONDITIONS

Jun 07, 2013

This is a License Agreement between Alice B Welsh Brochu ("You") and John Wiley and Sons ("John Wiley and Sons") provided by Copyright Clearance Center ("CCC"). The license consists of your order details, the terms and conditions provided by John Wiley and Sons, and the payment terms and conditions.

All payments must be made in full to CCC. For payment instructions, please see information listed at the bottom of this form.

License Number	3163640433113
License date	Jun 07, 2013
Licensed content publisher	John Wiley and Sons
Licensed content publication	Journal of Biomedical Materials Research
Licensed content title	Self-healing biomaterials
Licensed copyright line	Copyright © 2010 Wiley Periodicals, Inc.
Licensed content author	Alice B. W. Brochu,Stephen L. Craig,William M. Reichert
Licensed content date	Dec 9, 2010
Start page	492
End page	506
Type of use	Dissertation/Thesis
Requestor type	Author of this Wiley article
Format	Print and electronic
Portion	Figure/table
Number of figures/tables	1
Original Wiley figure/table number(s)	Figure 1, Table 4
Will you be translating?	No
Total	0.00 USD
Terms and Conditions	

TERMS AND CONDITIONS

This copyrighted material is owned by or exclusively licensed to John Wiley & Sons, Inc. or one of its group companies (each a "Wiley Company") or a society for whom a Wiley Company has exclusive publishing rights in relation to a particular journal (collectively "WILEY"). By clicking "accept" in connection with completing this licensing transaction, you agree that the following terms and conditions apply to this transaction (along with the billing and payment terms and conditions established by the Copyright Clearance Center

Inc., ("CCC's Billing and Payment terms and conditions"), at the time that you opened your RightsLink account (these are available at any time at http://myaccount.copyright.com).

Terms and Conditions

1. The materials you have requested permission to reproduce (the "Materials") are protected by copyright.

2.You are hereby granted a personal, non-exclusive, non-sublicensable, non-transferable, worldwide, limited license to reproduce the Materials for the purpose specified in the licensing process. This license is for a one-time use only with a maximum distribution equal to the number that you identified in the licensing process. Any form of republication granted by this license must be completed within two years of the date of the grant of this license (although copies prepared before may be distributed thereafter). The Materials shall not be used in any other manner or for any other purpose. Permission is granted subject to an appropriate acknowledgement given to the author, title of the material/book/journal and the publisher. You shall also duplicate the copyright notice that appears in the Wiley publication in your use of the Material. Permission is also granted on the understanding that nowhere in the text is a previously published source acknowledged for all or part of this Material. Any third party material is expressly excluded from this permission.

3. With respect to the Materials, all rights are reserved. Except as expressly granted by the terms of the license, no part of the Materials may be copied, modified, adapted (except for minor reformatting required by the new Publication), translated, reproduced, transferred or distributed, in any form or by any means, and no derivative works may be made based on the Materials without the prior permission of the respective copyright owner. You may not alter, remove or suppress in any manner any copyright, trademark or other notices displayed by the Materials. You may not license, rent, sell, loan, lease, pledge, offer as security, transfer or assign the Materials, or any of the rights granted to you hereunder to any other person.

4. The Materials and all of the intellectual property rights therein shall at all times remain the exclusive property of John Wiley & Sons Inc or one of its related companies (WILEY) or their respective licensors, and your interest therein is only that of having possession of and the right to reproduce the Materials pursuant to Section 2 herein during the continuance of this Agreement. You agree that you own no right, title or interest in or to the Materials or any of the intellectual property rights therein. You shall have no rights hereunder other than the license as provided for above in Section 2. No right, license or interest to any trademark, trade name, service mark or other branding ("Marks") of WILEY or its licensors is granted hereunder, and you agree that you shall not assert any such right, license or interest with respect thereto.

5. NEITHER WILEY NOR ITS LICENSORS MAKES ANY WARRANTY OR REPRESENTATION OF ANY KIND TO YOU OR ANY THIRD PARTY, EXPRESS, IMPLIED OR STATUTORY, WITH RESPECT TO THE MATERIALS OR THE ACCURACY OF ANY INFORMATION CONTAINED IN THE MATERIALS,

INCLUDING, WITHOUT LIMITATION, ANY IMPLIED WARRANTY OF MERCHANTABILITY, ACCURACY, SATISFACTORY QUALITY, FITNESS FOR A PARTICULAR PURPOSE, USABILITY, INTEGRATION OR NON-INFRINGEMENT AND ALL SUCH WARRANTIES ARE HEREBY EXCLUDED BY WILEY AND ITS LICENSORS AND WAIVED BY YOU.

6. WILEY shall have the right to terminate this Agreement immediately upon breach of this Agreement by you.

7. You shall indemnify, defend and hold harmless WILEY, its Licensors and their respective directors, officers, agents and employees, from and against any actual or threatened claims, demands, causes of action or proceedings arising from any breach of this Agreement by you.

8. IN NO EVENT SHALL WILEY OR ITS LICENSORS BE LIABLE TO YOU OR ANY OTHER PARTY OR ANY OTHER PERSON OR ENTITY FOR ANY SPECIAL, CONSEQUENTIAL, INCIDENTAL, INDIRECT, EXEMPLARY OR PUNITIVE DAMAGES, HOWEVER CAUSED, ARISING OUT OF OR IN CONNECTION WITH THE DOWNLOADING, PROVISIONING, VIEWING OR USE OF THE MATERIALS REGARDLESS OF THE FORM OF ACTION, WHETHER FOR BREACH OF CONTRACT, BREACH OF WARRANTY, TORT, NEGLIGENCE, INFRINGEMENT OR OTHERWISE (INCLUDING, WITHOUT LIMITATION, DAMAGES BASED ON LOSS OF PROFITS, DATA, FILES, USE, BUSINESS OPPORTUNITY OR CLAIMS OF THIRD PARTIES), AND WHETHER OR NOT THE PARTY HAS BEEN ADVISED OF THE POSSIBILITY OF SUCH DAMAGES. THIS LIMITATION SHALL APPLY NOTWITHSTANDING ANY FAILURE OF ESSENTIAL PURPOSE OF ANY LIMITED REMEDY PROVIDED HEREIN.

9. Should any provision of this Agreement be held by a court of competent jurisdiction to be illegal, invalid, or unenforceable, that provision shall be deemed amended to achieve as nearly as possible the same economic effect as the original provision, and the legality, validity and enforceability of the remaining provisions of this Agreement shall not be affected or impaired thereby.

10. The failure of either party to enforce any term or condition of this Agreement shall not constitute a waiver of either party's right to enforce each and every term and condition of this Agreement. No breach under this agreement shall be deemed waived or excused by either party unless such waiver or consent is in writing signed by the party granting such waiver or consent. The waiver by or consent of a party to a breach of any provision of this Agreement shall not operate or be construed as a waiver of or consent to any other or subsequent breach by such other party.

11. This Agreement may not be assigned (including by operation of law or otherwise) by you without WILEY's prior written consent.

12. Any fee required for this permission shall be non-refundable after thirty (30) days from receipt

13. These terms and conditions together with CCC's Billing and Payment terms and conditions (which are incorporated herein) form the entire agreement between you and WILEY concerning this licensing transaction and (in the absence of fraud) supersedes all prior agreements and representations of the parties, oral or written. This Agreement may not be amended except in writing signed by both parties. This Agreement shall be binding upon and inure to the benefit of the parties' successors, legal representatives, and authorized assigns.

14. In the event of any conflict between your obligations established by these terms and conditions and those established by CCC's Billing and Payment terms and conditions, these terms and conditions shall prevail.

15. WILEY expressly reserves all rights not specifically granted in the combination of (i) the license details provided by you and accepted in the course of this licensing transaction, (ii) these terms and conditions and (iii) CCC's Billing and Payment terms and conditions.

16. This Agreement will be void if the Type of Use, Format, Circulation, or Requestor Type was misrepresented during the licensing process.

17. This Agreement shall be governed by and construed in accordance with the laws of the State of New York, USA, without regards to such state's conflict of law rules. Any legal action, suit or proceeding arising out of or relating to these Terms and Conditions or the breach thereof shall be instituted in a court of competent jurisdiction in New York County in the State of New York in the United States of America and each party hereby consents and submits to the personal jurisdiction of such court, waives any objection to venue in such court and consents to service of process by registered or certified mail, return receipt requested, at the last known address of such party.

Wiley Open Access Terms and Conditions

Wiley publishes Open Access articles in both its Wiley Open Access Journals program [http://www.wileyopenaccess.com/view/index.html] and as Online Open articles in its subscription journals. The majority of Wiley Open Access Journals have adopted the Creative Commons Attribution License (CC BY) which permits the unrestricted use, distribution, reproduction, adaptation and commercial exploitation of the article in any medium. No permission is required to use the article in this way provided that the article is properly cited and other license terms are observed. A small number of Wiley Open Access journals have retained the Creative Commons Attribution Non Commercial License (CC BY-NC), which permits use, distribution and reproduction in any medium, provided the original work is properly cited and is not used for commercial purposes.

Online Open articles - Authors selecting Online Open are, unless particular exceptions apply, offered a choice of Creative Commons licenses. They may therefore select from the CC BY, the CC BY-NC and the Attribution-NoDerivatives (CC BY-NC-ND). The CC BY-NC-ND is more restrictive than the CC BY-NC as it does not permit adaptations or modifications without rights holder consent.

marketing purposes requires further explicit permission from Wiley and will be subject to a fee. Commercial purposes include:

- Copying or downloading of articles, or linking to such articles for further redistribution, sale or licensing;
- Copying, downloading or posting by a site or service that incorporates advertising with such content;
- The inclusion or incorporation of article content in other works or services (other than normal quotations with an appropriate citation) that is then available for sale or licensing, for a fee (for example, a compilation produced for marketing purposes, inclusion in a sales pack)
- Use of article content (other than normal quotations with appropriate citation) by for-profit organizations for promotional purposes
- Linking to article content in e-mails redistributed for promotional, marketing or educational purposes;
- Use for the purposes of monetary reward by means of sale, resale, license, loan, transfer or other form of commercial exploitation such as marketing products
- Print reprints of Wiley Open Access articles can be purchased from: corporatesales@wiley.com

The modification or adaptation for any purpose of an article referencing the CC BY-NC-ND License requires consent which can be requested from RightsLink@wiley.com .

Other Terms and Conditions:

BY CLICKING ON THE "I AGREE..." BOX, YOU ACKNOWLEDGE THAT YOU HAVE READ AND FULLY UNDERSTAND EACH OF THE SECTIONS OF AND PROVISIONS SET FORTH IN THIS AGREEMENT AND THAT YOU ARE IN AGREEMENT WITH AND ARE WILLING TO ACCEPT ALL OF YOUR OBLIGATIONS AS SET FORTH IN THIS AGREEMENT.

v1.8

If you would like to pay for this license now, please remit this license along with your payment made payable to "COPYRIGHT CLEARANCE CENTER" otherwise you will be invoiced within 48 hours of the license date. Payment should be in the form of a check or money order referencing your account number and this invoice number RLNK501038397.
Once you receive your invoice for this order, you may pay your invoice by credit card. Please follow instructions provided at that time.

Make Payment To:
Copyright Clearance Center
Dept 001
P.O. Box 843006
Boston, MA 02284-3006

For suggestions or comments regarding this order, contact RightsLink Customer Support: customercare@copyright.com or +1-877-622-5543 (toll free in the US) or +1-978-646-2777.

Gratis licenses (referencing $0 in the Total field) are free. Please retain this printable license for your reference. No payment is required.

Permission to reuse "Microencapsulation of 2-octylcyanoacrylate tissue adhesive for self-healing acrylic bone cement" for the contents of Chapter 2.

JOHN WILEY AND SONS LICENSE TERMS AND CONDITIONS

May 15, 2013

This is a License Agreement between Alice B Welsh Brochu ("You") and John Wiley and Sons ("John Wiley and Sons") provided by Copyright Clearance Center ("CCC"). The license consists of your order details, the terms and conditions provided by John Wiley and Sons, and the payment terms and conditions.

All payments must be made in full to CCC. For payment instructions, please see information listed at the bottom of this form.

License Number	31503? 120601
License date	May 2013
Licensed content publisher	John Wiley and Sons
Licensed content publication	Journal of Biomedical Materials Research
Licensed content title	Microencapsulation of 2-octylcyanoacrylate tissue adhesive for self-healing acrylic bone cement
Licensed copyright line	Copyright © 2012 Wiley Periodicals, Inc.
Licensed content author	Alice B. W. Brochu,William J. Chyan,William M. Reichert
Licensed content date	Jul 18, 2012
Start page	176
End page	177
Type of use	Dissertation/Thesis
Requestor type	Author of this Wiley article
Format	Print and electronic
Portion	Full article
Will you be translating?	No
Total	0.00 USD
Terms and Conditions	

TERMS AND CONDITIONS

This copyrighted material is owned by or exclusively licensed to John Wiley & Sons, Inc. or one of its group companies (each a "Wiley Company") or a society for whom a Wiley Company has exclusive publishing rights in relation to a particular journal (collectively "WILEY"). By clicking "accept" in connection with completing this licensing transaction, you agree that the following terms and conditions apply to this transaction (along with the billing and payment terms and conditions established by the Copyright Clearance Center Inc., ("CCC's Billing and Payment terms and conditions"), at the time that you opened your RightsLink account (these are available at any time at http://myaccount.copyright.com).

Terms and Conditions

1. The materials you have requested permission to reproduce (the "Materials") are protected by copyright.

2.You are hereby granted a personal, non-exclusive, non-sublicensable, non-transferable, worldwide, limited license to reproduce the Materials for the purpose specified in the licensing process. This license is for a one-time use only with a maximum distribution equal to the number that you identified in the licensing process. Any form of republication granted by this license must be completed within two years of the date of the grant of this license (although copies prepared before may be distributed thereafter). The Materials shall not be used in any other manner or for any other purpose. Permission is granted subject to an appropriate acknowledgement given to the author, title of the material/book/journal and the publisher. You shall also duplicate the copyright notice that appears in the Wiley publication in your use of the Material. Permission is also granted on the understanding that nowhere in the text is a previously published source acknowledged for all or part of this Material. Any third party material is expressly excluded from this permission.

3. With respect to the Materials, all rights are reserved. Except as expressly granted by the terms of the license, no part of the Materials may be copied, modified, adapted (except for minor reformatting required by the new Publication), translated, reproduced, transferred or distributed, in any form or by any means, and no derivative works may be made based on the Materials without the prior permission of the respective copyright owner. You may not alter, remove or suppress in any manner any copyright, trademark or other notices displayed by the Materials. You may not license, rent, sell, loan, lease, pledge, offer as security, transfer or assign the Materials, or any of the rights granted to you hereunder to any other person.

4. The Materials and all of the intellectual property rights therein shall at all times remain the exclusive property of John Wiley & Sons Inc or one of its related companies (WILEY) or their respective licensors, and your interest therein is only that of having possession of and the right to reproduce the Materials pursuant to Section 2 herein during the continuance of this Agreement. You agree that you own no right, title or interest in or to the Materials or any of the intellectual property rights therein. You shall have no rights hereunder other than the license as provided for above in Section 2. No right, license or interest to any trademark, trade name, service mark or other branding ("Marks") of WILEY or its licensors is granted hereunder, and you agree that you shall not assert any such right, license or interest with respect thereto.

5. NEITHER WILEY NOR ITS LICENSORS MAKES ANY WARRANTY OR REPRESENTATION OF ANY KIND TO YOU OR ANY THIRD PARTY, EXPRESS, IMPLIED OR STATUTORY, WITH RESPECT TO THE MATERIALS OR THE ACCURACY OF ANY INFORMATION CONTAINED IN THE MATERIALS, INCLUDING, WITHOUT LIMITATION, ANY IMPLIED WARRANTY OF MERCHANTABILITY, ACCURACY, SATISFACTORY QUALITY, FITNESS FOR A

PARTICULAR PURPOSE, USABILITY, INTEGRATION OR NON-INFRINGEMENT AND ALL SUCH WARRANTIES ARE HEREBY EXCLUDED BY WILEY AND ITS LICENSORS AND WAIVED BY YOU.

6. WILEY shall have the right to terminate this Agreement immediately upon breach of this Agreement by you.

7. You shall indemnify, defend and hold harmless WILEY, its Licensors and their respective directors, officers, agents and employees, from and against any actual or threatened claims, demands, causes of action or proceedings arising from any breach of this Agreement by you.

8. IN NO EVENT SHALL WILEY OR ITS LICENSORS BE LIABLE TO YOU OR ANY OTHER PARTY OR ANY OTHER PERSON OR ENTITY FOR ANY SPECIAL, CONSEQUENTIAL, INCIDENTAL, INDIRECT, EXEMPLARY OR PUNITIVE DAMAGES, HOWEVER CAUSED, ARISING OUT OF OR IN CONNECTION WITH THE DOWNLOADING, PROVISIONING, VIEWING OR USE OF THE MATERIALS REGARDLESS OF THE FORM OF ACTION, WHETHER FOR BREACH OF CONTRACT, BREACH OF WARRANTY, TORT, NEGLIGENCE, INFRINGEMENT OR OTHERWISE (INCLUDING, WITHOUT LIMITATION, DAMAGES BASED ON LOSS OF PROFITS, DATA, FILES, USE, BUSINESS OPPORTUNITY OR CLAIMS OF THIRD PARTIES), AND WHETHER OR NOT THE PARTY HAS BEEN ADVISED OF THE POSSIBILITY OF SUCH DAMAGES. THIS LIMITATION SHALL APPLY NOTWITHSTANDING ANY FAILURE OF ESSENTIAL PURPOSE OF ANY LIMITED REMEDY PROVIDED HEREIN.

9. Should any provision of this Agreement be held by a court of competent jurisdiction to be illegal, invalid, or unenforceable, that provision shall be deemed amended to achieve as nearly as possible the same economic effect as the original provision, and the legality, validity and enforceability of the remaining provisions of this Agreement shall not be affected or impaired thereby.

10. The failure of either party to enforce any term or condition of this Agreement shall not constitute a waiver of either party's right to enforce each and every term and condition of this Agreement. No breach under this agreement shall be deemed waived or excused by either party unless such waiver or consent is in writing signed by the party granting such waiver or consent. The waiver by or consent of a party to a breach of any provision of this Agreement shall not operate or be construed as a waiver of or consent to any other or subsequent breach by such other party.

11. This Agreement may not be assigned (including by operation of law or otherwise) by you without WILEY's prior written consent.

12. Any fee required for this permission shall be non-refundable after thirty (30) days from receipt

13. These terms and conditions together with CCC's Billing and Payment terms and conditions (which are incorporated herein) form the entire agreement between you and

WILEY concerning this licensing transaction and (in the absence of fraud) supersedes all prior agreements and representations of the parties, oral or written. This Agreement may not be amended except in writing signed by both parties. This Agreement shall be binding upon and inure to the benefit of the parties' successors, legal representatives, and authorized assigns.

14. In the event of any conflict between your obligations established by these terms and conditions and those established by CCC's Billing and Payment terms and conditions, these terms and conditions shall prevail.

15. WILEY expressly reserves all rights not specifically granted in the combination of (i) the license details provided by you and accepted in the course of this licensing transaction, (ii) these terms and conditions and (iii) CCC's Billing and Payment terms and conditions.

16. This Agreement will be void if the Type of Use, Format, Circulation, or Requestor Type was misrepresented during the licensing process.

17. This Agreement shall be governed by and construed in accordance with the laws of the State of New York, USA, without regards to such state's conflict of law rules. Any legal action, suit or proceeding arising out of or relating to these Terms and Conditions or the breach thereof shall be instituted in a court of competent jurisdiction in New York County in the State of New York in the United States of America and each party hereby consents and submits to the personal jurisdiction of such court, waives any objection to venue in such court and consents to service of process by registered or certified mail, return receipt requested, at the last known address of such party.

Wiley Open Access Terms and Conditions

Wiley publishes Open Access articles in both its Wiley Open Access Journals program [http://www.wileyopenaccess.com/view/index.html] and as Online Open articles in its subscription journals. The majority of Wiley Open Access Journals have adopted the Creative Commons Attribution License (CC BY) which permits the unrestricted use, distribution, reproduction, adaptation and commercial exploitation of the article in any medium. No permission is required to use the article in this way provided that the article is properly cited and other license terms are observed. A small number of Wiley Open Access journals have retained the Creative Commons Attribution Non Commercial License (CC BY-NC), which permits use, distribution and reproduction in any medium, provided the original work is properly cited and is not used for commercial purposes.

Online Open articles · Authors selecting Online Open are, unless particular exceptions apply, offered a choice of Creative Commons licenses. They may therefore select from the CC BY, the CC BY-NC and the Attribution-NoDerivatives (CC BY-NC-ND). The CC BY-NC-ND is more restrictive than the CC BY-NC as it does not permit adaptations or modifications without rights holder consent.

Wiley Open Access articles are protected by copyright and are posted to repositories and websites in accordance with the terms of the applicable Creative Commons license

redistribution, sale or licensing;

- Copying, downloading or posting by a site or service that incorporates advertising with such content;
- The inclusion or incorporation of article content in other works or services (other than normal quotations with an appropriate citation) that is then available for sale or licensing, for a fee (for example, a compilation produced for marketing purposes, inclusion in a sales pack)
- Use of article content (other than normal quotations with appropriate citation) by for-profit organizations for promotional purposes
- Linking to article content in e-mails redistributed for promotional, marketing or educational purposes;
- Use for the purposes of monetary reward by means of sale, resale, license, loan, transfer or other form of commercial exploitation such as marketing products
- Print reprints of Wiley Open Access articles can be purchased from: corporatesales@wiley.com

The modification or adaptation for any purpose of an article referencing the CC BY-NC-ND License requires consent which can be requested from RightsLink@wiley.com .

Other Terms and Conditions:

BY CLICKING ON THE "I AGREE..." BOX, YOU ACKNOWLEDGE THAT YOU HAVE READ AND FULLY UNDERSTAND EACH OF THE SECTIONS OF AND PROVISIONS SET FORTH IN THIS AGREEMENT AND THAT YOU ARE IN AGREEMENT WITH AND ARE WILLING TO ACCEPT ALL OF YOUR OBLIGATIONS AS SET FORTH IN THIS AGREEMENT.

v1.8

If you would like to pay for this license now, please remit this license along with your payment made payable to "COPYRIGHT CLEARANCE CENTER" otherwise you will be invoiced within 48 hours of the license date. Payment should be in the form of a check or money order referencing your account number and this invoice number RLNK501021928.

Once you receive your invoice f his order, you may pay your invoice by credit card. Please follow instructions prov d at that time.

Make Payment To:
Copyright Clearance Center
Dept 001
P.O. Box 843006
Boston, MA 02284-3006

For suggestions or comments regarding this order, contact RightsLink Customer Support: customercare@copyright.com or +1-877-622-5543 (toll free in the US) or +1-978-646-2777.

Gratis licenses (referencing $0 .he Total field) are free. Please retain this printable license for your reference. No ayment is required.

References

1. Keller, T.C., Samartzis, Dino, and F.H. Shen, *Arthritis. Encyclopedia of Global Health. SAGE Publications*, Thousand Oaks, USA: SAGE Publications.

2. *Arthritis*, in *Black's Medical Dictionary, 42nd Edition*. 2010, A&C Black.

3. Zeni, J.A., Jr., M.J. Axe, and L. Snyder-Mackler, *Clinical predictors of elective total joint replacement in persons with end-stage knee osteoarthritis.* Bmc Musculoskeletal Disorders, 2010. **11**.

4. *Osteoarthritis - Treatments and drugs*. 2012.

5. *Osteoarthritis*, in *Black's Medical Dictionary, 42nd Edition*. 2010, A&C Black.

6. Gharpuray, V.M., L.M. Keer, and J.L. Lewis, *Cracks emanating from circular voids or elastic inclusions in PMMA near a bone-implant interface.* Journal of Biomechanical Engineering-Transactions of the Asme, 1990. **112**(1): p. 22-28.

7. Coventry, M.C., *The History of Joint Replacement Arthroplasty*, in *Joint Replacement Arthroplasty*, B.F. Morrey, Editor. 2003, Elsevier Science: Philadelphia. p. 3-6.

8. Ahmed, A.M.a.B.F.M., *Polymethylmethacrylate*, in *Joint Replacement Arthroplasty*, B.F. Morrey, Editor. 2003, Elsevier Science: Philadelphia. p. 7-18.

9. Stryker. *Simplex P Bone Cement Products*. 2006 [cited 2010 February 20]; Available from: http://www.stryker.com/en-us/products/Orthopaedics/BoneCementSubstitutes/index.htm.

10. Giddings, V.L., et al., *A small punch test technique for characterizing the elastic modulus and fracture behavior of PMMA bone cement used in total joint replacement.* Biomaterials, 2001. **22**(13): p. 1875-1881.

11. Saha, S. and S. Pal, *Mechanical properties of bone cement - a review* Journal of Biomedical Materials Research, 1984. **18**(4): p. 435-462.

12. Lewis, G., *Alternative acrylic bone cement formulations for cemented arthroplasties: Present status, key issues, and future prospects.* Journal of Biomedical Materials Research Part B-Applied Biomaterials, 2008. **84B**(2): p. 301-319.

13. Inacio, M.C.S., et al., *Sex and risk of hip implant failure: assessing total hip arthroplasty outcomes in the United States.* JAMA internal medicine, 2013. **173**(6): p. 435-41.

14. Wong, J.M., et al., *Recent advances in designs, approaches and materials in total knee replacement: literature review and evidence today.* Journal of perioperative practice, 2011. **21**(5): p. 165-71.

15. Day, J.S., et al., *Prevalence and projections of total shoulder and elbow arthroplasty in the United States to 2015.* Journal of Shoulder and Elbow Surgery, 2010. **19**(8): p. 1115-1120.

16. Weinstein, A.M., et al., *Estimating the burden of total knee replacement in the United States.* The Journal of bone and joint surgery. American volume, 2013. **95**(5): p. 385-92.

17. Kurtz, S., *The Clinical Performance of UHMWPE in Hip Replacements*, in *UHMWPE Biomaterials Handbook*, S.M. Kurtz, Editor. 2009, Elsevier, Inc: San Diego.

18. Kurtz, S., et al., *Projections of primary and revision hip and knee arthroplasty in the United States from 2005 to 2030.* Journal of Bone and Joint Surgery-American Volume, 2007. **89A**(4): p. 780-785.

19. Fehring, T.K., et al., *Joint Replacement Access in 2016 A Supply Side Crisis.* Journal of Arthroplasty, 2010. **25**(8): p. 1175-1181.

20. Kurtz, S.M., et al., *Future Young Patient Demand for Primary and Revision Joint Replacement: National Projections from 2010 to 2030.* Clinical Orthopaedics and Related Research, 2009. **467**(10): p. 2606-2612.

21. Krause, W., R.S. Mathis, and L.W. Grimes, *Fatigue properties of acrylic bone cement: S-N, P-N, and P-S-N data* Journal of Biomedical Materials Research-Applied Biomaterials, 1988. **22**(A3): p. 221-244.

22. Ong, K.L., et al., *Risk of Subsequent Revision after Primary and Revision Total Joint Arthroplasty.* Clinical Orthopaedics and Related Research, 2010. **468**(11): p. 3070-3076.

23. Puckett, A.D., et al., *Improved orthopaedic bone cement formulations based on rubber toughening.* Critical Reviews in Biomedical Engineering, 2000. **28**(3-4): p. 457-461.

24. Pellicci, P.M., et al., *Revision total hip arthroplasty* Clinical Orthopaedics and Related Research, 1982(170): p. 34-41.

25. Bhatt, H. and T. Goswami. *Implant wear mechanisms-basic approach*. 2008.

26. Kurtz, S.M., *The UHMWPE handbook: ultra-high molecular weight polyethylene in total joint replacement*. 2004, San Diego: Elsevier Academic Press.

27. Edidin, A.A. and S.M. Kurtz, *Influence of mechanical behavior on the wear of 4 clinically relevant polymeric biomaterials in a hip simulator.* Journal of Arthroplasty, 2000. **15**(3): p. 321-331.

28. Ovcharenko, A., G. Halperin, and I. Etsion, *Experimental Study of a Creeping Polymer Sphere in Contact With a Rigid Flat.* Journal of Tribology-Transactions of the Asme, 2009. **131**(1).

29. Guandalini, L., M. Baleani, and M. Viceconti, *A procedure and criterion for bone cement fracture toughness tests.* Proceedings of the Institution of Mechanical Engineers Part H-Journal of Engineering in Medicine, 2004. **218**(H6): p. 445-450.

30. Molino, L.N. and L.D.T. Topoleski, *Effect of BaSO4 on the fatigue crack propagation rate of PMMA bone cement.* Journal of Biomedical Materials Research, 1996. **31**(1): p. 131-137.

31. Ryd, L., et al., *ROENTGEN STEREOPHOTOGRAMMETRIC ANALYSIS AS A PREDICTOR OF MECHANICAL LOOSENING OF KNEE PROSTHESES.* Journal of Bone and Joint Surgery-British Volume, 1995. **77B**(3): p. 377-383.

32. Bauer, T.W. and J. Schils, *The pathology of total joint arthroplasty I. Mechanisms of implant fixation.* Skeletal Radiology, 1999. **28**(8): p. 423-432.

33. Jacobs, J.J., et al., *Wear debris in total joint replacements.* Journal of the American Academy of Orthopaedic Surgeons, 1994. **2**(4): p. 212-220.

34. Jeffers, J.R.T., et al., *Cement mantle fatigue failure in total hip replacement: Experimental and computational testing.* Journal of Biomechanics, 2007. **40**(7): p. 1525-1533.

35. Bauer, T.W. and J. Schils, *The pathology of total joint arthroplasty - II. Mechanisms of implant failure.* Skeletal Radiology, 1999. **28**(9): p. 483-497.

36. Abu-Amer, Y., I. Darwech, and J.C. Clohisy, *Aseptic loosening of total joint replacements: mechanisms underlying osteolysis and potential therapies.* Arthritis Research & Therapy, 2007. **9**.

37. Ingham, E. and J. Fisher, *The role of macrophages in osteolysis of total joint replacement.* Biomaterials, 2005. **26**(11): p. 1271-1286.

38. Raab, S., A.M. Ahmed, and J.W. Provan, *THE QUASISTATIC AND FATIGUE PERFORMANCE OF THE IMPLANT - BONE-CEMENT INTERFACE.* Journal of Biomedical Materials Research, 1981. **15**(2): p. 159-182.

39. Katti, K.S., *Biomaterials in total joint replacement.* Colloids and Surfaces B-Biointerfaces, 2004. **39**(3): p. 133-142.

40. Engh, C.A., et al., *A QUANTITATIVE-EVALUATION OF PERIPROSTHETIC BONE-REMODELING AFTER CEMENTLESS TOTAL HIP-ARTHROPLASTY.* Journal of Bone and Joint Surgery-American Volume, 1992. **74A**(7): p. 1009-1020.

41. Jacobs, J.J., et al., *Wear particles.* Journal of Bone and Joint Surgery-American Volume, 2006. **88A**: p. 99-102.

42. Sabokbar, A., R. Pandey, and N.A. Athanasou, *The effect of particle size and electrical charge on macrophage-osteoclast differentiation and bone resorption.* Journal of Materials Science-Materials in Medicine, 2003. **14**(9): p. 731-738.

43. Lewis, G., S. Janna, and A. Bhattaram, *Influence of the method of blending an antibiotic powder with an acrylic bone cement powder on physical, mechanical, and thermal properties of the cured cement.* Biomaterials, 2005. **26**(20): p. 4317-4325.

44. Moran, E., I. Byren, and B.L. Atkins, *The diagnosis and management of prosthetic joint infections.* Journal of Antimicrobial Chemotherapy, 2010. **65**: p. iii45-iii54.

45. Jamsen, E., et al., *Prevention of deep infection in joint replacement surgery A review.* Acta Orthopaedica, 2010. **81**(6): p. 660-666.

46. Lewis, G., *Properties of Antibiotic-Loaded Acrylic Bone Cements for Use in Cemented Arthroplasties: A State-of-the-Art Review.* Journal of Biomedical Materials Research Part B-Applied Biomaterials, 2009. **89B**(2): p. 558-574.

47. Brochu, A.B.W., S.L. Craig, and W.M. Reichert, *Self-healing biomaterials.* Journal of Biomedical Materials Research Part A, 2011. **96A**(2): p. 492-506.

48. Kenny, S.M. and M. Buggy, *Bone cements and fillers: A review.* Journal of Materials Science-Materials in Medicine, 2003. **14**(11): p. 923-938.

49. Manley, M.T., et al., *Fixation of acetabular cups without cement in total hip arthroplasty - A comparison of three different implant surfaces at a minimum duration of follow-up of five years.* Journal of Bone and Joint Surgery-American Volume, 1998. **80A**(8): p. 1175-1185.

50. Hirakawa, K., et al., *Mechanisms of failure of total hip replacements - Lessons learned from retrieval studies.* Clinical Orthopaedics and Related Research, 2004(420): p. 10-17.

51. Bauer, T.W., et al., *UNCEMENTED ACETABULAR COMPONENTS - HISTOLOGIC ANALYSIS OF RETRIEVED HYDROXYAPATITE-COATED AND POROUS IMPLANTS.* Journal of Arthroplasty, 1993. **8**(2): p. 167-177.

52. Coathup, M.J., et al., *A comparison of bone remodelling around hydroxyapatite-coated, porous-coated and grit-blasted hip replacements retrieved at post-mortem.* Journal of Bone and Joint Surgery-British Volume, 2001. **83B**(1): p. 118-123.

53. Simonet, W.S., et al., *Osteoprotegerin: A novel secreted protein involved in the regulation of bone density.* Cell, 1997. **89**(2): p. 309-319.

54. Ulrich-Vinther, M., et al., *Recombinant adeno-associated virus-mediated osteoprotegerin gene therapy inhibits wear debris-induced osteolysis.* Journal of Bone and Joint Surgery-American Volume, 2002. **84A**(8): p. 1405-1412.

55. Schwarz, E.M., R.J. Looney, and R.J. O'Keefe, *Anti-TNF-alpha therapy as a clinical intervention for periprosthetic osteolysis.* Arthritis Research, 2000. **2**(3): p. 165-168.

56. Merkel, K.D., et al., *Tumor necrosis factor-alpha mediates orthopedic implant osteolysis.* American Journal of Pathology, 1999. **154**(1): p. 203-210.

57. Sato, M. and W. Grasser, *EFFECTS OF BISPHOSPHONATES ON ISOLATED RAT OSTEOCLASTS AS EXAMINED BY REFLECTED LIGHT-MICROSCOPY.* Journal of Bone and Mineral Research, 1990. **5**(1): p. 31-40.

58. Carano, A., et al., *BISPHOSPHONATES DIRECTLY INHIBIT THE BONE-RESORPTION ACTIVITY OF ISOLATED AVIAN OSTEOCLASTS INVITRO.* Journal of Clinical Investigation, 1990. **85**(2): p. 456-461.

59. Rahaman, M.N., et al., *Ceramics for prosthetic hip and knee joint replacement.* Journal of the American Ceramic Society, 2007. **90**(7): p. 1965-1988.

60. Sathish, S., et al., *Studies on the corrosion and wear behavior of the laser nitrided biomedical titanium and its alloys.* Materials Science & Engineering C-Materials for Biological Applications, 2010. **30**(3): p. 376-382.

61. Long, M. and H.J. Rack, *Titanium alloys in total joint replacement - a materials science perspective.* Biomaterials, 1998. **19**(18): p. 1621-1639.

62. Dearnley, P.A., *A review of metallic, ceramic and surface-treated metals used for bearing surfaces in human joint replacements.* Proceedings of the Institution of Mechanical Engineers Part H-Journal of Engineering in Medicine, 1999. **213**(H2): p. 107-135.

63. Kessler, M.R., *Self-healing: a new paradigm in materials design.* Proceedings of the Institution of Mechanical Engineers Part G-Journal of Aerospace Engineering, 2007. **221**: p. 479-495.

64. Kessler, M.R., N.R. Sottos, and S.R. White, *Self-healing structural composite materials.* Composites Part a-Applied Science and Manufacturing, 2003. **34**(8): p. 743-753.

65. White, S.R., et al., *Autonomic healing of polymer composites.* Nature, 2001. **409**(6822): p. 794-797.

66. Blaiszik, B.J., et al., *Microcapsules filled with reactive solutions for self-healing materials.* Polymer, 2009. **50**(4): p. 990-997.

67. Blaiszik, B.J., N.R. Sottos, and S.R. White, *Nanocapsules for self-healing materials.* Composites Science and Technology, 2008. **68**(3-4): p. 978-986.

68. Yuan, Y.C., et al., *Self healing in polymers and polymer composites. Concepts, realization and outlook: A review.* Express Polymer Letters, 2008. **2**(4): p. 238-250.

69. Toohey, K.S., et al., *Self-healing materials with microvascular networks.* Nature Materials, 2007. **6**: p. 581-585.

70. Moore, N.C. *Self-healing Concrete for Safer, More Durable Infrastructure*. 2009 April 24, 2009 [cited 2009; Available from: http://www.sciencedaily.com/releases/2009/04/090422175336.htm.

71. Andersson, H.M., M.W. Keller, J.S. Moore, N.R. Sottos, and S.R. White, *Self Healing Polymers and Composites*, in *Self Healing Materials: an Alternative Approach to 20 Centuries of Materials Science*, S.v.d. Zwaag, Editor. 2007, Springer: AA Dordrecht, The Netherlands. p. 19-44.

72. Kessler, M.R. and S.R. White, *Self-activated healing of delamination damage in woven composites.* Composites Part a-Applied Science and Manufacturing, 2001. **32**(5): p. 683-699.

73. Bergman, S.D., F. Wuld, *Re-Mendable Polymers*, in *Self Healing Materials: an Alternative Approach to 20 Centuries of Materials Science*, S.v.d. Zwaag, Editor. 2007, Springer: AA Dordrecht, the Netherlands. p. 45-68.

74. Cho, S.H., et al., *Polydimethylsiloxane-based self-healing materials.* Advanced Materials, 2006. **18**(8): p. 997-+.

75. Rule, J.D., et al., *Wax-protected catalyst microspheres for efficient self-healing materials.* Advanced Materials, 2005. **17**(2): p. 205-+.

76. Rule, J.D., N.R. Sottos, and S.R. White, *Effect of microcapsule size on the performance of self-healing polymers.* Polymer, 2007. **48**(12): p. 3520-3529.

77. Biggs, P., L. Jones II, B. Wellborn, G. Lewis. *A Self-healing PMMA Bone Cement: Influence of Crystal Size of Grubbs' Catalyst*. in *25th Southern Biomedical Engineering Conference 2009*. 2009.

78. Liu, X., et al., *Characterization of diene monomers as healing agents for autonomic damage repair.* Journal of Applied Polymer Science, 2006. **101**(3): p. 1266-1272.

79. Lee, J.K., et al., *Characterization of dicyclopentadiene and 5-ethylidene-2-norbornene as self-healing agents for polymer composite and its microcapsules.* Macromolecular Research, 2004. **12**(5): p. 478-483.

80. Odom, S.A., et al., *A Self-healing Conductive Ink.* Advanced Materials, 2012. **24**(19): p. 2578-2581.

81. Jin, H.H., et al., *Self-healing thermoset using encapsulated epoxy-amine healing chemistry.* Polymer, 2012. **53**(2): p. 581-587.

82. Wool, R.P., *A material fix.* Nature, 2001. **409**(6822): p. 773-774.

83. Therriault, D., S.R. White, and J.A. Lewis, *Chaotic mixing in three-dimensional microvascular networks fabricated by direct-write assembly.* Nature Materials, 2003. **2**(4): p. 265-271.

84. Lewis, G., et al., *A room-temperature autonomically-healing PMMA bone cement: influence of composition on fatigue crack propagation rate.* Journal of Applied Biomaterials & Biomechanics, 2009. **7**(2): p. 90-96.

85. Brown, E.N., *Use of the tapered double-cantilever beam geometry for fracture toughness measurements and its application to the quantification of self-healing.* Journal of Strain Analysis for Engineering Design, 2011. **46**(3): p. 167-186.

86. Jin, H., et al., *Fracture and fatigue response of a self-healing epoxy adhesive.* Polymer, 2011. **52**(7): p. 1628-1634.

87. Brown, E.N., S.R. White, and N.R. Sottos, *Retardation and repair of fatigue cracks in a microcapsule toughened epoxy composite - Part 1: Manual infiltration.* Composites Science and Technology, 2005. **65**(15-16): p. 2466-2473.

88. Brown, E.N., S.R. White, and N.R. Sottos, *Retardation and repair of fatigue cracks in a microcapsule toughened epoxy composite - Part II: In situ self-healing.* Composites Science and Technology, 2005. **65**(15-16): p. 2474-2480.

89. Brown, E.N., S.R. White, and N.R. Sottos, *Fatigue crack propagation in microcapsule-toughened epoxy.* Journal of Materials Science, 2006. **41**(19): p. 6266-6273.

90. Kuehn, K.D., W. Ege, and U. Gopp, *Acrylic bone cements: mechanical and physical properties.* Orthopedic Clinics of North America, 2005. **36**(1): p. 29-+.

91. *ASTM International F451-08*, in *Standard Specification for Acrylic Bone Cement*. 2008.

92. *ASTM International D638-10*, in *Standard Test Method for Tensile Properties of Plastics*. 2010.

93. Harper, E.J., J.C. Behiri, and W. Bonfield, *Flexural and fatigue properties of a bone cement based upon polyethylmethacrylate and hydrxyapatite.* Journal of Materials Science-Materials in Medicine, 1995. **6**(12): p. 799-803.

94. *International Standard 5833:2002(E)*, in *Implants for surgery- Acrylic resin cements*. 2002.

95. Perek, J. and R.M. Pilliar, *Fracture toughness of composite acrylic bone cements* Journal of Materials Science-Materials in Medicine, 1992. **3**(5): p. 333-344.

96. Graham, J., et al., *Fracture and fatigue properties of acrylic bone cement - The effects of mixing method, sterilization treatment, and molecular weight.* Journal of Arthroplasty, 2000. **15**(8): p. 1028-1035.

97. Lewis, G., *Apparent fracture toughness of acrylic bone cement: effect of test specimen configuration and sterilization method.* Biomaterials, 1999. **20**(1): p. 69-78.

98. Lewis, G. and S. Mladsi, *Correlation between impact strength and fracture toughness of PMMA-based bone cements.* Biomaterials, 2000. **21**(8): p. 775-781.

99. Soltesz, U., *The influence of loading conditions on the lifetimes in fatigue testing of bone cements* Journal of Materials Science-Materials in Medicine, 1994. **5**(9-10): p. 654-656.

100. Soltész, U., R. Schäfer, R. Jaeger, U. Gopp, and K.-D. Kühn, *Fatigue Testing of Bone Cements - Comparison of Testing Arrangements.* Journal of ASTM International, 2005. **2**.

101. Swanson, S.A.V., M.A.R. Freeman, *The Scientific Basis of Joint Replacement*, ed. S.A.V.a.M.A.R.F. Swanson. 1977, New York: John Wiley and Sons Inc.

102. Ling, R.S.M. and A.J.C. Lee, *Porosity reduction in acrylic cement is clinically irrelevant.* Clinical Orthopaedics and Related Research, 1998(355): p. 249-253.

103. Burr, D.B., et al., *Bone remodeling in response to in vivo fatigue microdamage* Journal of Biomechanics, 1985. **18**(3): p. 189-&.

104. Caler, W.E. and D.R. Carter, *Bone creep fatigue damage accumulation* Journal of Biomechanics, 1989. **22**(6-7): p. 625-635.

105. Lewis, G., *Fatigue testing and performance of acrylic bone-cement materials: State-of-the-art review.* Journal of Biomedical Materials Research Part B-Applied Biomaterials, 2003. **66B**(1): p. 457-486.

106. Kuehn, K.-D., *Bone Cements. Up-to-Date Comparison of Physical and Chemical Properties of Commercial Materials*. 2000, Heidelberg: Springer.

107. Davies, J.P., et al., *Comparison of the mechanical properties of Simplex P, Zimmer Regular, and LVC bone cements.* Journal of Biomedical Materials Research, 1987. **21**(6): p. 719-730.

108. Lee, A.J.C., R.S.M. Ling, and J.D. Wrighton, *Some properties of polymethylmethacrylate with reference to its use in orthopedic surgery* Clinical Orthopaedics and Related Research, 1973(95): p. 281-287.

109. Kurtz, S.M., et al., *Static and fatigue mechanical behavior of bone cement with elevated barium sulfate content for treatment of vertebral compression fractures.* Biomaterials, 2005. **26**(17): p. 3699-3712.

110. Lewis, G. and S. Mladsi, *Effect of sterilization method on properties of Palacos (R) R acrylic bone cement.* Biomaterials, 1998. **19**(1-3): p. 117-124.

111. Lewis, G., et al., *Influence of two changes in the composition of an acrylic bone cement on its handling, thermal, physical, and mechanical properties.* Journal of Materials Science-Materials in Medicine, 2007. **18**(8): p. 1649-1658.

112. Crowninshield, R., RA Brand, RC Johnston, JC Milroy, *The effect of femoral stem cross-sectional geometry on cement stresses in total hip reconstruction.* Clin Orthop Relat Res, 1980. **146**: p. 71-77.

113. Almeida, T., et al., *Preliminary evaluation of the in vitro cytotoxicity of PMMA-co-EHA bone cement.* Materials Science & Engineering C-Materials for Biological Applications, 2011. **31**(3): p. 658-662.

114. Granchi, D., et al., *In vitro effects of bone cements on the cell cycle of osteoblast-like cells* Biomaterials, 1995. **16**(15): p. 1187-1192.

115. Harper, E.J., M. Braden, and W. Bonfield, *Mechanical properties of hydroxyapatite reinforced poly(ethylmethacrylate) bone cement after immersion in a physiological solution: influence of a silane coupling agent.* Journal of Materials Science-Materials in Medicine, 2000. **11**(8): p. 491-497.

116. Brochu, A.B.W., *Microencapsulation of Octylcyanoacrylate for Applications as a Healing Agent in a Self-healing Bone Cement*. 2011, Duke University: United States -- North Carolina.

117. Jyoti, M.A. and H.-Y. Song, *Initial in vitro biocompatibility of a bone cement composite containing a poly-epsilon-caprolactone microspheres.* Journal of Materials Science-Materials in Medicine, 2011. **22**(5): p. 1333-1342.

118. Lopes, M.A., et al., *Flow cytometry for assessing biocompatibility.* Journal of Biomedical Materials Research, 1998. **41**(4): p. 649-656.

119. Nayab, S.N., F.H. Jones, and I. Olsen, *Modulation of the human bone cell cycle by calcium ion-implantation of titanium.* Biomaterials, 2007. **28**(1): p. 38-44.

120. Martin, J.Y., et al., *Effect of titanium surface roughness on proliferation, differentiation, and protein synthesis of human osteoblast-like cells (MG63)* Journal of Biomedical Materials Research, 1995. **29**(3): p. 389-401.

121. Clover, J. and M. Gowen, *ARE MG-63 AND HOS TE85 HUMAN OSTEOSARCOMA CELL-LINES REPRESENTATIVE MODELS OF THE OSTEOBLASTIC PHENOTYPE.* Bone, 1994. **15**(6): p. 585-591.

122. Clifford, C.J. and S. Downes, *A comparative study of the use of colorimetric assays in the assessment of biocompatibility.* Journal of Materials Science-Materials in Medicine, 1996. **7**(10): p. 637-643.

123. Monner, D.A., *An assay for growth of mouse bone marrow cells in microtiter liquid culture using the tetrazolium salf MTT and its application to studies of myelopoiesis* Immunology Letters, 1988. **19**(4): p. 261-268.

124. Denizot, F. and R. Lang, *Rapid colorimetric assay for cell growth and survival-modifications to the tetrazolium dye procedure giving improved sensitivity and reliability* Journal of Immunological Methods, 1986. **89**(2): p. 271-277.

125. Mosmann, T., *Rapid colorimetrix assay for cellular growth and survival - application to proliferation and cytotoxicity assays.* Journal of Immunological Methods, 1983. **65**(1-2): p. 55-63.

126. Ciapetti, G., et al., *In vitro evaluation of cell/biomaterial interaction by MTT assay.* Biomaterials, 1993. **14**(5): p. 359-364.

127. Uggeri, J., et al., *Calcein-AM is a detector of intracellular oxidative activity.* Histochemistry and Cell Biology, 2004. **122**(5): p. 499-505.

128. Invitrogen. *Breakthrough cell proliferation assays - Click-iT® EdU cell proliferation assays replace BrdU.* Available from: http://tools.invitrogen.com/content/sfs/brochures/f-073563%20click-it-r4_hr.pdf.

129. Sun, J.-Y., et al., *The effect of the ionic products of Bioglass (R) dissolution on human osteoblasts growth cycle in vitro.* Journal of Tissue Engineering and Regenerative Medicine, 2007. **1**(4): p. 281-286.

130. Dolbeare, F., et al., *Flow cytometric measurement of total DNA content and incorporated bromodeoxyuridine* Proceedings of the National Academy of Sciences of the United States of America-Biological Sciences, 1983. **80**(18): p. 5573-5577.

131. Wright, T.M. and R.P. Robinson, *Fatigue crack propagation in polymethylmethacrylate bone cements* Journal of Materials Science, 1982. **17**(9): p. 2463-2468.

132. Milios, J., G.C. Papanicolaou, and R.J. Young, *Dynamic crack propagation behavior of rubber-toughened poly(methyl methacrylate)* Journal of Materials Science, 1986. **21**(12): p. 4281-4288.

133. Pal, S. and S. Saha, *STRESS-RELAXATION AND CREEP-BEHAVIOR OF NORMAL AND CARBON-FIBER REINFORCED ACRYLIC BONE-CEMENT.* Biomaterials, 1982. **3**(2): p. 93-96.

134. Kawate, K., et al., *Importance of a thin cement mantle - Autopsy studies of eight hips.* Clinical Orthopaedics and Related Research, 1998(355): p. 70-76.

135. Race, A., et al., *Early cement damage around a femoral stem is concentrated at the cement/bone interface.* Journal of Biomechanics, 2003. **36**(4): p. 489-496.

136. Welsh, R.P., R.M. Pilliar, and I. Macnab, *SURGICAL IMPLANTS - ROLE OF SURFACE POROSITY IN FIXATION TO BONE AND ACRYLIC.* Journal of Bone and Joint Surgery-American Volume, 1971. **A 53**(5): p. 963-&.

137. Beaumont, P.W.R. and B. Plumpton, *STRENGTH OF ACRYLIC BONE CEMENTS AND ACRYLIC CEMENT STAINLESS STEEL INTERFACES .2. SHEAR-STRENGTH OF AN ACRYLIC CEMENT STAINLESS STEEL INTERFACE.* Journal of Materials Science, 1977. **12**(9): p. 1853-1856.

138. Lennon, A.B., B.A.O. McCormack, and P.J. Prendergast, *The relationship between cement fatigue damage and implant surface finish in proximal femoral prostheses.* Medical Engineering & Physics, 2003. **25**(10): p. 833-841.

139. Verdonschot, N. and R. Huiskes, *The effects of cement-stem debonding in THA on the long-term failure probability of cement.* Journal of Biomechanics, 1997. **30**(8): p. 795-802.

140. Stolk, J., N. Verdonschot, and R. Huiskes, *Stair climbing is more detrimental to the cement in hip replacement than walking.* Clinical Orthopaedics and Related Research, 2002(405): p. 294-305.

141. Allen, M.J., et al., *Tissue response to in situ polymerization of a new two-solution bone cement: Evaluation in a sheep model.* Journal of Biomedical Materials Research Part B-Applied Biomaterials, 2006. **79B**(2): p. 441-452.

142. Kim, K.J., Y. Kobayashi, and T. Itoh, *Osteolysis model with continuous infusion of polyethylene particles.* Clinical Orthopaedics and Related Research, 1998(352): p. 46-52.

143. Okada, Y., et al., *Repair of segmental bone defects using bioactive bone cement: Comparison with PMMA bone cement.* Journal of Biomedical Materials Research, 1999. **47**(3): p. 353-359.

144. Hautamaki, M.P., et al., *Repair of bone segment defects with surface porous fiber-reinforced polymethyl methacrylate (PMMA) composite prosthesis - Histomorphometric incorporation model and characterization by SEM.* Acta Orthopaedica, 2008. **79**(4): p. 555-564.

145. Coulthard, P., et al., *Tissue adhesives for closure of surgical incisions.* Cochrane Database of Systematic Reviews, 2010(5).

146. Castner, D.G. and B.D. Ratner, *Biomedical surface science: Foundations to frontiers.* Surface Science, 2002. **500**(1-3): p. PII S0039-6028(01)01587-4.

147. Ratner, B.D., *A paradigm shift: biomaterials that heal.* Polymer International, 2007. **56**: p. 1183-1185.

148. Chen, P.Y., et al., *Structure and mechanical properties of selected biological materials.* Journal of the Mechanical Behavior of Biomedical Materials, 2008. **1**(3): p. 208-226.

149. Meyers, M.A., et al., *Biological materials: Structure and mechanical properties.* Progress in Materials Science, 2008. **53**(1): p. 1-206.

150. Hsieh, K.H., C.C. Tsai, and D.M. Chang, *VAPOR AND GAS-PERMEABILITY OF POLYURETHANE MEMBRANES .2. EFFECT OF FUNCTIONAL-GROUP.* Journal of Membrane Science, 1991. **56**(3): p. 279-287.

151. Hsieh, K.H., C.C. Tsai, and S.M. Tseng, *VAPOR AND GAS-PERMEABILITY OF POLYURETHANE MEMBRANES .1. STRUCTURE PROPERTY RELATIONSHIP.* Journal of Membrane Science, 1990. **49**(3): p. 341-350.

152. Hong, K. and S. Park, *Preparation of polyurethane microcapsules with different soft segments and their characteristics.* Reactive & Functional Polymers, 1999. **42**(3): p. 193-200.

153. Santerre, J.P., et al., *Understanding the biodegradation of polyurethanes: From classical implants to tissue engineering materials.* Biomaterials, 2005. **26**(35): p. 7457-7470.

154. Shukla, P.G., et al., *Preparation and characterization of microcapsules of water-soluble pesticide monocrotophos using polyurethane as carrier material.* Journal of Microencapsulation, 2002. **19**(3): p. 293-304.

155. Shukla, P.G. and S. Sivaram, *Microencapsulation of the water-soluble pesticide Monocrotophos by an oil in oil interfacial polyaddition method.* Journal of Microencapsulation, 1999. **16**(4): p. 517-521.

156. Frere, W., L. Danicher, and P. Gramain, *Preparation of polyurethane microcapsules by interfacial polycondensation.* European Polymer Journal, 1998. **34**(2): p. 193-199.

157. Cho, J.S., A. Kwon, and C.G. Cho, *Microencapsulation of octadecane as a phase-change material by interfacial polymerization in an emulsion system.* Colloid and Polymer Science, 2002. **280**(3): p. 260-266.

158. Su, J.F., et al., *Preparation and characterization of polyurethane microcapsules containing n-octadecane with styrene-maleic anhydride as a surfactant by interfacial polycondensation.* Journal of Applied Polymer Science, 2006. **102**(5): p. 4996-5006.

159. Torini, L., J.F. Argillier, and N. Zydowicz, *Interfacial polycondensation encapsulation in miniemulsion.* Macromolecules, 2005. **38**(8): p. 3225-3236.

160. Johnsen, H. and R.B. Schmid, *Preparation of polyurethane nanocapsules by miniemulsion polyaddition.* Journal of Microencapsulation, 2007. **24**(8): p. 731-742.

161. Mizuno, K., Y. Taguchi, and M. Tanaka, *The effect of the surfactant adsorption layer on the growth rate of the polyurethane capsule shell.* Journal of Chemical Engineering of Japan, 2005. **38**(1): p. 45-48.

162. Gaudin, F. and N. Sintes-Zydowicz, *Core-shell biocompatible polyurethane nanocapsules obtained by interfacial step polymerisation in miniemulsion.* Colloids and Surfaces a-Physicochemical and Engineering Aspects, 2008. **331**(1-2): p. 133-142.

163. Hong, K. and S. Park, *Characterization of ovalbumin-containing polyurethane microcapsules with different structures.* Polymer Testing, 2000. **19**(8): p. 975-984.

164. Kim, M.D., et al., *Segmented polyurethane-based microparticles: Synthesis, properties, and isoniazid encapsulation and kinetics of release.* Polymer Science Series A, 2006. **48**(12): p. 1257-1262.

165. Yang, J.L., et al., *Microencapsulation of Isocyanates for Self-Healing Polymers.* Macromolecules, 2008. **41**(24): p. 9650-9655.

166. Keller, M.W. and N.R. Sottos, *Mechanical properties of microcapsules used in a self-healing polymer.* Experimental Mechanics, 2006. **46**(6): p. 725-733.

167. Caruso, M.M., et al., *Robust, Double-Walled Microcapsules for Self-Healing Polymeric Materials.* Acs Applied Materials & Interfaces, 2010. **2**(4): p. 1195-1199.

168. Brown, E.N., et al., *In situ poly(urea-formaldehyde) microencapsulation of dicyclopentadiene.* Journal of Microencapsulation, 2003. **20**(6): p. 719-730.

169. Dunne, N.J. and J.F. Orr, *Curing characteristics of acrylic bone cement.* Journal of Materials Science-Materials in Medicine, 2002. **13**(1): p. 17-22.

170. Angeles Corcuera, M., et al., *Effect of Diisocyanate Structure on the Properties and Microstructure of Polyurethanes Based on Polyols Derived from Renewable Resources.* Journal of Applied Polymer Science, 2011. **122**(6): p. 3677-3685.

171. Brochu, A.B.W., W.J. Chyan, and W.M. Reichert, *Microencapsulation of 2-octylcyanoacrylate tissue adhesive for self-healing acrylic bone cement.* Journal of biomedical materials research. Part B, Applied biomaterials, 2012. **100B**(7): p. 1764-72.

172. Dabagh, M., M.J. Abdekhodaie, and M.T. Khorasani, *Effects of polydimethylsiloxane grafting on the calcification, physical properties, and biocompatibility of polyurethane in a heart valve.* Journal of Applied Polymer Science, 2005. **98**(2): p. 758-766.

173. Kidane, A.G., et al., *Current Developments and Future Prospects for Heart Valve Replacement Therapy.* Journal of Biomedical Materials Research Part B-Applied Biomaterials, 2009. **88B**(1): p. 290-303.

174. Perez, M.A., J.M. Garcia-Aznar, and M. Doblare, *Does Increased Bone-Cement Interface Strength have Negative Consequences for Bulk Cement Integrity? A Finite Element Study.* Annals of Biomedical Engineering, 2009. **37**(3): p. 454-466.

175. Hoey, D. and D. Taylor, *Quantitative analysis of the effect of porosity on the fatigue strength of bone cement.* Acta Biomaterialia, 2009. **5**(2): p. 719-726.

176. Singer, A.J. and H.C. Thode, *A review of the literature on octylcyanoacrylate tissue adhesive.* American Journal of Surgery, 2004. **187**(2): p. 238-248.

177. *Palacos R Instructions for use*, in *Zimmer Surgical, Inc*. 2012: Dover.

178. Brown, E.N., S.R. White, and N.R. Sottos, *Microcapsule induced toughening in a self-healing polymer composite.* Journal of Materials Science, 2004. **39**(5): p. 1703-1710.

179. Jackson, A.C., et al., *Silica-Protected Micron and Sub-Micron Capsules and Particles for Self-Healing at the Microscale.* Macromolecular Rapid Communications, 2011. **32**(1): p. 82-87.

180. Brown, E.N., N.R. Sottos, and S.R. White, *Fracture testing of a self-healing polymer composite.* Experimental Mechanics, 2002. **42**(4): p. 372-379.

181. Brochu, A.B.W., G.A. Evans, W.M. Reichert ***Mechanical and cytotoxicity testing of acrylic bone cement embedded with microencapsulated 2-octyl cyanoacrylate***. Journal of Biomedical Materials Research Part B-Applied Biomaterials, 2013, accepted

182. Lewis, G. and G.E. Austin, *MECHANICAL-PROPERTIES OF VACUUM-MIXED ACRYLIC BONE-CEMENT.* Journal of Applied Biomaterials, 1994. **5**(4): p. 307-314.

183. Lewis, G. and S.I. Janna, *Effect of fabrication pressure on the fatigue performance of Cemex XL acrylic bone cement.* Biomaterials, 2004. **25**(7-8): p. 1415-1420.

184. Lewis, G. and A. Sadhasivini, *Estimation of the minimum number of test specimens for fatigue testing of acrylic bone cement.* Biomaterials, 2004. **25**(18): p. 4425-4432.

185. Johnson, J.A., et al., *FATIGUE OF ACRYLIC BONE-CEMENT - EFFECT OF FREQUENCY AND ENVIRONMENT.* Journal of Biomedical Materials Research, 1989. **23**(8): p. 819-831.

186. Freitag, T.A. and S.L. Cannon, *FRACTURE CHARACTERISTICS OF ACRYLIC BONE CEMENTS .2. FATIGUE.* Journal of Biomedical Materials Research, 1977. **11**(4): p. 609-624.

187. Lopes, P., et al., *New PMMA-co-EHA glass-filled composites for biomedical applications: Mechanical properties and bioactivity.* Acta Biomaterialia, 2009. **5**(1): p. 356-362.

188. Lopes, P.P., et al., *Preparation and study of in vitro bioactivity of PMMA-co-EHA composites filled with a Ca-3(PO4)(2)-SiO2-MgO glass.* Materials Science & Engineering C-Biomimetic and Supramolecular Systems, 2008. **28**(4): p. 572-577.

189. Ono, S., et al., *Development of New Bone Cement utilizing Low Toxicity Monomers.* Journal of Medical and Dental Sciences, 2008. **55**(2): p. 189-196.

190. *International Standard 10993-12:2012*, in *Biological evaluation of medical devices -- Part 12: Sample preparation and reference materials*. 2012, ISO: Switzerland.

191. Kaplan, M. and K. Baysal, *In vitro toxicity test of ethyl 2-cyanoacrylate, a tissue adhesive used in cardiovascular surgery, by fibroblast cell culture method.* Heart Surgery Forum, 2005. **8**(3): p. E169-E172.

192. Ciapetti, G., et al., *TOXICITY OF CYANOACRYLATES IN-VITRO USING EXTRACT DILUTION ASSAY ON CELL-CULTURES.* Biomaterials, 1994. **15**(2): p. 92-96.

193. Clover, J. and M. Gowen, *Are MG63 and HOS human osteosarcoma cell lines representative models of the osteoblastic phenotype* Bone, 1994. **15**(6): p. 585-591.

194. Knetsch, M.L.W., N. Olthof, and L.H. Koole, *Polymers with tunable toxicity: A reference scale for cytotoxicity testing of biomaterial surfaces.* Journal of Biomedical Materials Research Part A, 2007. **82A**(4): p. 947-957.

195. Alt, V., et al., *An in vitro assessment of the antibacterial properties and cytotoxicity of nanoparticulate silver bone cement.* Biomaterials, 2004. **25**(18): p. 4383-4391.

196. Kim, S.B., et al., *The characteristics of a hydroxyapatite-chitosan-PMMA bone cement.* Biomaterials, 2004. **25**(26): p. 5715-5723.

197. Kim, H.S., et al., *The cytotoxic effect of methotrexate loaded bone cement on osteosarcoma cell lines.* International Orthopaedics, 2001. **25**(6): p. 343-348.

198. Linder, L., *The tissue response to bone cement*, in *Biocompatibility of orthopedic implants*, D.F. Williams, Editor. 1982, CRC Press: Boca Raton.

199. Thumwanit, V. and U. Kedjarune, *Cytotoxicity of polymerized commercial cyanoacrylate adhesive on cultured human oral fibroblasts.* Australian Dental Journal, 1999. **44**(4): p. 248-252.

200. Evans, C.E., G.C. Lees, and I.A. Trail, *Cytotoxicity of cyanoacrylate adhesives to cultured tendon cells.* Journal of Hand Surgery-British and European Volume, 1999. **24B**(6): p. 658-661.

201. Weber, S.C. and M.W. Chapman, *Adhesives in orthopaedic surgery. A review of the literature and in vitro bonding strengths of bone-bonding agents.* Clinical Orthopaedics and Related Research, 1984(191): p. 249-261.

202. Leonard, F., et al., *Tissue adhesives and hemostasis-inducing compounds: The alkyl cyanoacrylates.* J Biomed Mat Res, 1967. **1**((1)): p. 3-9.

203. Vinters, H.V., et al., *The histotoxicity of cyanoacrylates - a selective review* Neuroradiology, 1985. **27**(4): p. 279-291.

204. Matsumoto, T., et al., *Higher homologous cyanoacrylate tissue adhesives in surgery of internal organs.* Archives of Surgery, 1967. **94**(6): p. 861-&.

205. Gandham, V.D., A.B.W. Brochu, and W.M. Reichert, *Microencapsulation of Liquid Cyanoacrylate via In situ Polymerization for Self-healing Bone Cement Application.* MRS Online Proceedings Library, 2012. **1417**: p. null-null.

206. Evans, S.L., *Fatigue crack propagation under variable amplitude loading in PMMA and bone cement.* Journal of Materials Science-Materials in Medicine, 2007. **18**(9): p. 1711-1717.

207. Jasty, M., et al., *The initiation of failure in cemented femoral components of hip arthroplasties.* Journal of Bone and Joint Surgery-British Volume, 1991. **73**(4): p. 551-558.

208. Fini, M., et al., *A bone substitute composed of polymethylmethacrylate and alpha-tricalcium phosphate: results in terms of osteoblast function and bone tissue formation.* Biomaterials, 2002. **23**(23): p. 4523-4531.

209. Lohmann, C.H., et al., *Ceramic and PMMA particles differentially affect osteoblast phenotype.* Biomaterials, 2002. **23**(8): p. 1855-1863.

210. Clohisy, J.C., et al., *Tumor necrosis factor-alpha mediates polymethylmethacrylate particle-induced NF-kappa B activation in osteoclast precursor cells.* Journal of Orthopaedic Research, 2002. **20**(2): p. 174-181.

Biography

Alice Bradbury Welsh Brochu
May 12, 1986
Raleigh, NC

Education

Duke University; Durham, NC
Ph.D. in Biomedical Engineering, September 2013
M.S. in Biomedical Engineering, May 2011
Center for Biomolecular and Tissue Engineering (CBTE) Certificate

North Carolina State University; Raleigh, NC
B.S. in Biomedical Engineering, May 2008
Summa Cum Laude
University Honors Program
Dean's List, every semester

Publications

1. **Brochu, A.B.W**., G.A. Evans, W.M. Reichert. Mechanical and cytotoxicity testing of acrylic bone cement embedded with microencapsulated 2-octyl cyanoacrylate. *Journal of Biomedical Materials Research Part B*, 2013, accepted.

2. **Brochu, A.B.W**., W.J. Chyan, W.M. Reichert. Microencapsulation of 2-octylcyanoacrylate tissue adhesive for self-healing acrylic bone cement. *Journal of Biomedical Materials Research Part B*, 2012. 100B(7):1764–1772.

3. Gandham, V.D., **A.B.W. Brochu**, and W.M. Reichert, Microencapsulation of Liquid Cyanoacrylate via In situ Polymerization for Self-Healing Bone Cement Application. *MRS Proceedings*, 1417, mrsf11-1417-kk01-06 doi:10.1557/opl.2012.1014.

4. **Brochu, A.B.W**. Microencapsulation of Octylcyanoacrylate for Applications as a Healing Agent in a Self-healing Bone Cement. Master's Thesis, Duke University, 2011.

5. **Brochu, A.B.W**., S.L. Craig, W.M. Reichert, Self-healing biomaterials. *Journal of Biomedical Materials Research Part A*, 2011. 96A(2): 492-506.

Honors

Duke University CBTE Kewaunee Lectureship Graduate Student Poster Award 4/13

James B. Duke Fellowship	8/08-8/12
Duke University CBTE Kewaunee Lectureship Graduate Student Poster Award	4/12
CBTE NIH Predoctoral Fellow	7/09-7/11
NSF Graduate Research Fellowship Honorable Mention	2010
The Honor Society of Phi Kappa Phi	2007-present
Research Experience for Undergraduates Fellow, Duke University	5/07-7/07
Tau Beta Pi Honors Engineering Society	2006-present
Howard Hughes Medical Institute Summer Research Intern	5/06-8/06